6

Random closed sets II – The general case

6.1 Basic properties

6.1.1 Introduction

Random closed sets serve as general mathematical models for irregular geometrical patterns, such as porous media. In the planar case they are sometimes called *random area patterns*. Random closed sets play a central rôle in stochastic geometry. Chapter 3 presents an important special case of a random set — the Boolean model. In this chapter a more general theory is considered.

What today are known as random sets occur relatively early in the literature of probability theory. Systematic studies can be found as early as in the decade of the thirties; the famous book by Kolmogorov (1933, p. 41) contains the phrase 'region ... whose shape depends on chance', and Kolmogorov gives there a mean-value formula closely related to Formula (6.23) below. Furthermore, in 1937 he studied a particular case of the Boolean model, in the context of crystallisation; see the KJMA theory in Section 6.6.4 on p. 273. Further early studies of particular random set models can be found in the literature of the 1940s and 1950s; see the references in Section 3.1.2.

Foundations of the modern theory of random closed sets were laid by Choquet (1954) in his work on *capacities*. Matheron (1967, 1975) studied random closed sets in locally compact separable Hausdorff spaces (LCS spaces). A more general theory has been published by Kendall (1974); this derives from work in the 1960s in which Davidson played an important part (see the remarks in Kendall, 1974). Modern references are the books Goutsias *et al.* (1997), Jeulin (1997), Molchanov (1993, 2005), Nguyen (2006) and Schneider and Weil (2008).

Random sets also play a rôle in the theory of control and optimisation. This theory uses so-called multivalued functions, which can be considered to be random sets provided their parameter space is endowed with a certain probability distribution (see Artstein, 1984b; Salinetti

Stochastic Geometry and its Applications, Third Edition.
Sung Nok Chiu, Dietrich Stoyan, Wilfrid S. Kendall and Joseph Mecke.

and Wets, 1986; Aubin and Frankowska, 1990). Moreover, random set theory provides tools for the statistical inference for the set of parameter values that are observationally equivalent under the given data and maintained assumptions (Beresteanu *et al.*, 2011). The literature also discusses random fuzzy sets (see e.g. Kruse and Meyer, 1987; Bandemer and Näther, 1992; Dozzi *et al.*, 2001; Li *et al.*, 2002; Nguyen, 2005; Krätschmer, 2006; Nguyen and Wu, 2006; and Fu and Zhang, 2008).

In this chapter, the theory of Matheron (1975) will be presented, but only for the particular case in which the random sets lie in $\mathbb{R}^d$. (A reader who is familiar with the theory of locally compact separable Hausdorff spaces will observe that the generalisation is straightforward.) As a matter of convention the random sets considered here are *closed*; that is, the boundaries of the sets are included in the sets themselves.

6.1.2 Random set definition

The hitting σ-algebra $\mathcal{F}$

Random sets can be considered and characterised in many ways, typically by employing some system of deterministic test sets and then analysing the intersections of random sets with these test sets. Thus two choices must be made: first of the system of test sets, and then of the nature of measurement of the intersection. For example, if the random set Ξ might be infinite in extent then the test sets are best chosen to be bounded. On the other hand, as Kendall (1974) points out, some measurements (such as the Lebesgue measure of the intersection $\Xi \cap T$ for test sets T) are not always appropriate. (The measure-related way is briefly discussed in Section 7.3.4.) Rather, to quote Kendall, 'instead of working with some version of the "size" of $\Xi \cap T$ we should merely note whether $\Xi \cap T$ is empty or not'. This means of measurement, the mere observation of whether the intersection is void, is fundamental to the modern random set theories as developed by Matheron and Kendall. The hitting σ-algebra $\mathcal{F}$ is closely related to this means of measurement.

Suppose that $\mathbb{F}$ is the family of all closed subsets of $\mathbb{R}^d$. Then $\mathcal{F}$ denotes the smallest σ-algebra of subsets of $\mathbb{F}$ that contains all the 'hitting sets':

$$\mathbb{F}_K = \{F \in \mathbb{F} : F \cap K \neq \emptyset\} \qquad \text{for } K \in \mathbb{K}.$$

Thus the system of test sets is the system $\mathbb{K}$ of all compact subsets of $\mathbb{R}^d$; and the measurement of the intersection is simply an observation of whether or not the intersection is void. The hitting σ-algebra $\mathcal{F}$, also known as the *Effros σ-algebra* in the context of general topology, is built out of a family of assertions about whether or not the random set hits particular compact subsets.

Important properties of $\mathcal{F}$ can be found in Beer (1993), Molchanov (2005) and Schneider and Weil (2008); it can be shown that $\mathcal{F}$ is the Borel σ-algebra with respect to a suitable topology (the Fell topology) on $\mathbb{F}$.

Random closed sets

A random closed set Ξ is a random variable taking values in $[\mathbb{F}, \mathcal{F}]$. So Ξ is an $(\mathcal{A}, \mathcal{F})$-measurable mapping of a probability space $[\Omega, \mathcal{A}, \mathbf{P}]$ into $[\mathbb{F}, \mathcal{F}]$. This means that probabilities can be assigned to statements about Ξ when the statements are composed out of assertions

that Ξ hits compact sets. Thus Ξ generates a distribution P on $[\mathbb{F}, \mathcal{F}]$ called the *distribution* of Ξ, with $P(A) = \mathbf{P}(\Xi \in A)$ for every $A \in \mathcal{F}$.

Simple examples of random sets

The full sophistication of the formal definition of random sets is not needed in order to appreciate many examples, such as:

- random points,
- closed balls of random centre positions and radii,
- closed cubes with random corner positions and edge lengths.

More complicated random sets can be generated by using set-theoretic operations such as $\cup$, $\cap$ and $\oplus$. It can be shown that these operations have suitable measurability properties, so that the resulting structures are indeed still random closed sets. An important example of a random closed set generated by such means is the Boolean model in Chapter 3, the definition of which uses the operations of set union and translation.

6.1.3 Capacity functional and Choquet theorem

Capacity functional

An effective means of characterising the distribution P of a random set Ξ is given by the *capacity functional* T_Ξ. It is defined by

$$T_\Xi(K) = \mathbf{P}(\Xi \cap K \neq \emptyset) = P(\mathbb{F}_K), \tag{6.1}$$

where K is any compact subset of $\mathbb{R}^d$. That means, $T_\Xi(K)$ is the probability that the random set Ξ hits the set K. Considered as a function on $\mathbb{K}$ the capacity functional is actually an *alternating Choquet capacity of infinite order* (Matheron, 1975). That is to say, $T_\Xi(K)$ satisfies

(a) upper semicontinuity: if $K_n \downarrow K$ then $T_\Xi(K_n) \downarrow T_\Xi(K)$,

(b) complete alternation: $S_n(K; K_1, \ldots, K_n) \geq 0$, for all n,

where

$$S_n(K; K_1, \ldots, K_n) = S_{n-1}(K; K_1, \ldots, K_{n-1}) - S_{n-1}(K \cup K_n; K_1, \ldots, K_{n-1}),$$

and $S_0(K) = 1 - T_\Xi(K)$; here K and $K_1, \ldots, K_n$ are compact subsets of $\mathbb{R}^d$. Note that $S_n(K; K_1, \ldots, K_n)$ is equal to

$$\mathbf{P}(\Xi \cap K = \emptyset,\ \Xi \cap K_1 \neq \emptyset,\ \ldots,\ \Xi \cap K_n \neq \emptyset),$$

and that

(c) $$T_\Xi(\emptyset) = 0,$$

and

(d) $$0 \leq T_\Xi(K) \leq 1 \qquad \text{for } K \in \mathbb{K}.$$

The Choquet theorem

The Choquet theorem on capacities gives a precise characterisation of the distribution of a random closed set: the distribution is completely determined by knowledge of the capacity functional.

Theorem 6.1. *Let T be a functional on $\mathbb{K}$. Then there is a (necessarily unique) distribution P on $\mathcal{F}$ with*

$$P(\mathbb{F}_K) = T(K)$$

if and only if T is an alternating Choquet capacity of infinite order and such that

$$0 \le T(K) \le 1 \qquad \text{for } K \in \mathbb{K},$$

and $T(\emptyset) = 0$, that is, T satisfies conditions (a)–(d) above.

The necessity of these conditions is clear from the discussion above. The sufficiency is plausible, since the hitting sets $\mathbb{F}_K$ generate $\mathcal{F}$; a proof can be found in Schneider and Weil (2008, pp. 22–31). It is based on the original proof of Matheron (1975) and uses an idea of Salinetti and Wets (1986). Other proofs are given in Berg *et al.* (1984) and Norberg (1989), who use harmonic analysis on semigroups and lattice theory, respectively; see also Molchanov (2005, pp. 13–18).

If the random closed set satisfies additional properties then it may be possible to determine its distribution using a smaller family of hitting sets; see Cressie and Laslett (1987) and Molchanov (2005, pp. 18–20). For example, the distribution of a *convex* random compact set Ξ is determined by the probabilities

$$\mathbf{P}(\Xi \subset K) \qquad \text{for compact convex } K.$$

The Choquet theorem shows that capacity functionals play a describing rôle for random closed sets similar to that distribution functions play for random variables. Several distributional properties of random closed sets can be succinctly expressed in terms of their capacity functionals. For example, convergence in distribution is ensured if and only if the corresponding capacity functionals are convergent; see Norberg (1984), Kallenberg (2002, p. 325) and Molchanov (2005, p. 86).

6.1.4 Distributional properties

Independence

Two random closed sets Ξ_1 and Ξ_2 are said to be *independent* if for arbitrary A_1 and A_2 in $\mathcal{F}$

$$\mathbf{P}(\Xi_1 \in A_1,\ \Xi_2 \in A_2) = \mathbf{P}(\Xi_1 \in A_1)\,\mathbf{P}(\Xi_2 \in A_2). \tag{6.2}$$

By the Choquet theorem this is equivalent to the condition

$$\mathbf{P}(\Xi_1 \cap K_1 \neq \emptyset,\ \Xi_2 \cap K_2 \neq \emptyset) = T_{\Xi_1}(K_1)\,T_{\Xi_2}(K_2) \tag{6.3}$$

for all compact K_1 and K_2. If two random closed sets Ξ_1 and Ξ_2 are independent, then the capacity functional of $\Xi_1 \cup \Xi_2$ is given by

$$T_{\Xi_1 \cup \Xi_2}(K) = T_{\Xi_1}(K) + T_{\Xi_2}(K) - T_{\Xi_1}(K)T_{\Xi_2}(K) \qquad \text{for } K \in \mathbb{K}. \tag{6.4}$$

Stationarity and isotropy

A random closed set Ξ is said to be *stationary* if Ξ and the translated sets $\Xi_x = \Xi + x$ all have the same distribution, whatever x in $\mathbb{R}^d$ may be. Again the Choquet theorem shows that this holds if and only if the capacity functional is translation-invariant, that is,

$$T_\Xi(K) = T_\Xi(K_x) \tag{6.5}$$

for every compact K and every x in $\mathbb{R}^d$. The proof of this uses the equalities

$$\begin{aligned} T_\Xi(K) &= \mathbf{P}(\Xi \cap K \neq \emptyset) \\ &= \mathbf{P}\big((\Xi - x) \cap K \neq \emptyset\big) \\ &= \mathbf{P}\big(\Xi \cap (K + x) \neq \emptyset\big) = T_\Xi(K_x). \end{aligned}$$

A random closed set is said to be *stationary and isotropic* (or *motion-invariant*) if for every rigid motion $\boldsymbol{m}$ the distributions of Ξ and of $\boldsymbol{m}\Xi$ are the same. As before an equivalent condition can be given using capacity functionals:

$$T_\Xi(K) = T_\Xi(\boldsymbol{m}K) \tag{6.6}$$

for all such $\boldsymbol{m}$ and $K \in \mathbb{K}$.

Sometimes stationary random $\mathbb{S}$-sets (random closed sets that are almost surely elements of the extended convex ring $\mathbb{S}$, i.e. almost surely locally polyconvex; see Section 1.8) satisfying a certain integrability condition are called *standard random sets*; see Schneider and Weil (2008, p. 397). For example, Boolean models with convex grains are standard.

Ergodicity

Consider the translated family of sets

$$A_x = \{F_x : F \in A\}$$

for $A \in \mathcal{F}$ and x in $\mathbb{R}^d$. A random closed set Ξ (or its distribution P) is said to be *metrically transitive* (with respect to the family of spatial translations) if the condition on A that

$$P\big((A \setminus A_x) \cup (A_x \setminus A)\big) = 0 \qquad \text{for all } x \in \mathbb{R}^d \tag{6.7}$$

always implies that $P(A)$ is zero or one. Condition (6.7) means (if events of probability zero are neglected) that Ξ belongs or fails to belong to A and to A_x simultaneously. Consequently if Ξ is metrically transitive then assertions that are translation-invariant (make no explicit or implicit reference to the location of Ξ) are either almost certainly true or almost certainly false.

A random set Ξ is *ergodic* if

$$\lim_{n\to\infty} \frac{1}{v_d(W_n)} \int_{W_n} P(A_x \cap B)\,\mathrm{d}x = P(A)P(B) \tag{6.8}$$

for any two A and B in $\mathcal{F}$ and any convex averaging sequence of windows $\{W_n\}$.

It can be shown (see Daley and Vere-Jones, 2008, Exercise 12.2.3, and Heinrich, 1992b) that a stationary Ξ is ergodic if and only if it is metrically transitive.

A sufficient condition for ergodicity is the *mixing property*:

$$P(A \cap B_x) \to P(A)P(B) \qquad \text{for all } A, B \text{ in } \mathcal{F}, \tag{6.9}$$

or, equivalently, in terms of capacity functional

$$1 - T_\Xi(K \cup K'_x) \to \big(1 - T_\Xi(K)\big)\big(1 - T_\Xi(K')\big) \qquad \text{for all } K, K' \text{ in } \mathbb{K}, \tag{6.10}$$

as $\|x\| \to \infty$. Stationary Boolean models and homogeneous Poisson processes are mixing (see Schneider and Weil, 2008, Section 9.3).

The use of the property of ergodicity may be summarised as follows: statistical averages can be expressed by limits of arithmetic or spatial averages. For example, the classical ergodic theorem states that under metrical transitivity (with respect to iterates of a measure-preserving transformation T) the arithmetic averages

$$\big(f(TX) + \cdots + f(T^n X)\big)\Big/ n$$

converge as $n \to \infty$ to $\mathbf{E}\big(f(X)\big)$, when f is a bounded measurable function, T^k the k^{th} iterate of T, and X a random variable. Nguyen (1979) and Nguyen and Zessin (1979a) proved ergodic theorems for 'spatial processes', in which spatial averages replace arithmetic averages.

A simple case of such results concerns spatial processes of the form

$$X_B = h(B \cap \Xi) \qquad \text{for } B \text{ a fixed bounded Borel subset of } \mathbb{R}^d,$$

where h is a suitable function. Such a case arises, for example, in the study of statistics of random sets and in the definition of 'densities' of random sets; see Schneider and Weil (2008, Sections 9.2–9.3) and Section 6.3.6.

In order to discuss this, notation must be introduced to describe the kind of spatial averaging being used. Let C_0 denote the semi-open cube,

$$C_0 = \left\{(x_1, \ldots, x_d) \in \mathbb{R}^d : -\frac{1}{2} \le x_i < \frac{1}{2}\right\}.$$

Clearly, the whole space can be divided into translates of C_0.

Theorem 6.2. *(Nguyen and Zessin, 1979a) Suppose that Ξ is a stationary ergodic random closed set and that there is given a measurable mapping $h : \mathcal{B}^d \to \mathbb{R}$ with*

$$h(B + x) = h(B) \qquad \textit{for each } B \in \mathcal{B}^d \textit{ and all } x \in \mathbb{R}^d \quad \textit{(translation-invariance),}$$

and

$$h(B_1 \cup B_2) = h(B_1) + h(B_2) \qquad \textit{for all disjoint } B_1, B_2 \quad \textit{(additivity).}$$

Further, let $\{W_n\}$ be a convex averaging sequence of windows.

(1) If there exists a positive constant c such that

$$\mathbf{E}\big(|h(K \cap \Xi)|\big) \le c \qquad \text{for all convex bodies } K \subset C_0,$$

then

$$\lim_{n\to\infty} \mathbf{E}\left(\left|\frac{h(W_n \cap \Xi)}{v_d(W_n)} - \mathbf{E}\big(h(C_0 \cap \Xi)\big)\right|\right) = 0. \tag{6.11}$$

(2) If there exists a nonnegative random variable ξ of finite mean such that

$$|h(K \cap \Xi)| \le \xi \qquad \mathbf{P}\text{-almost surely for all convex bodies } K \subset C_0,$$

then

$$\lim_{n\to\infty} \frac{h(W_n \cap \Xi)}{v_d(W_n)} = \mathbf{E}\big(h(C_0 \cap \Xi)\big) \qquad \mathbf{P}\text{-almost surely}. \tag{6.12}$$

Thus the spatial average $h(W_n \cap \Xi)/v_d(W_n)$ converges to the statistical average $\mathbf{E}\big(h(C_0 \cap \Xi)\big)$ under the conditions of stationarity and ergodicity, and the latter average is regarded as the density of h; see Section 6.3.6.

Case (1) of Theorem 6.2 provides a weaker form of convergence than case (2). In later applications, the class $\mathcal{B}^d$ is sometimes replaced by the convex ring $\mathcal{R}$.

6.1.5 Miscellany

Random fields

From any random closed set Ξ a random field $\{Y(x) : x \in \mathbb{R}^d\}$ can be constructed as the indicator function of the set Ξ. That is

$$Y(x) = \mathbf{1}_\Xi(x) \qquad \text{for } x \text{ in } \mathbb{R}^d. \tag{6.13}$$

This correspondence is of use in applying methods of the statistics of random fields to the statistical analysis of random sets. Conversely, from a random field a random closed set can be obtained as an excursion set by truncating the random field at a fixed level; see Section 6.6.3. Buryachenko (2007) tries to circumvent random sets by using indicator functions.

Another constructed random field is

$$V_\Xi(x) = v_d\big(B(x, r) \cap \Xi\big), \tag{6.14}$$

the volume of Ξ in the ball $B(x, r)$ of radius r centred at x; see p. 287.

Random marked sets

A *random marked set* is a random field with a random set as support. That means, it is a pair (Ξ, Z) where Ξ is a random closed set in $\mathbb{R}^d$ and Z a real-valued random mapping defined on

Ξ. Random marked sets were introduced in Ballani *et al.* (2012), where precise definitions are given. Three examples are:

(1) Random field over a level u.
Start with a random field $\{Y(x) : x \in \mathbb{R}^d\}$ which has continuous realisations and a fixed real number u, the level. Take as random set the u-level excursion set $\Xi = \{x \in \mathbb{R}^d : Y(x) \geq u\}$ (discussed in detail in Section 6.6.3) and define Z by

$$Z(x) = Y(x) \qquad \text{for } x \in \Xi.$$

For x lying outside Ξ, $Z(x)$ is not defined. Wrong results will be obtained if the covariance function of $\{Y(x)\}$ is estimated from (Ξ, Z) by the usual geostatistical methods ignoring the fact that outside of Ξ no values of the field can be observed.

(2) Marked point process.
A marked point process $\Psi = \{[x_n; m_n]\}$ can be considered as a random marked set, if $\Xi = \Phi = \{x_n\}$, that is, the ground process is the random supporting set, and $m_n = Z(x_n)$ for $x_n \in \Phi$.

(3) Marked fibre process.
Take a fibre process, that is, a random collection of curves (fibres) in space as considered in Section 8.4, and mark each fibre point x by a real value $Z(x)$. This value may come from an independent random field $\{Y(x)\}$ as in example (1) via $Z(x) = Y(x)$ or may depend on the given fibre, for example as $Z(x) =$ tube thickness in x, if the fibre stands for a tube with variable thickness. See Section 8.6 for further discussion of marked fibre processes and related objects.

The notion of 'stochastic processes with random domains' (Molchanov, 2005, pp. 319–22) is closely related to this concept of random marked sets.

Ballani *et al.* (2012) study second-order characteristics of random marked sets.

Comparison of random closed sets

The random closed set Ξ_2 is *stochastically larger than* Ξ_1, denoted by $\Xi_1 \subseteq_{\text{st}} \Xi_2$, if there exist random closed sets N_1 and N_2, distributed respectively as Ξ_1 and Ξ_2, such that $N_1 \subset N_2$ almost surely.

Norberg (1992a,b) showed that $\Xi_1 \subseteq_{\text{st}} \Xi_2$ if and only if

$$\mathbf{P}\left(\bigcap_{i=1}^{n}(\Xi_1 \cap K_i \neq \emptyset)\right) \leq \mathbf{P}\left(\bigcap_{i=1}^{n}(\Xi_2 \cap K_i \neq \emptyset)\right) \tag{6.15}$$

for all n and all compact sets $K_1, K_2, \ldots \in \mathbb{K}$; see also Molchanov (2005, Theorem 4.42).

Formula (6.15) implies

$$T_{\Xi_1}(K) \leq T_{\Xi_2}(K), \tag{6.16}$$

but the converse is not true; see Norberg (1992b) and Müller and Stoyan (2002, p.247).

Comparisons of Boolean models and of RSA (see Section 6.5.3) and dead leaves models with respect to $\subseteq_{\text{st}}$ are briefly discussed in Müller and Stoyan (2002, Section 7.4).

Szekli (1995) considers comparison based on comparison of the empty space distribution function. This is greatly extended in Last and Szekli (2011) to the empty space hazard function, which leads to comparison of clustering degrees for germ–grain models.

Stoyan and Stoyan (1980b) consider some partial orderings, weaker than $\subseteq_{\mathrm{st}}$, of random closed sets. Cascos and Molchanov (2003) introduce orderings based on the Aumann expectation; see Formula (6.17) below and Cascos (2010).

Simulation of random sets

Lantuéjoul (2002) presents efficient algorithms for the simulation, including perfect simulation (Kendall and Thönnes, 1999; Møller, 2001), of several random set models described in this book. Simulation of Gaussian random fields, which are needed for generating for example excursion sets or marked random sets, is described in Schlather (2001b) using the R statistical programming language.

6.2 Random compact sets

6.2.1 Definition of means

A random compact set is simply a random closed set that is compact with probability one. Random compact sets are of interest as components of stationary random sets but also as models of particles or small objects of technological, biological or geological origin. Some stochastic models of such sets are considered in Molchanov (1993), Stoyan and Stoyan (1994) and Molchanov and Stoyan (1995). Of particular interest are typical cells of tessellations (see Chapter 9), convex hulls of points (see Reitzner, 2010), and sets resulting from limit procedures.

Beginning with Aumann (1965) several authors have suggested definitions of set-valued means of random compact sets (see Stoyan and Stoyan, 1994, Section 8.3, and Molchanov, 2005, Chapter 2). The typical pattern of such definitions is as follows:

(1) assign to the random compact set Ξ a (family of) random function(s);

(2) use a suitable definition for determining a (family of) mean function(s);

(3) determine a set which corresponds to this (these) mean function(s).

Selection expectation

Aumann's original definition is

$$\mathbf{E}(\Xi) = \{\mathbf{E}(X) : X \text{ is a selection of } \Xi \text{ with } \mathbf{E}(\|X\|) < \infty\}. \tag{6.17}$$

A *selection* of Ξ is a random point X in $\mathbb{R}^d$ with $\mathbf{P}(X \in \Xi) = 1$. Since $\mathbf{E}(\|X\|)$ is finite for all X, $\mathbf{E}(\Xi)$ itself is compact. Furthermore, $\mathbf{E}(\Xi)$ is convex and coincides with $\mathbf{E}(\mathrm{conv}\Xi)$, with the exception that the probability space is atomic. If Ξ is convex, then the definition can be re-expressed in terms of the support function (see Section 1.6): $\mathbf{E}(\Xi)$ satisfies

$$s\big(\mathbf{E}(\Xi), u\big) = \mathbf{E}\big(s(\Xi, u)\big) \qquad \text{for } u \in S^{d-1}, \tag{6.18}$$

which is sufficient to uniquely determine a member in the family of convex compact sets. If Ξ is isotropic, then $\mathbf{E}(\Xi)$ is a ball centred at o. Often $\mathbf{E}(\Xi)$ is called the *Aumann expectation* or *selection expectation* of Ξ.

The average breadth of the Aumann expectation of Ξ coincides with the expected average breadth of Ξ:

$$\mathbf{E}\big(\overline{b}(\Xi)\big) = \overline{b}\big(\mathbf{E}(\Xi)\big), \tag{6.19}$$

and consequently an analogous equality holds for the perimeter in the planar convex case. Thus the Aumann expectation of a random ball centred at o is the ball with mean diameter.

For volume and area such relations do not hold; instead, there is an inequality for area in the planar case:

$$\mathbf{E}\left(\sqrt{A(\Xi)}\right) \leq \sqrt{A\big(\mathbf{E}(\Xi)\big)}. \tag{6.20}$$

Many authors have established limit theorems for random compact sets. Artstein and Vitale (1975) prove that for a sequence of i.i.d. random compact sets Ξ, Ξ_1, Ξ_2, ... with $\mathbf{E}(\sup\{\|x\| : x \in \Xi\}) < \infty$,

$$\frac{1}{n}(\Xi_1 \oplus \cdots \oplus \Xi_n) \to \mathbf{E}(\Xi) \qquad \text{almost surely} \tag{6.21}$$

with respect to the Hausdorff metric; see also Artstein (1984a). Weil (1982a) proves a central limit theorem, which corresponds to the strong law of large numbers given in (6.21).

For other limit theorems involving the Minkowski sum, such as the law of iterated logarithm, renewal theorems and ergodic theorems, as well as limit theorems for unions and convex hulls of random compact sets, generalising classical results of extreme value theory; see Molchanov (1993) and Molchanov (2005, Chapters 3–4).

Other expectations

An alternative natural way of defining a mean for a random compact set Ξ is the use of the *coverage function*,

$$p_\Xi(x) = \mathbf{E}\big(\mathbf{1}_\Xi(x)\big) = T_\Xi(\{x\}) \qquad \text{for } x \in \mathbb{R}^d, \tag{6.22}$$

that is, the mean of the indicator function of Ξ. Another form is

$$p_\Xi(x) = \mathbf{P}(x \in \Xi) \qquad \text{for } x \in \mathbb{R}^d. \tag{6.23}$$

In this case the mean is not a set but a function taking values between 0 and 1. Perhaps one may consider $p_\Xi(x)$ as the membership function of a fuzzy set (see e.g. Dubois and Prade, 2000; Nguyen and Wu, 2006). The mean volume of Ξ satisfies

$$\mathbf{E}\big(v_d(\Xi)\big) = \int_{\mathbb{R}^d} p_\Xi(x)\mathrm{d}x. \tag{6.24}$$

If Ξ is isotropic then $p_\Xi(x)$ depends only on $\|x\|$.

A third mean-set definition is the *Vorob'ev mean*. The idea is to take the excursion set of the coverage function $p_\Xi(x)$ such that the volume of the excursion set and the mean volume

of Ξ coincide:

$$\mathbf{E}_{\mathrm{V}}(\Xi) = \{x \in \mathbb{R}^d : p_{\Xi}(x) \geq u\}, \tag{6.25}$$

where u is determined by

$$v_d\big(\{x \in \mathbb{R}^d : p_{\Xi}(x) \geq u\}\big) = \mathbf{E}\big(v_d(\Xi)\big). \tag{6.26}$$

If u is not unique then take the infimum of all such u. Vorob'ev's definition is quite natural: the mean set $\mathbf{E}_{\mathrm{V}}(\Xi)$ satisfies the inequality

$$\mathbf{E}\big(v_d(\Xi \triangle \mathbf{E}_{\mathrm{V}}(\Xi)\big) \leq \mathbf{E}v_d(\Xi \triangle B)$$

for all Borel sets B with $v_d(B) = \mathbf{E}\big(v_d(\Xi)\big)$. Here $\triangle$ denotes the symmetric difference operator:

$$C \triangle D = C \setminus D \cup D \setminus C.$$

In this sense $\mathbf{E}_{\mathrm{V}}(\Xi)$ is that set of area $\mathbf{E}\big(v_d(\Xi)\big)$ that is best fitted to Ξ. Heinrich *et al.* (2012) proposed a consistent estimator of $\mathbf{E}_{\mathrm{V}}(\Xi)$ from discretised independent realisations of Ξ.

Molchanov (2005, Chapter 3) discusses mean sets defined by various distance functions and, when restricted to star-shaped sets, radius-vector function. Jankowski and Stanberry (2010, 2012) define mean sets and mean boundaries, and construct their confidence regions, using signed distance functions; see Osher and Fedkiw (2003).

There are also attempts to define variances, which are positive numbers characterising variability; see Stoyan and Stoyan (1994, Section 8.3.5).

The application of ideas of mean sets to samples of particles such as sand grains is difficult since for these only shape and size are of interest, while spatial position is disregarded. Stoyan and Molchanov (1997) show how to proceed: the particles are shifted and rotated before determining a mean.

The book Stoyan and Stoyan (1994) studies systematically summary characteristics and, in Section 8.5, models for particles. The papers Stoyan *et al.* (2002) and Ballani and van den Boogaart (2013) present particle models with Gibbs distributions, for pixel sets and polytopes, respectively. Further models are mentioned in Molchanov (2005, pp. 218–223) (Gaussian, p-stable and Minkowski infinitely divisible) and in Jónsdóttir *et al.* (2008). Figure 3.4 can be interpreted as a sample of a random compact set.

6.2.2 Mean-value formulae for convex random sets

In this section the random closed set Ξ is taken to be convex and compact with probability one. Thus the intrinsic volumes $V_k(\Xi)$ can be considered. It is assumed that their first moments are finite:

$$\overline{V}_k = \mathbf{E}\big(V_k(\Xi)\big) < \infty \qquad \text{for } k = 0, 1, \ldots, d. \tag{6.27}$$

The *Steiner*, *Crofton*, and other integral-geometric formulae will then be satisfied for Ξ almost surely, and analogous formulae will hold for the mean values. For example, corresponding to the Steiner formula there is

$$\mathbf{E}\left(v_d\big(\Xi \oplus b(o, r)\big)\right) = \sum_{k=0}^{d} b_{d-k} \overline{V}_k r^{d-k} \qquad \text{for } r \geq 0. \tag{6.28}$$

If Ξ has a distribution invariant with respect to rotations about the origin o, then the important so-called *generalised Steiner formula*

$$\mathbf{E}\big(v_d(\Xi \oplus K)\big) = \frac{1}{b_d} \sum_{k=0}^{d} \frac{b_k b_{d-k}}{\binom{d}{k}} \overline{V}_k V_{d-k}(K) \tag{6.29}$$

holds for every compact convex K. Its proof rests on the Hadwiger characterisation theorem: the functional $h(K)$ appearing in Formula (1.44) is

$$h(K) = \mathbf{E}\big(v_d(\Xi \oplus K)\big),$$

which can be shown to be motion-invariant, C-additive, and monotone in the compact set K. Thus from the Hadwiger theorem $h(K)$ is a linear combination of the $V_k(K)$ and its coefficients can be derived by setting $K = B(o, r)$.

In the important planar and spatial cases Formula (6.29) takes on the forms:

$$\mathbf{E}\big(A(\Xi \oplus K)\big) = \overline{A} + \frac{\overline{L}\, L(K)}{2\pi} + A(K) \qquad \text{if } d = 2 \tag{6.30}$$

and

$$\mathbf{E}\big(V(\Xi \oplus K)\big) = \overline{V} + \frac{\overline{\overline{b}}\, S(K)}{2} + \frac{\overline{S}\, \overline{b}(K)}{2} + V(K) \qquad \text{if } d = 3. \tag{6.31}$$

A similar generalisation can be carried out on Formulae (1.45) for the intrinsic volumes, and also for the generalised intrinsic volumes of sets in the convex ring $\mathcal{R}$.

A useful consequence of Formula (6.31) is that for the volume of the mean *excluded volume* of a random convex compact subset Ξ of $\mathbb{R}^3$:

$$\mathbf{E}\big(V(\Xi \oplus \check{\Xi})\big) = 2\overline{V} + \overline{\overline{b}} \cdot \overline{S}, \tag{6.32}$$

where $\check{\Xi}$ denotes a random closed set of the same distribution as $-\Xi$ but independent of Ξ.

6.3 Characteristics for stationary and isotropic random closed sets

6.3.1 The area or volume fraction

The area or volume fraction of a stationary random set Ξ is the mean volume of Ξ intersected with the unit cube C_0, that is,

$$p = \mathbf{E}\big(v_d(\Xi \cap C_0)\big). \tag{6.33}$$

If Ξ models the pore network of a porous medium, then p is the *porosity*. The volume fraction is the most important random set characteristic and plays a rôle similar to that of the intensity of a point process. Unfortunately, in the literature different symbols are used, for example ϕ or η, and even in this book the notations V_V and A_A are used from time to time as alternatives

to p; see Section 10.2.2. The meaning of V_V is 'volume of Ξ per unit volume', and A_A is analogous. These two symbols appear when the dimension of the space is emphasised.

It is the case that

$$p = \mathbf{P}(o \in \Xi) = \mathbf{P}(x \in \Xi) = T_\Xi(\{o\}) \qquad \text{for } x \in \mathbb{R}^d, \tag{6.34}$$

which results from the stationarity of Ξ by the following chain of equalities:

$$\begin{aligned}
\mathbf{E}\big(v_d(\Xi \cap C_0)\big) &= \mathbf{E}\left(\int_{\mathbb{R}^d} \mathbf{1}_{\Xi \cap C_0}(x)\,\mathrm{d}x\right) \\
&= \mathbf{E}\left(\int_{C_0} \mathbf{1}_\Xi(x)\,\mathrm{d}x\right) \\
&= \int_{C_0} \mathbf{E}\big(\mathbf{1}_\Xi(x)\big)\,\mathrm{d}x \\
&= \int_{C_0} \mathbf{P}(x \in \Xi)\,\mathrm{d}x = \mathbf{P}(o \in \Xi),
\end{aligned}$$

since by stationarity $\mathbf{P}(x \in \Xi) = \mathbf{P}(o \in \Xi)$ for all x in $\mathbb{R}^d$.

The volume fraction can arise in other ways, which are described as follows.

(a) If the volume (or coverage) measure V_Ξ is defined on $\mathbb{R}^d$ by

$$V_\Xi(B) = v_d(\Xi \cap B) \qquad \text{for all Borel sets } B, \tag{6.35}$$

then V_Ξ is a stationary random measure; see Chapter 7. Its *intensity* is p.

(b) Let v be the translation-invariant measure on $\mathbb{R}^d$ defined by

$$v(B) = \mathbf{E}\big(v_d(\Xi \cap B)\big) \qquad \text{for all Borel sets } B. \tag{6.36}$$

It is finite on bounded Borel sets. Suppose that K is a convex body with inner points. Then the corresponding *density*

$$D_V(\Xi) = \frac{v(K)}{v_d(K)} \tag{6.37}$$

exists and equals p.

(c) Suppose that Ξ is ergodic and K is as in (b). Then the ergodic theorem given in Theorem 6.2 states that the ratio

$$\frac{v_d\big(\Xi \cap (rK)\big)}{v_d(rK)}$$

converges to p almost surely as $r \to \infty$.

6.3.2 The covariance

Just as p describes the first-order structure of Ξ, the *covariance* or *two-point probability function* deals with the second-order structure. (Note that the term is 'covariance' and not

'covariance function'.) As for volume fraction so here different symbols are used, for example $\gamma_2(r)$ (Frisch and Stillinger, 1963) and $S_2(r)$ (Torquato, 2002).

Clearly, for the covariance to be an effective measure of second-order structure the volume fraction p must be positive, since otherwise the covariance will be identically zero. Some random sets, such as point or fibre processes, have $p = 0$ and their second-order structure is described directly by moment measures. (The covariance is essentially a product density corresponding to the random volume measure defined by (6.35).)

The covariance is defined by

$$C(\mathbf{r}) = C_\Xi(\mathbf{r}) = \mathbf{P}(o \in \Xi, \mathbf{r} \in \Xi) = T_\Xi(\{o, \mathbf{r}\}) \qquad \text{for } \mathbf{r} \in \mathbb{R}^d. \tag{6.38}$$

It satisfies the equations

$$C(\mathbf{r}) = \mathbf{P}(o \notin \Xi, \mathbf{r} \notin \Xi) + 2p - 1, \tag{6.39}$$

which is proved as on p. 74, and

$$C(\mathbf{r}) = \mathbf{P}(o \in \Xi \ominus \check{B}), \tag{6.40}$$

where $B = \{o, \mathbf{r}\}$ (a set composed of two points) and $\check{B} = -B$. Thus $C(\mathbf{r})$ is the volume fraction of the set Ξ eroded by the structuring element B. Formula (6.40) is a simple consequence of the definition of the operation of erosion:

$$o \in \Xi \ominus \check{B} \text{ if and only if } o \in \Xi \text{ and } \mathbf{r} \in \Xi.$$

Formula (6.38) is the same as

$$C(\mathbf{r}) = \mathbf{P}\big(o \in \Xi \cap (\Xi - \mathbf{r})\big). \tag{6.41}$$

This provides a basis for statistical estimation of $C(\mathbf{r})$ as a volume fraction.

There is a close relation between $C(\mathbf{r})$ and the *covariance function* of the random field associated with Ξ: the mean of the stationary random field

$$\{\mathbf{1}_\Xi(x) : x \in \mathbb{R}^d\}$$

is given by $\mathbf{E}\big(\mathbf{1}_\Xi(x)\big) = p$, and its covariance function $k(\mathbf{r})$ is

$$k(\mathbf{r}) = \mathbf{E}\left(\big(\mathbf{1}_\Xi(o) - p\big)\big(\mathbf{1}_\Xi(\mathbf{r}) - p\big)\right) = C(\mathbf{r}) - p^2, \tag{6.42}$$

as can be seen on expanding the product. Notice that, in contrast to $k(\mathbf{r})$, the covariance $C(\mathbf{r})$ is not centred.

The covariance function is often normalised by dividing by $k(o) = p(1 - p)$, which gives the *correlation function* or *Debye X-ray correlation function*

$$\kappa(\mathbf{r}) = \frac{k(\mathbf{r})}{k(o)} \qquad \text{for } \mathbf{r} \in \mathbb{R}^d, \tag{6.43}$$

with

$$k(o) = p(1 - p),$$

If Ξ is not only stationary but also isotropic then the functions $C(\mathbf{r})$, $k(\mathbf{r})$ and $\kappa(\mathbf{r})$ depend only on the distance $r = \|\mathbf{r}\|$. For simplicity the argument is then written as a scalar r, and

the function symbols are retained, for example:

$$C(\mathbf{r}) = C(\|\mathbf{r}\|) = C(r) \qquad \text{for motion-invariant } \Xi.$$

The function

$$g(r) = \frac{C(r)}{p^2}$$

is sometimes called *pair correlation function*. Indeed it is the pair correlation function of the volume measure; see Section 7.3.4. The function

$$\gamma(r) = C(0) - C(r) \qquad \text{for } r \geq 0 \tag{6.44}$$

is also known as the *variogram*.

Note that

$$C(0) = C(o) = p, \tag{6.45}$$

and if Ξ satisfies the mixing property, then

$$C(\infty) = p^2. \tag{6.46}$$

Not every nonnegative function $C(r)$ with $C(0) = p$ and $C(\infty) = p^2$ is the covariance of a random set. A necessary condition is that the corresponding covariance function $k(r)$ is positive definite. Torquato (2006) and Jiao *et al.* (2007, 2010) discussed necessary and sufficient conditions for the reconstructions of random sets from a given covariance. In general, $C(r)$ alone does not determine uniquely the distribution of a random set.

Analysis of the three functions $C(r)$, $k(r)$ and $\kappa(r)$ allows for information to be gained about the structure of Ξ even in the case where no image of Ξ is available as, for example, in the cases of X-ray scattering analysis, or geological exploration by means of boreholes. Figure 6.1 shows possible forms of $C(r)$ by giving three typical images of samples of planar random sets together with corresponding empirical covariances (determined by image analyser). Thus the functions can be used in a descriptive analysis. They also have theoretical uses in determining the accuracy of statistical estimators; see Section 6.4.2. Integrating the correlation function leads to the *integral range* a_V (Matheron, 1971), which is, despite the name, a volume defined by

$$a_V = \int_{\mathbb{R}^d} \kappa(\mathbf{r}) \mathrm{d}\mathbf{r}. \tag{6.47}$$

This value gives an approximation of the size of the representative volume element for the determination of volume fraction; see Section 6.4.6.

Finally the three functions can be used directly in estimation of model parameters, for example in the Boolean model as demonstrated in Example 3.3.

Let the random set Ξ be almost surely regular closed (coinciding with the closure of its interior) and suppose that the specific surface area $S_V^{(d)}$ of the boundary $\partial\Xi$ of Ξ is finite (see Section 7.3.4 for a definition of specific surface area). Then the first derivative $C'(0+)$ is related to $S_V^{(d)}$ by

$$S_V^{(d)} = -\frac{db_d}{b_{d-1}} C'(0+), \tag{6.48}$$

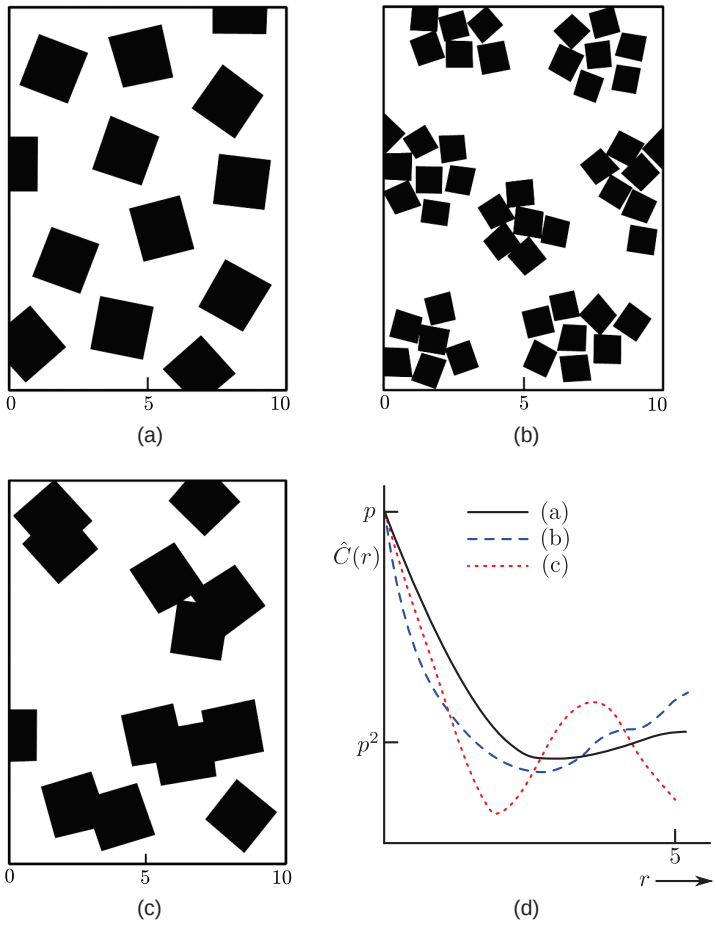

Figure 6.1 Forms of the covariance $C(r)$ for realisations of three different random closed sets sharing the same volume fraction p. The form of $C(r)$ allows conclusions to be drawn concerning the properties of the corresponding random sets, such as the inter-particle distances or the tendency to clustering. See also Figures 6.2 and 6.4.

as discovered by Debye *et al.* (1957) and Guinier and Fournet (1995). In the particular cases of $d = 1, 2$ or 3 the coefficient of $-C'(0+)$ is 2, π or 4, respectively. See Berryman (1987), Kiderlen and Jensen (2003) and Gokhale *et al.* (2005) for the anisotropic case.

Proof of Formula (6.48). The proof is given here for $d = 3$; for $d = 2$ it is analogous. Let $\boldsymbol{g}$ be an oriented line through o. Then the set $\partial\Xi \cap \boldsymbol{g}$ of intersection points of the boundary of Ξ with the line $\boldsymbol{g}$ is a stationary point process on $\boldsymbol{g}$. It has finite intensity P_L, where P_L is connected to $S_V^{(3)} = S_V$ by the stereological formula (see Section 8.5.2)

$$P_L = \frac{S_V}{2}. \tag{6.49}$$

Now suppose that $\{x_n\}$ is the point process of left endpoints of the intervals forming the connected components of $\Xi^{\mathrm{int}} \cap \boldsymbol{g}$ or chords in Ξ (recall that $\boldsymbol{g}$ is oriented, so 'left' has a meaning along $\boldsymbol{g}$). Attach a mark l_n to each x_n by defining l_n to be the length of the corresponding connected component of $\Xi^{\mathrm{int}} \cap \boldsymbol{g}$ starting in x_n. The marked point process $\Psi = \{[x_n; l_n]\}$ inherits stationarity from Ξ and has intensity $\lambda = S_V/4$, the half of the value given by (6.49).

The random set $\Xi \cap \boldsymbol{g}$ can be viewed as a subset of the real line $\mathbb{R}$. Its covariance $C(r)$ coincides with the covariance of Ξ. Because of (6.40), $C(r)$ is equal to the length fraction of the eroded set

$$(\Xi \cap \boldsymbol{g}) \ominus \{o, r\} = \big\{x \in \mathbb{R} : \{x, x + r\} \subset \Xi \cap \boldsymbol{g}\big\},$$

and so it follows that $C(0) - C(r)$ is the length fraction of the set $\{x \in \Xi \cap \boldsymbol{g} : x + r \notin \Xi \cap \boldsymbol{g}\}$. In other words,

$$C(0) - C(r) = \mathbf{E}\big(\nu_1(\{x \in \Xi \cap \boldsymbol{g} : x + r \notin \Xi \cap \boldsymbol{g}\} \cap [0, 1])\big). \tag{6.50}$$

This equation yields upper and lower bounds for $C(0) - C(r)$ for small r ($r < 1$). The upper bound is

$$\mathbf{E}\left(\sum_{n: x_n + l_n \in [0, 1+r]} r\right),$$

and the lower bound is

$$r\mathbf{E}\left(\sum_{n: x_n + l_n \in [r, 1]} \mathbf{1}(l_n > r)\right) - r\mathbf{E}\left(\sum_{n: x_n \in [0,1]} \mathbf{1}(d_\Psi(x_n) \le r)\right),$$

where $d_\Psi(x_n)$ is the distance from x_n to its nearest neighbour in Ψ.

Applying the Campbell theorem (4.29) for marked point processes to both bounds yields

$$(1 - r)\lambda \mathbf{P}(l > r) - \lambda \mathbf{P}\big(d_\Psi(o) \le r\big) \le \frac{C(0) - C(r)}{r} \le (1 + r)\lambda,$$

where l follows the same distribution as l_n. Letting $r \to 0$ leads to

$$C'(0+) = -\lambda = -\frac{S_V}{4},$$

since $\mathbf{P}\big(d_\Psi(o) \le 0\big) = 0$. □

The second derivative $C''(0+)$ has also been studied; see Ciccariello (1995) and Böhm and Schmidt (2003), who showed that it is given by the values at $r = 0$ of the chord length probability density functions (see Section 6.3.4) for Ξ and its complement.

It has proved useful in many applications since Debye *et al.* (1957) to approximate complicated covariances by a simpler form, the so-called *exponential covariance*

$$C_{\mathrm{e}}(r) = p(1 - p)\mathrm{e}^{-\alpha r} + p^2 \qquad \text{for } r \ge 0, \tag{6.51}$$

where α is a positive parameter describing the degree of variability or randomness in the random closed set. The corresponding covariance function and correlation function are given by

$$k_e(r) = p(1-p)\mathrm{e}^{-\alpha r} \tag{6.52}$$

and

$$\kappa_e(r) = \mathrm{e}^{-\alpha r} \tag{6.53}$$

both for $r \geq 0$. In the spatial case ($d = 3$) it can be shown that

$$\alpha = \frac{S_V}{4V_V(1-V_V)}, \tag{6.54}$$

with

$$V_V = p;$$

see Ohser and Tscherny (1988). This is a useful expression of the theoretical quantity α in terms of quantities that can be easily estimated statistically. Under the assumption of the exponential covariance (6.51), the integral range defined in (6.47) is equal to

$$a_V = \frac{d!\, b_d}{\alpha^d}. \tag{6.55}$$

Sometimes a structure with an exponential covariance is called 'Debye random medium'. A simple example can be constructed as follows. Consider a Poisson line (or plane) tessellation with parameter ϱ as described in Section 9.5. Let each cell of the tessellation be painted independently of the others, painted black with probability p and white with probability $1-p$. Then the closure of the union of all black cells is a planar (spatial) random closed set with exponential covariance, with parameter $\alpha = \varrho$. Ohanian (1973) gave examples of random sets with exponential covariances but with curved boundaries.

Zachary and Torquato (2011) generalised $C(r)$ by using a function defined as in (6.38), where Ξ is replaced by $\Xi \oplus B(o, \delta)$ or $\Xi \ominus B(o, \delta)$. In the first case also structures with $p = 0$, for example fibre processes, can be analysed.

In some cases it is easy to give the covariance of sets obtained by set-theoretic operations. For the closure of the *complement* $(\Xi^{\mathrm{c}})^{\mathrm{cl}}$ of Ξ it is

$$C_{(\Xi^{\mathrm{c}})^{\mathrm{cl}}}(\mathbf{r}) = C_{\Xi}(\mathbf{r}) - 2p + 1, \tag{6.56}$$

and for the intersection $\Xi_1 \cap \Xi_2$ of two independent stationary closed random sets Ξ_1 and Ξ_2

$$C_{\Xi_1 \cap \Xi_2}(\mathbf{r}) = C_{\Xi_1}(\mathbf{r}) \cdot C_{\Xi_2}(\mathbf{r}). \tag{6.57}$$

If the two sets Ξ_1 and Ξ_2 are dependent, then their spatial correlation may be described by the *cross-covariance*

$$C_{12}(\mathbf{r}) = C_{\Xi_1, \Xi_2}(\mathbf{r}) = \mathbf{P}(o \in \Xi_1, \mathbf{r} \in \Xi_2). \tag{6.58}$$

An example of a pair of stationary dependent sets is Ξ_1 and Ξ_2, where Ξ_2 is constructed by Ξ_1 and a third set Ξ_3, which are both stationary and independent, by

$$\Xi_2 = (\Xi_3 \setminus \Xi_1)^{\mathrm{cl}}.$$

Here

$$C_{12}(\mathbf{r}) = \mathbf{P}(o \in \Xi_1, \mathbf{r} \in \Xi_2) = \big(p_1 - C_{\Xi_1}(\mathbf{r})\big)p_3,$$

where p_1 and p_3 are the volume fractions of Ξ_1 and Ξ_3, respectively.

Also *n-point probability functions* are of interest; see for example the monograph Torquato (2002). However, the theoretical determination of these functions for random set models is notoriously complicated.

6.3.3 Contact distribution functions

It is frequently the case that random sets must be considered for which identification of single particles or pores is inappropriate. Nevertheless, some kind of measurement of 'size' would be desired. The *contact distribution functions* $H_B(r)$ provide a useful tool for this, as explained in Section 3.1.7. This concept was introduced by Prager (1969), and Delfiner (1972) and Serra (1982, Chapter XIII) discussed its general value. Hug *et al.* (2002a) is an excellent survey on contact distributions.

The following presents a sketch of the theory for the stationary case. A contact distribution function depends on the choice of a *structuring element* B, which is a convex body. If B contains the origin o then $H_B(r)$ is defined by

$$H_B(r) = 1 - \mathbf{P}(o \notin \Xi \oplus r\check{B} \,|\, o \notin \Xi), \tag{6.59}$$

or

$$H_B(r) = 1 - \frac{\mathbf{P}(o \notin \Xi \oplus r\check{B})}{1 - p} \qquad \text{for } r \geq 0. \tag{6.60}$$

The numerator of the second term is

$$1 - \text{volume fraction of the set } \Xi \oplus r\check{B}.$$

The function $H_B(r)$ is indeed a distribution function if B is compact and convex with o an inner point. Then even a probability density function $h_B(r)$ exists,

$$h_B(r) = H_B'(r);$$

see Hansen *et al.* (1999). If B is compact and star-shaped (e.g. B is a segment with endpoint at o) then the additional conditions of $p > 0$ and Ξ mixing are necessary; see Heinrich (1993).

Sometimes the *empty space function* $F_B(r)$ is used, defined by

$$F_B(r) = \mathbf{P}(o \in \Xi \oplus r\check{B}) \qquad \text{for } r \geq 0. \tag{6.61}$$

The corresponding distribution has an atom of size p at $r = 0$. It can be interpreted as the distribution function of the random distance $d_B(o, \Xi)$ in the B-metric from a test point (which is

represented by o) to Ξ, which is zero if the test point is in Ξ. In some context, the corresponding hazard function $\eta_B(r)$ is also useful:

$$\eta_B(r) = \frac{f_B(r)}{1 - F_B(r)} \qquad \text{for } r > 0, \tag{6.62}$$

where $f_B(r)$ is the derivative (and also the density) of $F_B(r)$ and exists whenever $h_B(r)$ exists.

The empty space function can be extended to a distribution function on the whole real line by

$$F_B(r) = \begin{cases} \mathbf{P}(o \in \Xi \oplus r\check{B}) & \text{for } r \geq 0, \\ \mathbf{P}(o \in \Xi \ominus |r|B) & \text{for } r < 0. \end{cases} \tag{6.63}$$

This is the distribution function of the signed distance in the B-metric from a test point to the boundary of Ξ, which has negative sign if the test point is in Ξ. Note that the negative branch of Formula (6.63) uses $|r|B$, not $|r|\check{B}$ as might be expected; see van Lieshout (1999).

Analogous functions can be defined by replacing $\oplus$ and $\ominus$ by opening $\circ$ and closing $\bullet$; see van Lieshout (1999). The counterpart of the extended $F_B(r)$ is there called '*size distribution function*'. Sivakumar and Goutsias (1999) and Goutsias and Batman (2000) discuss a discrete analogue of the corresponding probability density function, called *size density*, defined in Formula (6.143) , which is a valuable tool in practical image analysis; see for example Asano *et al.* (2003), Fletcher and Evans (2005) and Land and Wilkison (2009).

Hug *et al.* (2002a) consider random distances from test sets (replacing the test point o above by a compact set) to random sets. Ohser and Schladitz (2009, Section 5.5.1) consider distances from a second set Ψ, which stands for a third constituent in a sample, to Ξ.

The cases of particular practical importance are those of the two extremes: the *linear contact distribution function* $H_l(r)$, in which B is a segment of unit length (in the case of anisotropy the orientation of this segment is of importance; see Section 6.3.5); and the *spherical contact distribution function* $H_s(r)$, in which B is the unit ball (disc) centred at o in the spatial (planar) case. (Note that the empty space function $F_B(r)$ defined in (6.61) often, if not always, employs a spherical B in practice.) Figure 6.2 shows the empirical $H_s(r)$ for the three patterns shown in Figure 6.1. These curves reveal information on the distributional properties of the size of the particles. Also of practical interest is the case of B a square (cube) or a disc in $\mathbb{R}^3$, leading to $H_q(r)$ and $H_d(r)$; see p. 83.

The quantity $1 - H_s(r)$ is the conditional probability that a test point is the centre of a ball of radius r lying completely outside Ξ, given that the test point in question does not belong to Ξ. Thus the spherical contact distribution function $H_s(r)$ is also referred to as 'the law of first contact'. It can be seen also as the distribution function of the Euclidean distance from o to Ξ,

$$H_s(r) = \mathbf{P}(d(o, \Xi) \leq r | \, o \notin \Xi) \qquad \text{for } r \geq 0. \tag{6.64}$$

In the isotropic case and if Ξ has a sufficiently smooth boundary, the spherical contact distribution function is related to the specific surface area by

$$S_V^{(d)} = (1 - p)H_s'(0+), \tag{6.65}$$

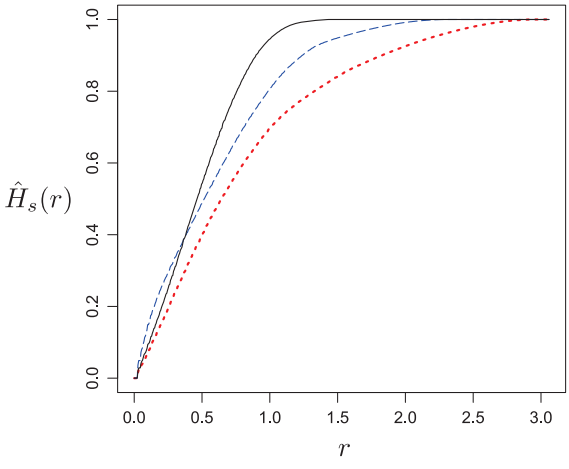

Figure 6.2 Forms of the spherical contact distribution function $H_s(r)$ for the three random set realisations (key: — (a); - - - (b); $\cdots$ (c)) of Figure 6.1. The form of $H_s(r)$ allows conclusions to be drawn concerning the distributional properties of the corresponding random sets. Because of the nearly uniform distribution of the grain positions in (a) the distances between test points and the random set are particularly small, while in (c) large distances are possible. See also Figures 6.1 and 6.4.

see Last and Schassberger (1998) and Hug *et al.* (2002a). Kiderlen and Rataj (2006) showed what happens for general B and stationary Ξ. They used a general theory to explain the Formulae (6.65) and (6.48). Ballani (2006b, 2011) studied two-point spherical contact distribution functions (where the condition '$o \notin \Xi$' is replaced by '$x_1 \notin \Xi, x_2 \notin \Xi$' and two radii r_1 and r_2 appear) and showed that the partial derivatives with respect to r_1 and r_2 are related to the second-order product density of the corresponding surface measure.

The second derivative $H_s''(0+)$ is related to a random geometrical signed measure as shown by Last and Schassberger (2001).

The survey Hug *et al.* (2002a) contains formulae for contact distributions for many random set models, and it considers also the nonstationary case, while Last and Holtmann (1999) give formulae for $H_s(r)$ for various germ–grain models.

The contact distributions introduced above characterise primarily the complement of the random set Ξ of interest: the scaled structuring element rB is placed outside of Ξ. Therefore, the contact distributions could be called 'outer' contact distributions. Of course, analogously, 'inner' contact distributions can be defined by using $(\Xi^c)^{cl}$, the closure of the complement of Ξ.

Rataj (1993) suggests a rather general approach to contact distances and their estimation including edge-corrections. There it is shown that distributions of contact distances cannot be derived from the finite-order characteristics of the corresponding random set. If the set is observable only within a compact window, then the observed contact distances are censored; see Rataj (1993) for relevant mathematical models.

Other summarising functional characteristics of random closed sets are the granulometry functions and functions constructed by opening and closing; see Matheron (1975) and Ripley (1988).

6.3.4 Chord length distributions

While Section 1.7.3 considers chords through convex compact sets, this section studies chords through stationary random sets. These are generated by intersecting the random set Ξ of interest by a directed line $\boldsymbol{g}$. The result is an alternating sequence of random chords inside and outside of Ξ. As for the contact distributions, the chords outside of Ξ are considered in the following. The complementary theory can be simply obtained by interchanging the rôles of Ξ and its complement.

The linear contact distribution function $H_l(r)$ characterises the distribution of chord lengths of the complement of Ξ. In fact, $H_l(r)$ is the distribution function of residual chord length in the direction of a test line segment which begins at a fixed point o, under the condition that o does not belong to Ξ. This is illustrated in Figure 6.3.

This interpretation must be considered in the light of the difference between 'length-biased' and 'unbiased' sampling of chord lengths. For suppose that $\boldsymbol{g}$ is a directed line containing the test segment and consider as on p. 220 the stationary point process $\boldsymbol{g} \cap \partial\Xi$. One may consider $\boldsymbol{g} \cap \partial\Xi$ to be a point process on $\mathbb{R}$ and assume that its intensity is finite. Then from $\boldsymbol{g} \cap \partial\Xi$ one may construct a marked point process $\{[x_n; r_n]\}$. Here $\{x_n\}$ is the sequence of right endpoints of chords in Ξ and r_n is the length of the chord outside of Ξ whose right endpoint is x_n. The corresponding mark distribution function $L(r)$ is the length distribution function of the typical chord of the complement of Ξ, selected in a fashion corresponding to the Palm distribution of the marked point process $\{[x_n; r_n]\}$, which is not length-biased. The distribution functions $L(r)$ and $H_l(r)$ are linked by

$$H_l(r) = \frac{1}{m_L} \int_0^r \big(1 - L(x)\big)\, \mathrm{d}x, \tag{6.66}$$

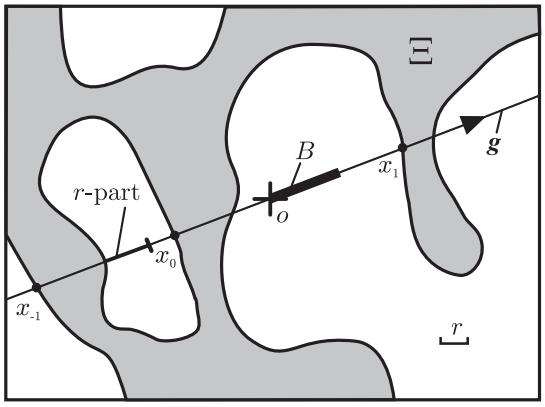

Figure 6.3 Intersection of a closed random set Ξ (shown in grey) and a line $\boldsymbol{g}$ (the direction of the line being defined by a structuring element B that is a segment). The right endpoints of the chords outside of Ξ $\ldots, x_{-1}, x_0, x_1, \ldots$ form a point process. The r-part of a chord is the set of all points of distance more than r from the right endpoint. The symbol $+$ indicates the location of the origin o.

where m_L is the mean typical chord length

$$m_L = \int_0^\infty x \, \mathrm{d}L(x) \tag{6.67}$$

with $0 < m_L < \infty$.

Proof of Formula (6.66). First, note that the marked point $[x_n; r_n]$ corresponds to a chord of length r_n with right endpoint x_n. For a chord $[x_n; r_n]$ of length greater than r let the 'r-part' be the subset of points in the chord further than r from the right endpoint. Thus the r-part has length $\max\{0, r_n - r\}$; see Figure 6.3. Then $1 - H_l(r)$ is the conditional probability that o lies in an r-part, given that o does not lie in Ξ. Hence $1 - H_l(r)$ is the quotient of $L_L(r)$ (the length fraction of the union of all r-parts) by L_L. If λ is the intensity of the process $\{x_n\}$ of right endpoints then

$$L_L = \lambda m_L$$

and

$$L_L(r) = \lambda \int_r^\infty (x - r) \, \mathrm{d}L(x),$$

so

$$1 - H_l(r) = \frac{L_L(r)}{L_L} = \frac{1}{m_L} \int_r^\infty (x - r) \, \mathrm{d}L(x),$$

and Formula (6.66) follows by integration by parts. □

Up to this point attention has focused on chords lying outside of Ξ. As mentioned above, if Ξ has positive volume fraction p, then also chords inside of Ξ make sense. These can be analysed as above simply by exchanging the rôles of Ξ and $(\Xi^{\mathrm{c}})^{\mathrm{cl}}$.

Chords outside of Ξ also make sense if Ξ consists of fragments of curves ($d = 2$) or of surfaces ($d = 3$). Last and Schassberger (1996) express $H_l(r)$ in terms of the Palm distribution of the fibre (or surface) process of the boundary of Ξ.

By means of the stereological Formulae (8.37) and (10.3) it is easy to show that the mean chord length m_L satisfies

$$m_L = \frac{\pi(1 - A_A)}{L_A} \qquad \text{if } d = 2, \tag{6.68}$$

and

$$m_L = \frac{4(1 - V_V)}{S_V} \qquad \text{if } d = 3. \tag{6.69}$$

If Ξ is a Boolean model of convex grains, or a semi-Markovian random set in the sense of Matheron (1975), then the chords of the complement of Ξ have an exponential distribution. In the case of a Boolean model this is a consequence of Formulae (6.66) and (3.58).

6.3.5 Directional analysis of random closed sets

Anisotropy is exhibited by many patterns that may be modelled as random closed sets. Such anisotropy can be quantified by analysis of $C(\mathbf{r})$ and $H_l(r)$, by means of varying the direction of $\mathbf{r}$ and of the linear segment used in the definition of the linear contact distribution. Figure 6.4(a) shows a planar pattern exhibiting clear anisotropy, and Figures 6.4(b) and (c) show $C(\mathbf{r})$ and $H_l(r)$ measured for $(\Xi^c)^{cl}$ in two perpendicular directions. One direction is parallel to the bottom line of Figure 6.4(a), the other perpendicular. The differences resulting from anisotropy are readily observed. Other techniques for studying the anisotropy of random sets are presented in Weil (1988), Stoyan and Beneš (1991) and Molchanov *et al.* (1993). In the second paper the case of germ–grain models is considered.

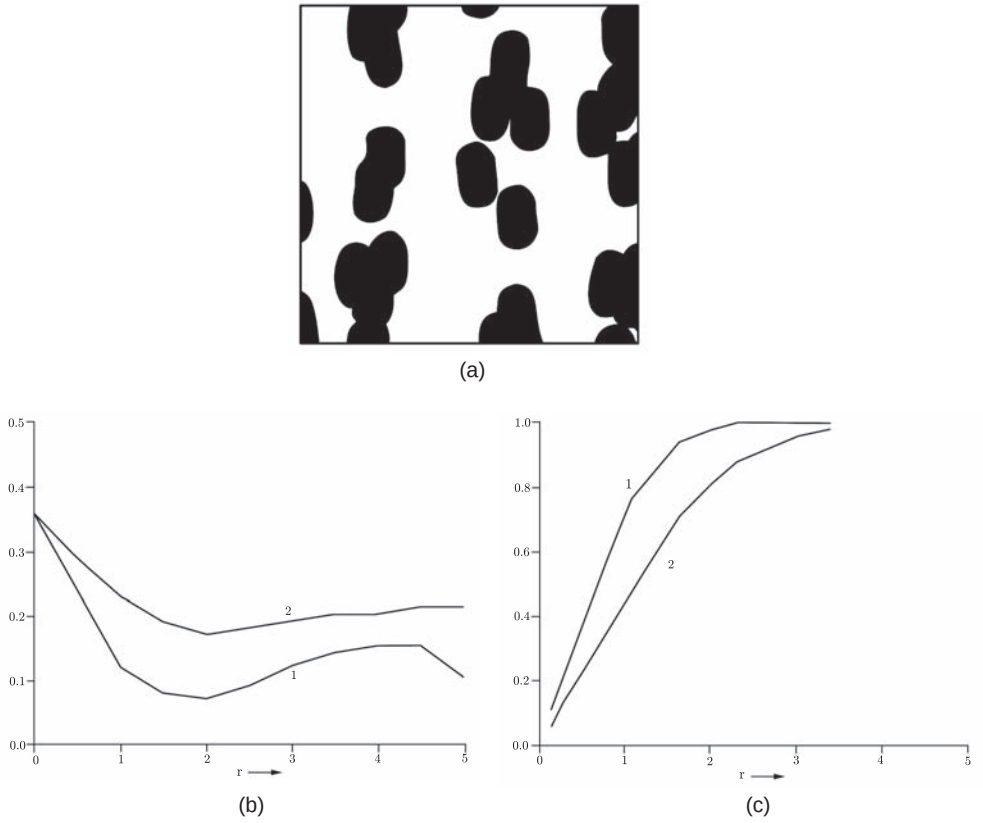

Figure 6.4 (a) An anisotropic area pattern. (b) Estimate of $C(\mathbf{r})$ for two directions (vertically and horizontally). (c) Estimate of $H_l(r)$ for the complement $(\Xi^c)^{cl}$ using the same directions as in (b). Horizontal direction ($\rightarrow$), curves 1; vertical direction $\uparrow$, curves 2.

In the context of surface processes, Section 8.5 provides methods for the statistical analysis of the distribution of surface normals of random closed sets.

6.3.6 Intensities or densities of random closed sets

A given random closed set Ξ is associated with various random measures. One example is the *volume measure* V_Ξ, which is defined by

$$V_\Xi(B) = \nu_d(B \cap \Xi) \qquad \text{for } B \text{ a bounded Borel set.}$$

Other examples include the *curvature measures* discussed in Section 7.3.4.

If such an associated random measure μ_Ξ is stationary then it has an *intensity* $\lambda(\mu_\Xi)$. When $\lambda(\mu_\Xi)$ is finite and positive it is an instructive characteristic of Ξ. The *specific surface* $S_V^{(d)}$ arises in this fashion as the mean surface area of Ξ per unit volume. If $S_V^{(d)}$ is to be well-defined then either assumptions on the smoothness of $\partial\Xi$ must be imposed or the notion of surface area must be modified. Zähle (1982, 1983) discussed suitable modifications of surface area for random closed sets.

Another approach to define densities is via the ergodic theorem. Let h be an additive translation-invariant functional on the Borel sets or on some subsystem of the Borel sets. Suppose that the limit

$$\overline{h}(\Xi) = \lim_{n\to\infty} \frac{\mathbf{E}\big(h(\Xi \cap W_n)\big)}{\nu_d(W_n)} \tag{6.70}$$

exists (c.f. Theorem 6.2 on p. 210) for all convex averaging sequences $\{W_n\}$. Then $\overline{h}(\Xi)$ is said to be the *h-density* of Ξ; see Schneider and Weil (2008, Section 9.2).

In particular, if $h(\cdot)$ is the k^{th} intrinsic volume $V_k(\cdot)$, its density v_k, defined as

$$v_k = \lim_{n\to\infty} \frac{\mathbf{E}\big(V_k(\Xi \cap W_n)\big)}{\nu_d(W_n)}, \tag{6.71}$$

is the *specific k^{th} intrinsic volume*, which is the intensity of the corresponding signed curvature measure; see Section 7.3.4.

Last but not least, the *morphological functions* of K. Mecke must be mentioned here; see Mecke (2000) and p. 84 for application in the context of Boolean model. These functions provide a very powerful tool for the statistical description of random sets. (Note that K. Mecke speaks in his papers not about 'morphological functions' but of 'Minkowski functionals'.) The idea is simple and natural, explained here for the three-dimensional case: Consider the dilated random set $\Xi \oplus B(o, r)$ and determine the corresponding densities of intrinsic volumes as functions of the dilation radius r. In the case of volume density or volume fraction, the morphological function is nothing else than the empty space function; in the case of specific surface area it has a close relation to the probability density function of the spherical contact distribution. However, analogous functions related to integral of mean curvature and Euler–Poincaré number yield additional information. The last one, related to the specific connectivity number, is particularly informative. It is also quite useful to show all four functions (of r) in parallel (similarly as in Figure 6.6) and to compare them; see Mecke (2000) and Arns *et al.* (2002).

6.4 Nonparametric statistics for stationary random closed sets

6.4.1 Introduction

This section presents nonparametric methods for the estimation of p, $C(r)$ and $H_B(r)$, and discusses the problem of determining the accuracy of estimation for p. The data are given in an observation window W. Throughout the section the random closed set Ξ under consideration is assumed to be stationary and, in most cases, isotropic. Statistical methods for the particular case of germ–grain models, excursion sets and birth-and-growth models are discussed in Sections 6.5.7, 6.6.3 and 6.6.4, respectively.

Many of the estimators presented are in fact estimators of the capacity functional $T_\Xi(K)$ for special K. If edge-effects are ignored, in the stationary case $T_\Xi(K)$ can be estimated by means of a grid G of n lattice points u by

$$\hat{T}_\Xi(K) = \frac{1}{n} \sum_{u \in G} \mathbf{1}(\Xi \cap K + u \neq \emptyset). \tag{6.72}$$

If the random set Ξ is not stationary, $T_\Xi(K)$ can be estimated from n independent samples $\{\Xi_i\}$ of Ξ:

$$\hat{T}_\Xi(K) = \frac{1}{n} \sum_{i=1}^{n} \mathbf{1}(\Xi_i \cap K \neq \emptyset). \tag{6.73}$$

Little is known of the theoretical properties of the estimators given. If Ξ is ergodic then many of them are consistent for increasing windows. Under certain mixing conditions some of the estimators can be shown to be asymptotically normal.

6.4.2 Estimation of the area or volume fraction p

The methods described here are based on sampling Ξ in the fixed bounded window W of observation by a finite grid of isolated points, a system of parallel lines or planes, or the whole W. The isotropy property is not required for their application.

The point-count method (Thompson, 1930; Glagolev, 1933)

A grid of points $x_1, \ldots, x_n$ in W is used and p is estimated by

$$\hat{p}_p = \frac{1}{n} \left(\sum_{i=1}^{n} \mathbf{1}_\Xi(x_i) \right), \tag{6.74}$$

the fraction of grid points lying in Ξ. This estimator is today frequently applied in image analysis, where the grid points are the centre points of the pixels. (One speaks about 'Gauss digitisation', see e.g. Ohser and Schladitz, 2009.)

The estimator $\hat{p}_p$ is unbiased since

$$\mathbf{E}(\hat{p}_p) = \frac{1}{n} \sum_{i=1}^{n} \mathbf{E}\big(\mathbf{1}_\Xi(x_i)\big) = \frac{1}{n}\, np = p. \tag{6.75}$$

Its variance σ_p^2 is given by

$$\sigma_p^2 = \frac{1}{n^2}\mathbf{E}\left(np - \sum_{i=1}^{n} \mathbf{1}_\Xi(x_i)\right)^2 = \frac{1}{n^2}\left(np(1-p) + 2\sum_{i>j} k(r_{ij})\right), \tag{6.76}$$

where $r_{ij} = \|x_i - x_j\|$ and $k(r)$ is the covariance function of Ξ. Formula (6.76) follows from expanding the square

$$\left(np - \sum_{i=1}^{n} \mathbf{1}_\Xi(x_i)\right)^2 = \left(\sum_{i=1}^{n}\big(p - \mathbf{1}_\Xi(x_i)\big)\right)^2.$$

The variance formula (6.76) depends both on the grid geometry and the form of the covariance function $k(r)$. If $k(r)$ decays to zero quickly then approximations are available. A very simple example is

$$\sigma_p^2 \approx \frac{p(1-p)}{n}. \tag{6.77}$$

This would be the exact variance were the indicators $\mathbf{1}_\Xi(x_i)$ independent. Many authors have studied point-count methods; see, for example, Matérn (1986) and Diggle and ter Braak (1982). Also random sampling points are used; if the covariance function $k(r)$ is decreasing then, for fixed n, the estimation variance is greater than for the grid case.

Example 6.1. *Approximation of estimation variance for the point-count method in the planar case*
Suppose the grid is quadratic of mesh width Δ and the covariance function $k(r)$ is of exponential form with $\alpha\Delta \gg 1$. Neglecting edge-effects and only considering up to second-nearest neighbours in the grid lead to

$$\sum_{i \neq j} k(r_{ij}) = 4np(1-p)\exp(-\alpha\Delta)\big(1 + \exp(-(\sqrt{2}-1)\alpha\Delta)\big),$$

and thus

$$\sigma_p^2 \approx \frac{1}{n}p\Big((1-p) + 8(1-p)\exp(-\alpha\Delta)\big(1 + \exp(-(\sqrt{2}-1)\alpha\Delta)\big)\Big). \tag{6.78}$$

The lineal method (Rosiwal, 1898)

An array of N parallel line segments, each of length l, is placed in the window W of observation. The volume fraction p is estimated by

$$\hat{p}_l = \frac{L}{Nl}, \tag{6.79}$$

where L is the (random) total length of line segments intersecting Ξ. As for the point-count method, this estimator is unbiased. Its accuracy has been studied in Stoyan (1979b) and Stoyan and Steyer (1979) for the planar case, with reference also to the interline distance. The particular models used in these studies were either of exponential covariance (6.51) or

formed by a Boolean model of spherical grains. In the case of exponential covariance with large α the estimation variance σ_l^2 of $\hat{p}_l$ is approximately

$$\sigma_l^2 \simeq \frac{2p(1-p)\left(1-\dfrac{1}{\alpha l}\right)}{N\alpha l}. \tag{6.80}$$

In the case of a planar sample of a motion-invariant three-dimensional set, σ_l^2 can be expressed in terms of V_V and S_V approximately by

$$\sigma_l^2 \simeq \frac{8V_V^2(1-V_V)^2}{NlS_V}, \tag{6.81}$$

using (6.54). It should be noted that in case of anisotropy the lineal method, based on parallel lines in a fixed orientation, may be affected adversely by the relationship between axes of anisotropy and the common direction of the sampling lines.

The density method

The volume fraction p is estimated in the spirit of volume measure density by the *empirical volume fraction*

$$\hat{p}_v = \frac{\nu_d(\Xi \cap W)}{\nu_d(W)}. \tag{6.82}$$

Measurement errors occur only through the bounded nature of the window, if pixelisation errors are ignored. The estimation variance σ_v^2 is given by

$$\sigma_v^2 = \mathbf{E}\big((\hat{p}_v - p)^2\big) = \frac{1}{\nu_d(W)^2}\int_W \int_W k(\|x-y\|)\,\mathrm{d}x\,\mathrm{d}y. \tag{6.83}$$

The domain of integration in the variance is W, meaning that the variance depends on the shape and size of the window W of observation. If the window is suitably large (in the sense of extending far in all directions, as for example in the case of a ball or disc of large radius) then an approximate formula is available:

$$\sigma_v^2 \simeq \frac{p(1-p)a_V}{\nu_d(W)}, \tag{6.84}$$

where a_V is the integral range defined in (6.47). In the particular case of an exponential covariance given in (6.51) with parameter α the variance becomes

$$\sigma_v^2 \simeq \frac{d!\,b_d\,p(1-p)}{\alpha^d\,\nu_d(W)}, \tag{6.85}$$

see Ohser and Mücklich (2000, Section 5.1) and Kanit *et al.* (2003). Use of Formula (6.54) leads in the three-dimensional case to

$$\sigma_v^2 \simeq \frac{512V_V^4(1-V_V)^4}{S_V^3\nu_d(W)}. \tag{6.86}$$

The formulae given here can also be applied in the context of image analysis if the pixel size is very small in comparison to the details of the random set Ξ investigated.

Heinrich (2005) presents a rigorous study of the limit behaviour of the empirical volume fraction for large windows W.

Example 6.2. *Comparison of estimation variances of the point-count, lineal, and density methods in the planar case*
To illustrate the methods discussed above, consider a random closed set of exponential covariance with $\alpha = 5\,\mathrm{m}^{-1}$, observed through a square sampling window W of dimension $30 \times 30\,\mathrm{m}^2$. For the point-count method a square grid is used with $31 \times 31 = 961$ points with mesh width $\Delta = 1\,\mathrm{m}$. For the lineal method 31 parallel lines (parallel also to a window side) are employed, each of length 30 m and with separation distance 1 m.

In the case of area fraction $p = 0.10$ Formulae (6.78), (6.80) and (6.85) yield the following approximate estimation variances, as compared with exact values given in parentheses, obtained by numerical integration:

$$\sigma_p^2 = 0.010 \quad (0.0098),$$
$$\sigma_l^2 = 0.006 \quad (0.0059),$$
$$\sigma_v^2 = 0.005 \quad (0.0046).$$

It is typical that the approximations have small positive biases.

In this case, greater use of information contained in the window is rewarded by lower estimation variance. However, this is not always so; see the interesting discussion in Baddeley and Cruz-Orive (1995).

6.4.3 Estimation of the covariance

Using Formula (6.40) the covariance $C(\mathbf{r})$ can be estimated as the volume fraction of the set $\Xi \ominus \{o, \mathbf{r}\}$. Under the assumption of isotropy the same estimator can be used for $C(r)$ with $\|\mathbf{r}\| = r$. For lattice data this is equivalent to

$$\hat{C}(r) = \frac{\sum_{i=1}^{n-1} \sum_{j=i+1}^{n} \mathbf{1}_\Xi(x_i)\mathbf{1}_\Xi(x_j)\mathbf{1}(\|x_i - x_j\| = r)}{\sum_{i=1}^{n-1} \sum_{j=i+1}^{n} \mathbf{1}_\Xi(x_i)\mathbf{1}_\Xi(x_j)}, \tag{6.87}$$

where x_i and x_j are lattice points of a finite grid. (Of course, the denominator must be positive.) For large samples, which are typical for materials research and physics, Fourier methods are recommended; see Ohser and Schladitz (2009, Chapter 6).

If normalised forms of the covariance are estimated and the sampling window is small, it makes sense to use distance-adapted estimators $\hat{p}(r)$ of p. This was shown in Mattfeldt and Stoyan (2000) for the pair correlation function $g(r) = C(r)/p^2$. In this case it is then natural to use the adapted $\hat{p}(r)$ resulting from the same reduced window from which $C(r)$ is estimated.

6.4.4 Second-order analysis with random fields

The analysis of the spatial variability of random sets should not be limited to analysis of the covariance $C(r)$, which is related to the volume measure; see Section 7.3.4. Arns *et al.* (2005) demonstrate an approach which includes also the other curvature measures $\Phi_{\Xi,k}$ explained in Section 7.3.4.

The idea is to construct for a given random set Ξ random fields $\{Z_k(x)\}$, called the *intrinsic volume fields*, for $k = 0, 1, \ldots, d$ by

$$Z_k(x) = \Phi_{\Xi,k}\big(B(x, R)\big) \qquad \text{for } x \in \mathbb{R}^d, \tag{6.88}$$

that is, the value $Z_k(x)$ is given by the value of the k^{th} curvature measure Φ_k corresponding to Ξ for the ball $B(x, R)$ of radius R centred at x. Here the radius R is a procedure parameter controlling the smoothness of the field. For example, $Z_d(x) = \nu_d\big(\Xi \cap B(x, R)\big)$ and if $d = 3$ and $k = 2$ then $Z_2(x)$ is the half surface area content of Ξ in $B(x, R)$ (where the surface of the ball $B(x, R)$ is excluded), and its mean is $\frac{1}{2}S_V \cdot \frac{4}{3}\pi R^3$.

These random fields can be constructed numerically and analysed statistically by methods of geostatistics, that is, by statistical methods for random fields. This is explained in Arns *et al.* (2005) for samples of foams and sandstone. Figure 6.5 shows a ($1.4\,\text{mm}^3$) sample of Fontainebleau sandstone of porosity 13% and the corresponding empirical covariance $C(r)$.

Figure 6.6 shows the empirical normalised variograms of the corresponding random fields. Recall that for a random field $Z_k(x)$ the variogram $\gamma_k(r)$ is given by

$$\gamma_k(r) = \frac{1}{2}\,\mathbf{E}\left(\big(Z_k(o) - Z_k(\mathbf{r})\big)^2\right). \tag{6.89}$$

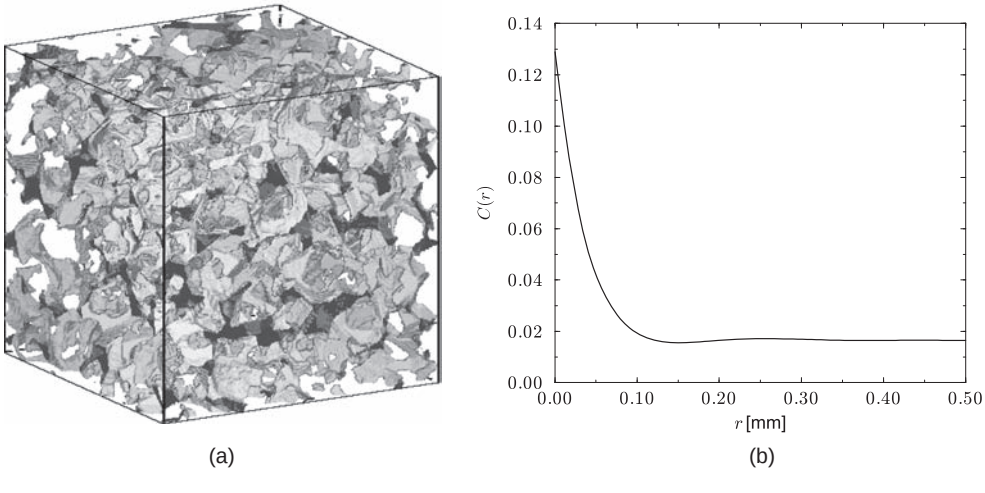

Figure 6.5 (a) A ($1.4\,\text{mm}^3$) sample of Fontainebleau sandstone of porosity 13%, and (b) the corresponding empirical covariance $C(r)$ of the pore space. Reproduced from Arns *et al.* (2005) with permission of Springer.

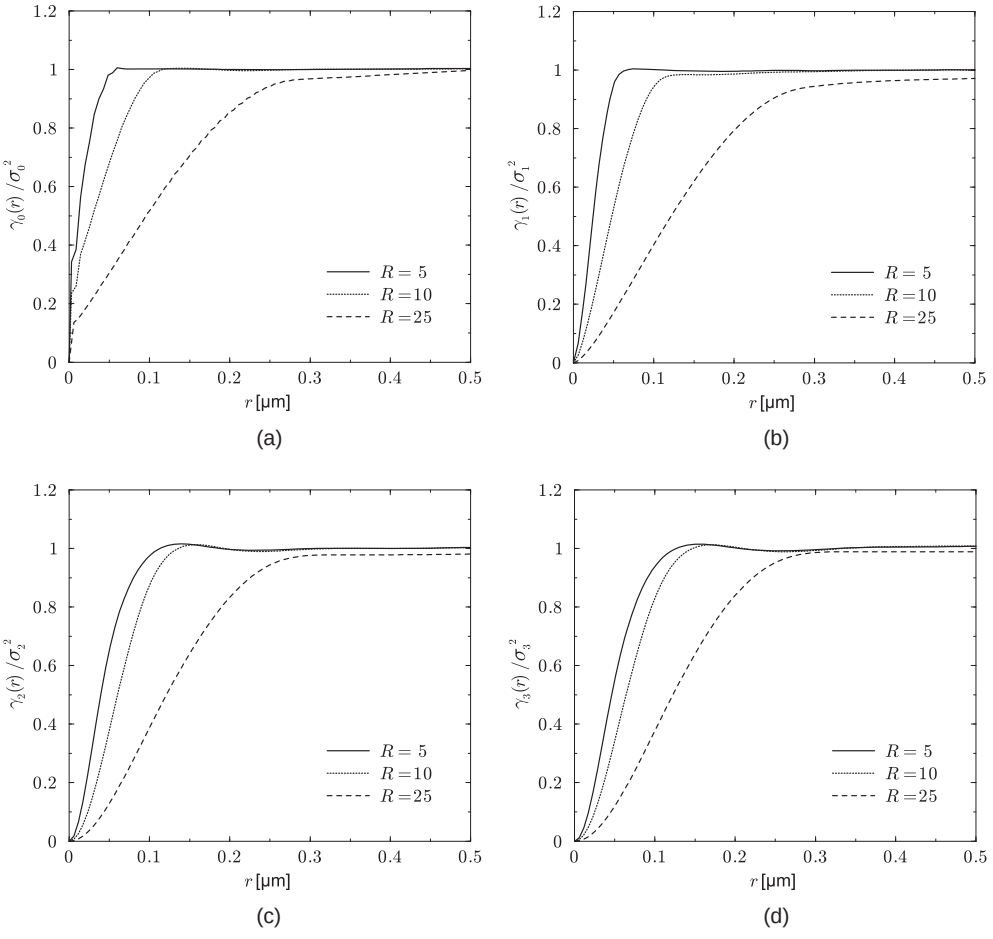

Figure 6.6 Normalised variograms $\gamma_k(r)/\sigma_k^2$ of the intrinsic volume fields for the Fontainebleau sandstone. (a) Euler–Poincaré characteristic, (b) integral of mean curvature, (c) surface area, and (d) volume. Reproduced from Arns *et al.* (2005) with permission of Springer.

(Because of the factor $\frac{1}{2}$, some authors call $\gamma_k(r)$ the *semi-variogram*.) It is natural to normalise it by the variance σ_k^2 of $Z_k(o)$. The (normalised) variograms show that the variability of volume and surface distribution are similar and higher than that of integral of mean curvature and Euler–Poincaré characteristic. The variogram $\gamma_3(r)$, as an alternative to $C(r)$, characterises the variability of volume distribution. The range of correlation for volume is about 0.3 mm.

6.4.5 Estimation of contact distributions

Since $\big(1 - H_B(r)\big)(1 - p)$ is the volume fraction of the stationary random set $\Xi \oplus r\check{B}$, methods in Section 6.4.2 are applicable, where B satisfies the conditions on p. 223. The following considers only the case where area or volume measurement is possible. From the definition

of $H_B(r)$ and the minus-sampling estimator (Section 6.5.7) of it is

$$\hat{H}_B(r) = 1 - \frac{1}{1-\hat{p}} \left(1 - \frac{v_d\big((W \ominus r\check{B}) \cap (\Xi \oplus r\check{B})\big)}{v_d(W \ominus r\check{B})} \right) \qquad \text{for } r \geq 0. \tag{6.90}$$

For the particular case of the spherical contact distribution $H_s(r)$, the estimator in (6.90) can be written as

$$\hat{H}_s(r) = 1 - \frac{1}{1-\hat{p}} \left(1 - \frac{v_d\big((W \ominus B(o,r)) \cap (\Xi \oplus B(o,r))\big)}{v_d\big(W \ominus B(o,r)\big)} \right) \qquad \text{for } r \geq 0. \tag{6.91}$$

An estimator of $H_s(r)$ in the spirit of Hanisch's D-estimator (4.124) is

$$\hat{H}_s(r) = 1 - \frac{1}{1-\hat{p}} \left(1 - \int_W \frac{\mathbf{1}\big(x \in W \ominus B(o, d(x))\big)\mathbf{1}(d(x) \leq r)}{v_d\big(W \ominus B(o, d(x))\big)} \, \mathrm{d}x \right) \quad \text{for } r \geq 0. \tag{6.92}$$

Here $d(x) = d(x, \Xi)$ is the Euclidean distance from x to Ξ; if $x \in \Xi$ then $d(x) = 0$. In practical application the integral becomes a sum, which is based on a grid of test points.

If $\hat{p}$ is unbiased then the above estimators of $H_s(r)$ are ratio-unbiased. Mayer (2004) showed how the estimator (6.90) can be efficiently applied.

Hansen *et al.* (1996) and Baddeley and Gill (1997) suggested Kaplan–Meier estimators for $H_B(r)(1-p)$ and the corresponding hazard rate. They argued that the latter is a good characteristic for model choice. Chiu and Stoyan (1998) showed that the ideas behind the Hanisch and Kaplan–Meier estimator are similar.

The distance-adapted $\hat{p}(r)$ mentioned in the previous section can of course be employed also here. However, the simulation in Stoyan *et al.* (2001) suggests that $\hat{p}(r)$ may not be better than the simple estimator $\hat{p}$ for the purposes of estimating $H_B(r)$.

6.4.6 Representative volume elements

A question of great practical importance in the planning of statistical analysis and in calculations of macroscopic properties of structures with random microstructure is the size of the necessary window W of observation or calculation. If this window is too small, edge-effects may play a rôle too great and typical fluctuations of the studied random sets are perhaps overlooked. Using a terminology that first appeared in the context of *homogenisation*, this book speaks of, even in the two-dimensional case, *representative volume elements* (RVEs). The size of the RVE is called *relevant volume* (RV).

In the case of a study of fluid permeability, for example, one takes a sample of the random set representing the porous medium of interest. The flow behaviour in the sample is studied using partial differential equation solvers and the permeability of a homogeneous sample of equal size is determined. If the sample (i.e. observation window W) is small, then edge-effects may play some rôle so that the observed porosity variability cannot be considered as typical. Consequently, the results obtained are not representative. Larger samples deliver estimates which should be (in favourable cases) closer to values that would be obtained for infinitely extended samples, which correspond to the statistically homogeneous case. However, the samples should be kept sufficiently small in order to be considered as volume elements (i.e. differential elements) of the continuum model of the porous medium. The smallest sample that is large enough to guarantee sufficiently small errors is the RVE (Nemat-Nasser and Hori,

1999). That is to say, an RVE and its size RV, which has to be interpreted as a lower bound, depend on a user-prescribed upper bound of statistical error and are only meaningful if this statistical tolerance is given.

The determination of an RVE is, of course, difficult. It depends both on the variability of the random set and on the physical quantity of interest and the summary characteristic being considered (see Freudenthal, 1950, Kanit *et al.*, 2003, Stroeven *et al.*, 2004, and Buryachenko, 2007). If the same summary statistic is considered, random sets with irregularly scattered large components require larger RVEs than random sets with many small and regularly distributed particles. On the other hand, for a fixed microstructure, a larger RVE is required for a precise estimation of the covariance $C(r)$ or spherical contact distribution function $H_s(r)$ than for the estimation of volume fraction p, say.

In classical statistics, sample size calculations require some prior knowledge on the nature of the data that will be analysed, such as their variation. A similar requirement holds in the context of random sets. It is impossible to determine the RVE without any *a priori* knowledge of the distribution of the random set investigated. A straightforward approach for acquiring *a priori* knowledge is a *pilot study* consisting of a preliminary statistical analysis of a small window (or a small number of windows if a series of windows have to be analysed). The expectation is that the pilot study yields a useful yet rough estimate of volume fraction p and some rough information on $C(r)$, perhaps the range of correlation.

If volume fraction p is of interest, the formulae in Section 6.4.2 may be used. In particular Formula (6.84) yields an approximation of RV for a prescribed precision σ_v^2 of the p-estimator. There the integral range plays an important rôle.

For other characteristics either (a) statistical experiments or (b) reconstruction simulations may be used for the determination of RVEs. Method (a) assumes that it is possible to generate a series of nested windows of increasing size. The summary characteristics of interest are estimated from them in order to identify the minimum window size that can be considered representative, such that any further increase of the window size will essentially not change the statistical results further. Method (b) generates random set samples larger than the original pattern by the reconstruction simulation method described in Section 6.7, under the assumption that the pattern given in the single original observation window shows the typical process behaviour. Subsequently method (a) can be applied to the simulated patterns.

Two papers in which RVEs are thoroughly discussed from a statistical standpoint are Kanit *et al.* (2003) and Stroeven *et al.* (2004). The first paper considers as an example two-phase Voronoi tessellations (where the cells are coloured randomly black and white), the second one focuses on granular materials, that is, special germ–grain models.

6.5 Germ–grain models

6.5.1 Basic facts

In a natural generalisation of the Boolean model, (a) the Poisson point process of germs is replaced by a general point process and (b) the grains are permitted to be dependent. This leads to the class of *germ–grain models*. In particular, the generalisation allows for treatment of collections of non-overlapping grains, since independence between germ and grains, as in the Boolean model, may lead to overlapping of grains.

A formal definition starts with a marked point process $\Psi = \{[x_n; \Xi_n]\}$ where the points x_n lie in $\mathbb{R}^d$ and the marks Ξ_n are compact subsets of $\mathbb{R}^d$. A *germ–grain model* Ξ as defined by Hanisch (1981) arises from such a marked point process as the union

$$\Xi = \bigcup_{n=1}^{\infty} (\Xi_n + x_n) = (\Xi_1 + x_1) \cup (\Xi_2 + x_2) \cup \cdots . \tag{6.93}$$

The points x_n are the *germs* and the compact sets Ξ_n are the *grains* of the germ–grain model. Sometimes, Ψ is called a *germ–grain process* (Schneider and Weil, 2008), while Hall (1988) calls $\{\Xi_n + x_n\}$ a *coverage process*.

In the case when Ψ and Ξ are stationary it is useful to introduce the notion of the typical grain Ξ_0, which is a random compact set having the same distribution as the marks of the marked point process Ψ. It is a distribution on the space $\mathbb{K}$ of compact sets endowed with the σ-algebra $\mathcal{F}_{\mathbb{K}}$, the trace of $\mathcal{F}$ on $\mathbb{K}$. There may exist dependences between the grains, as well as between grains and germs. The intensity of the stationary germ process is denoted by λ.

Note that rotating the random set Ξ is not the same as rotating the germ–grain process Ψ, because for the latter, which is a marked point process, the rotation applies only to the germs (points) but not to the grains (marks); see p. 118. Thus, when speaking about rotation and isotropy, one has to be careful.

Every random closed set can be trivially decomposed to become a germ–grain model. Weil and Wieacker (1987) (see also Schneider and Weil, 2008, Section 4.3) provide a meaningful decomposition by showing that for every random closed set Ξ in $\mathbb{R}^d$, there is a point process in $\mathbb{F}$ such that the union of its 'points' (which are closed sets in $\mathbb{R}^d$) is equal to Ξ in such a way that invariance properties under rigid motion (e.g. stationarity and isotropy) of Ξ in $\mathbb{R}^d$ are preserved in the corresponding point process in $\mathbb{F}$. Moreover, if Ξ is a random $\mathbb{S}$-set satisfying a local finiteness condition (see Schneider and Weil, 2008, p. 119), then the corresponding point process takes place in $C(\mathbb{K})$ so that the 'points' are in this case convex bodies. Thus random $\mathbb{S}$-sets are essentially the same as germ–grain models with convex grains.

Random $\mathbb{S}$-sets Ξ have boundaries that are smooth enough for the definition of random curvature measures as in Chapter 7. These are examples of random measures accompanying Ξ, as described in Section 7.3.4. When Ξ is stationary then so are the random curvature measures.

6.5.2 Formulae for p and $C(r)$

Explicit formulae for general germ–grain models are complicated. The capacity functional T_Ξ can be expressed in terms of the generating functional G_Ψ of the marked point process Ψ,

$$T_\Xi(K) = \mathbf{P}(\Xi \cap K \neq \emptyset) = 1 - G_\Psi(v_K), \tag{6.94}$$

where K is compact and

$$v_K(x, C) = 1 - \mathbf{1}_{\check{C} \oplus K}(x) \qquad \text{for compact } C \text{ and } x \in \mathbb{R}^d. \tag{6.95}$$

The left-hand side of Formula (6.94) can be expressed in terms of the germ process $\{x_n\}$, denoted by Φ, and the capacity functional T_{Ξ_0} of the typical grain Ξ_0 so that it can be

rewritten as

$$T_{\Xi}(K) = 1 - \mathbf{E} \prod_{x \in \Phi} \big(1 - T_{\Xi_0}(K - x)\big). \tag{6.96}$$

When the grains are non-overlapping, which is to say when

$$(\Xi_i + x_i) \cap (\Xi_j + x_j) = \emptyset \qquad \text{for all } i \neq j$$

with probability one, and when, moreover, Ξ is stationary, then the volume fraction is given by

$$p = \lambda \overline{V}, \tag{6.97}$$

where $\overline{V} = \mathbf{E}\big(v_d(\Xi_0)\big)$ is the mean volume of the typical grain Ξ_0. Hall (1988, Section 3.8) gives bounds for p for the case of independent grains and Cox and Neyman–Scott germ processes.

In the case of non-overlapping grains and stationarity the intensities v_k of the intrinsic volume measures satisfy the analogous formula

$$v_k = \lambda \overline{V}_k, \tag{6.98}$$

where $\overline{V}_k = \mathbf{E}\big(V_k(\Xi_0)\big)$ is the mean of the k^{th} intrinsic volume of the typical grain Ξ_0, and the covariance $C(r)$ is the sum of two terms

$$C(r) = C_1(r) + C_2(r), \tag{6.99}$$

where the first term is the probability that the origin o and the second point $\mathbf{r}$, any point of $\mathbb{R}^d$ with $\|\mathbf{r}\| = r$, belong to the same grain, and the second term the probability that these two points belong to different grains. When the non-overlapping grains are independent, isotropic and convex with positive volume, (6.99) can be expressed as

$$C(r) = \lambda \overline{\gamma}_{\Xi_0}(r) + \int_{\mathbb{R}^d} \int_{\mathbb{R}^d} \mathbf{1}_{\Xi_0}(x) p_{\Xi_0}(x - \mathbf{r} + z) \varrho^{(2)}(z) \, \mathrm{d}x \, \mathrm{d}z, \tag{6.100}$$

where $\overline{\gamma}_{\Xi_0}(r)$ is the isotropised set covariance of the typical grain Ξ_0 and $p_{\Xi_0}(x)$ its coverage function. Furthermore, λ and $\varrho^{(2)}(r)$ are the intensity and second-order product intensity of the (motion-invariant) germ-process; see Hanisch (1984a,b).

Torquato (1991) discusses the form (6.99) of $C(r)$, which is also useful for interpreting empirical covariances. He calls $C_1(r)$ 'two-point cluster function' and $C_2(r)$ 'two-point blocking function'.

6.5.3 Models of mutually non-overlapping balls

Models of random systems of mutually non-overlapping balls are of great practical interest in biology, physics and materials science. The following discusses briefly some models for such structures. The text starts with models of larger density, which are of great practical interest but mathematically difficult to analyse.

The RSA model

RSA is an abbreviation for 'random sequential adsorption' (or 'addition'), a term used in physics and chemistry. The RSA model is also termed SSI model in the statistical literature, an abbreviation of 'simple sequential inhibition'. Since the model is used much more frequently in physics and chemistry than in statistics, the name RSA is used here. Evans (1993) and Talbot *et al.* (2000) are key references.

The RSA model yields a process taking place in a finite region W and is hence a model for a structure composed of finitely many balls. The pattern is constructed by iteratively and randomly placing centres of balls into W with radii following some distribution function. Once a ball is successfully placed, its position is permanently fixed. If a new ball intersects with an already existing ball, the new ball is rejected and another ball with a different centre and perhaps a new radius (or just the same radius) is generated, and so on. There is, furthermore, a model abbreviated CSA, meaning 'cooperative sequential adsorption' (Talbot *et al.*, 2000), where the probability of adsorption of a new ball is proportional to a Boltzmann factor involving interaction between the new ball and the pre-adsorbed balls.

Once it is impossible to place any new ball (then the 'jamming' state is attained) in W the process stops. The pattern formed by the balls is a sample of the random set to be generated.

Stoyan and Schlather (2000) discuss a stationary version of the model. In the case of random radii, the (proposal) distribution used to generate radii of new balls and the (resulting) distribution of the radii of adsorbed balls have to be distinguished, because larger balls are less likely than smaller balls to be adsorbed.

All numerical information for the RSA model (Evans, 1993) has been obtained by simulation, for sufficiently large W such that one could speak about 'stationary case'. The RSA model is simulated along the lines of the model description. For an efficient simulation close to jamming, the search for potential locations for new balls should make use of an efficient search algorithm; see Döge (2001).

The area and volume fraction A_A and V_V for the model with constant radii can be determined by simulation

$$A_A = 0.547 \quad \text{and} \quad V_V = 0.382\,.$$

Statistical methods for the dynamic RSA model are described in van Lieshout (2006). Provatas *et al.* (2000) consider closely related models where the balls are replaced by fibres.

Packings of hard balls

Random close packings of identical balls were already mentioned in Section 5.4. Following Torquato and Stillinger (2010), instead of 'close' this section uses the term 'jammed'. In jammed packings each particle is in contact with its nearest neighbours, whilst in not-jammed packings 'rattlers' (particles not in contact with the rigid cluster, called the backbone, of particles that are jammed) may exist.

Perhaps it is risky to write in a mathematical book about a structure for which to date there is no mathematical model. The great practical importance of random close packings is the reason for this short section; the reader is also referred to the book by Aste and Weaire (2008) and the survey papers Torquato and Stillinger (2010) and Stachurski (2011), the latter of which discusses applications in the theory of amorphous materials. Comparable structures exist in reality, as real random packings of real hard balls (which approximate ideal hard balls) and

have been often experimentally generated since Bernal (1960); see Aste *et al.* (2004, 2005) for more recent reports. Empirical studies by different authors have repeatedly established

(a) volume fraction $V_V = p = 0.64$;

(b) pair correlation function $g(r)$ of the point process of centres as in Figure 4.7.

The following approximation formulae are given for hard ball systems with general volume fraction V_V between 0.5 and 0.7 and radius R. The paper Lochmann *et al.* (2006) shows a sequence of pair correlation functions for different V_V.

Covariance

$$C(r) \approx V_V - \frac{S_V}{4}\, r + \frac{Z V_V}{4} \left(\frac{r}{2R}\right)^2 + O(r^3) \qquad \text{for } r \geq 0, \tag{6.101}$$

where Z is the mean coordination number, that is, the mean number of contacts of the typical ball with other balls; see Torquato (2002, p. 38), who refers to Frisch and Stillinger (1963). In the case of $V_V = 0.64$, for Z the value 6.05 was found for simulated packings (Bezrukov *et al.*, 2002). For experimental packings smaller values were obtained, for example, between 5 and 5.5 (Delaney *et al.*, 2010). From the standpoint of physicists, the simulated structures are such 'in the limit of zero friction'.

Linear contact distribution function

$$H_l(r) \approx 1 - \exp\left(-\frac{3V_V}{4(1-V_V)}\frac{r}{R}\right) \qquad \text{for } r \geq 0, \tag{6.102}$$

see Levitz and Tchoubar (1992), Lu and Torquato (1992) and Stoyan *et al.* (2011).

Density function of spherical contact distribution function

$$h_s(r) \approx \frac{2}{\sqrt{2\pi}\sigma} \exp\left(-\frac{r^2}{2\sigma^2}\right) \qquad \text{for } r \geq 0, \tag{6.103}$$

with

$$\sigma = \frac{(1-V_V)2R}{3\sqrt{2\pi}V_V}, \tag{6.104}$$

see Stoyan *et al.* (2011).

That these summary characteristics are used by various authors shows that the idea of a motion-invariant hard-ball-packed structure is widely accepted, though properly speaking it can refer only to ensembles made up of infinitely many balls.

Such structures have been simulated by various algorithms (differing only in detail), for example the Lubachevsky–Stillinger algorithm (see Donev *et al.*, 2005) and the force-biased algorithm (see Bezrukov *et al.*, 2002, and Illian *et al.*, 2008, p. 395). Simulation studies have often reproduced the results above. This leads the authors to believe that there does exist an

objective mathematical object called 'random jammed packing of hard balls', for which, one day, some genius will propose a mathematical model, which has in some approximation the properties above and will lead to a formula for V_V. Stoyan (1998) *conjectured* that

$$\boxed{V_V = \frac{2}{\pi}}, \tag{6.105}$$

see also Buryachenko (2007, p. 180). Already Scott (1960) gives the value $V_V = 0.6366$, which is very close to $2/\pi$, and it seems to be clear that he, as well as his contemporaries J. D. Bernal and J. L. Finney, believed that the true unknown value is indeed $2/\pi$. (Note that although Song *et al.*, 2008, argue, by interpreting the random jammed packing as the ground state of the ensemble of jammed matter, that the volume fraction V_V cannot exceed 0.634, their value 0.634 is not precise but just an approximate value.) And perhaps one day even a formula for $g(r)$ will be found. Then it may become clear whether at $r = 2R$ there is, in addition to the δ-component (resulting from the direct contacts of balls), also a pole.

This book assumes the existence of the set-theoretic union of the random jammed packing of hard balls as a motion-invariant random closed set, which in this section is denoted by Ξ.

This set Ξ is the base for another model, the *cherry-pit model* $\Xi_{\oplus r}$,

$$\Xi_{\oplus r} = \Xi \oplus B(o, r). \tag{6.106}$$

This means that all balls of Ξ are enlarged in such a way that the radii are increased by the value r, then being $R + r$. The enlargement leads to the possibility of overlapping of the larger balls. (The hard balls are the 'pits' and the enlarged ones the 'cherries'.) Clearly, also $\Xi_{\oplus r}$ is motion-invariant. (Note that in Torquato, 2002, the cherry-pit model is defined with respect to a Gibbs hard-core process.) Clearly, its volume fraction $V_{V,r}$ and specific surface area $S_{V,r}$ satisfy

$$V_{V,r} \to 1 \quad \text{and} \quad S_{V,r} \to 0 \qquad \text{for } r \to \infty.$$

From (6.103) and the fact that the spherical contact distribution function of $\Xi_{\oplus r}$ can be easily expressed by that of Ξ, the following approximations are obtained:

$$V_{V,r} \approx 1 - 2(1 - V_V)\left(1 - \Phi\left(\frac{r}{\sigma}\right)\right), \tag{6.107}$$

and

$$S_{V,r} \approx (1 - V_V)\frac{2}{\sqrt{2\pi}\sigma} \exp\left(-\frac{r^2}{2\sigma^2}\right), \tag{6.108}$$

where V_V denotes the volume fraction of the hard ball packing Ξ, $\Phi(x)$ is the standard Gaussian distribution function (with $\Phi(0) = \frac{1}{2}$), and σ is given by (6.104); see Elsner *et al.* (2009).

The case of balls of random diameters is considered for example in Lochmann *et al.* (2006). Hermann *et al.* (2013) discuss the corresponding cherry-pit model.

Moreover, there are also algorithms to pack ellipsoids, cylinders and polyhedra; see Bezrukov and Stoyan (2006), Bargiel (2008), Torquato and Stillinger (2010) and Jiao and Torquato (2011). Other algorithms try to simulate processes of sedimentation under the influence of gravity, which do not lead to stationary or equilibrium systems; see for example Jodrey and Tory (1979) and the experiment-oriented paper Royall *et al.* (2007).

Figure 6.7 A natural packing of cubical paving-stones. Courtesy of E. Rothe.

Also radial simulations have been used, where one irregular cluster of balls is placed at the origin and is then enlarged by adding successively layers of balls; see p. 165 of SKM95, and Stachurski (2011).

Figure 6.7 shows a natural random packing of cubical paving-stones.

The paper Ballani *et al.* (2006) gives an example for a statistical analysis of a structure which can be modelled by a packing of hard balls, some special kind of concrete. The first step was computerised tomography (CT) and led to pixel data. In the second step, methods of Bayesian image analysis (van Lieshout, 1995, and Winkler, 2003) were applied to segment the grains as non-overlapping ideal balls. For this simulated annealing was used. Having the data of balls, one could then apply methods of point process statistics; see also Ballani (2006a). An alternative approach is described in Thiedmann *et al.* (2012), which is suitable for more noisy data.

The Stienen model

Now two models are considered where some mathematics is possible. Unfortunately, these have densities much smaller than the models discussed above.

For the *Stienen model* (Stoyan, 1990a) the germ process is a homogeneous Poisson process of intensity λ. The grains are balls of random diameters: the diameter d_n of the ball around the germ point x_n is equal to the distance from x_n to its nearest neighbour. Figure 6.8 shows a simulated sample of this model for the planar case. Typically large balls are isolated, and small ones appear sometimes as isolated pairs. The stationary and isotropic marked point process $\{[x_n; d_n]\}$ is an example of a *dependently* marked Poisson process. Clearly, the Stienen model is not a Boolean model. By the way, it can also be interpreted as the system of *in*-balls (centred at the generating points) of the Poisson-Voronoi tessellation; see Section 9.7.

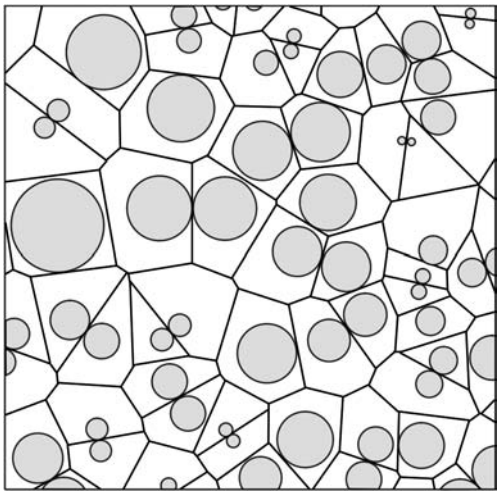

Figure 6.8 A sample of the planar Stienen model. The centres of the discs form a sample of a Poisson process; the disc diameters are equal to the corresponding nearest-neighbour distances. The polygons are the corresponding Dirichlet cells.

The volume fraction p can be calculated by means of Formula (6.97) as

$$p = \lambda b_d \cdot \int_0^\infty r^d \lambda b_d d r^{d-1} \exp(-\lambda b_d r^d)\, \mathrm{d}r,$$

which is $1/8$ in the case $d = 3$. Wiencek and Stoyan (1993) give for $d = 3$ the covariance $C(r)$, obtained by simulation. Schlather and Stoyan (1997) express $C(r)$ in integral form for $d \geq 2$. Olsbo (2007) calculates the correlation coefficient between the volume of the typical Poisson-Voronoi cell and the corresponding Stienen ball.

The Stienen model can be generalised by means of a reduction factor $\alpha\,(< 1)$: the corresponding marked point process is then $\{[x_n; \alpha d_n]\}$.

In the spatial case it is possible to calculate characteristics related to planar sections: the section disc diameter distribution functions, the intensity of the point process of section disc centres and even the pair correlation function of this point process; see Section 10.7.2.

The lilypond model

Häggström and Meester (1996) introduced a model closely related to the Stienen model. Consider a point process of germs in $\mathbb{R}^d$. Centred at these germs, grains start growing radially at the same instant with the same constant speed. A grain stops growing when it touches another grain. This germ–grain model of non-overlapping balls is called the *lilypond model*. A more formal definition (to allow non-Poisson germs) given by Daley and Last (2005) is that the lilypond model is a system of non-overlapping balls such that each ball is in touch with a ball of equal or smaller size. Heveling and Last (2006) showed that there always exists a unique lilypond system of balls for any germ process.

Obviously, the lilypond model contains as a subset the Stienen model of the same set of germs. Consequently, its volume fraction is larger than that of the Stienen model. Daley *et al.*

(1999, 2000) determined the volume fraction of the Poisson lilypond model:

$$p = \begin{cases} 1 - \mathrm{e}^{-1} & \text{for } d = 1, \\ 0.349 & \text{for } d = 2, \\ 0.186 & \text{for } d = 3, \end{cases} \tag{6.109}$$

the latter two values by simulation. The former paper also gives an exponential upper bound for the tail of the distribution of the size of the typical ball. Subexponential bounds for the tail of the size of the cluster (of touching balls) containing the origin are given in Last and Penrose (2013), where also central limit theorems for the total volume and the number of clusters in expanding windows are proved.

For a homogeneous Poisson germ process, Häggström and Meester (1996) proved that the model does not percolate, that is, there is no infinite cluster of touching balls. Daley and Last (2005) showed that there is also no percolation for a wide range of germ processes, including certain Poisson cluster, Cox and Gibbs processes satisfying some moment conditions. Obviously, for $d > 1$, if the radii of the balls in the Poisson lilypond model are increased by a sufficiently large fixed amount δ, then percolation occurs; the infimum of such δ is called the *critical enhancement* δ_c. Last and Penrose (2013) showed that δ_c is strictly positive, meaning that for sufficiently small $0 < \delta < \delta_c$, the union of balls enlarged by δ still does not percolate. Thus, in a Poisson lilypond, not every frog that is able to jump from one lily pad to another can travel infinitely far without getting into water; if its jump range is too small, it is still unable to do so.

Various

Pelikan *et al.* (1994) study germ–grain models where the grains are balls or cylinders with caps and the positions are given as in the RSA process. Cylindric grains also appear in the filament model in Stoica *et al.* (2010).

Biswal *et al.* (2009) report about a random-field-controlled germ–grain model of RSA type.

Other models come from the field of Gibbs processes; see Baddeley and Møller (1989), Mase (1985), Stoyan (1989), Stoyan and Stoyan (1994, p. 334), van Lieshout (1995), W. S. Kendall *et al.* (1999), Møller and Helisová (2010) and Coeurjolly *et al.* (2012). A simple example is the system of hard balls belonging to the Gibbs hard-core process as in Section 5.5.3.

6.5.4 Shot-noise germ–grain models

An interesting class of germ–grain processes with dependent grains is closely related to shot-noise fields. Its random-set version, the corresponding germ–grain model, is called the *SINR coverage process*, where SINR stands for *signal to interference and noise ratio* (Baccelli and Błaszczyszyn, 2009a, Chapter 7).

The construction starts from a shot-noise field $\{S_\Psi(x)\}$ as in Section 5.6 constructed using a marked point process $\Psi = \{[x_n; m_n]\}$ of intensity λ and a response function $s(x, m)$. The germs of the shot-noise germ–grain process are simply the points x_n, while the grains Ξ_n are constructed as follows:

$$\Xi_n = \big\{x \in \mathbb{R}^d : s(x - x_n, m_n) \geq t \cdot \big(w(x) + S_\Psi(x)\big)\big\}. \tag{6.110}$$

Here t is a nonnegative threshold, which can, in more general models, also depend on n, and $w(x)$ denotes external or thermal noise. Thus Ξ_n is the set where the signal from x_n is t times greater than the relevant noise and interference. The shot-noise germ–grain model Ξ is given by an equation analogous to (6.93).

Baccelli and Błaszczyszyn (2009a, Section 7.4) show that the grains Ξ_n defined in (6.110) are random closed sets, and under boundedness conditions they are also compact. The grains Ξ_n can be empty; they are not necessarily spherical or convex, can overlap and are in general mutually dependent. If $s(x, m)$ is defined by (5.106) with the simplified path-loss function, then each Ξ_n is not empty and contains always x_n, since $s(o, m) = \infty$.

Figure 6.9 shows a simulated shot-noise germ–grain model in a $2 \times 2\,\mathrm{km}^2$ window, with a homogeneous Poisson germ process of intensity $\lambda = 10\,\mathrm{km}^{-2}$, simplified path-loss response

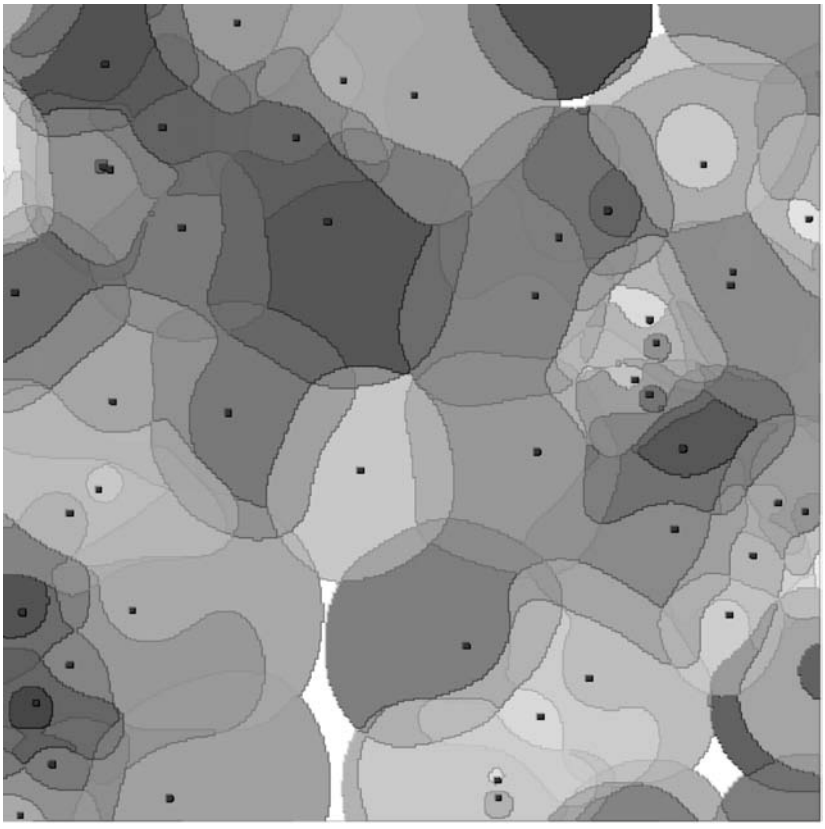

Figure 6.9 A simulated sample of a shot-noise germ–grain model. Different grey-tones mark different grains, the white phase is the complement of the random set Ξ. A grain corresponds to the region where the signal emitted with power of 1 W (Watt) by an antenna located at the corresponding germ can be received with the signal-to-interference-and-noise ratio not smaller than $t = 0.2$; the interference is caused by all other germs emitting also signals of power 1 W each, and modelled by the shot-noise, noise power $w(x) \equiv 10^{-10}$ W. The parameters are given in the text. Courtesy of B. Błaszczyszyn.

function $s(x, m) = L(\|x\|) = L(r)$, where

$$L(r) = (Ar)^{-\beta} \quad \text{(in Watt)} \tag{6.111}$$

with $A = 8000\,\text{km}^{-1}$ and $\beta = 3$, $w(x) \equiv 10^{-10}$ W (Watt) and $t = 0.2$. These parameters are quite realistic for power attenuation of radio signals.

In dependence on the model characteristics the grains have different shapes. Extremal cases are balls and Voronoi cells.

In the case that Ψ is an independently marked homogeneous Poisson process the distribution of the typical grain, denoted as Ξ_o, can be characterised analytically. The Slivnyak–Mecke formula makes it possible to consider the grain Ξ_o as if based on a germ at the origin o and mark m with the same mark distribution as the m_n and independent of Ψ as

$$\Xi_o = \big\{x \in \mathbb{R}^d : s(x, m) \geq t \cdot \big(w(x) + S_\Psi(x)\big)\big\}. \tag{6.112}$$

In particular, the mean volume of Ξ_o can be obtained as

$$\overline{V} = \int_{\mathbb{R}^d} p(x)\mathrm{d}x, \tag{6.113}$$

with

$$p(x) = \mathbf{P}(x \in \Xi_o). \tag{6.114}$$

For the planar case of the simplified path-loss function in (6.111) with $A > 0$ and $\beta > 2$, $w(x) \equiv 0$ and exponentially distributed marks, the coverage probability is given by

$$p(x) = \exp(-\lambda \|x\|^2 t^{2/\beta} K), \tag{6.115}$$

where

$$K = \frac{2\pi}{\beta}\Gamma\big(\frac{2}{\beta}\big)\Gamma\big(1 - \frac{2}{\beta}\big) = \frac{2\pi^2}{\beta \sin(2\pi/\beta)} \tag{6.116}$$

(Baccelli and Błaszczyszyn, 2009a, Example 5.6, and Baccelli and Błaszczyszyn, 2009b, Proposition 16.1). Note that (6.115) and (6.116) do not contain the parameter of the exponential mark distribution and A. The volume fraction p is difficult to obtain, but clearly the qualitative relation

$$p = \lambda \overline{V} - O(\lambda^2) \tag{6.117}$$

holds.

Baccelli and Błaszczyszyn (2009a,b) present many results for this germ–grain process, for example information on the set covariance $\gamma_{\Xi_o}(r)$ of the typical grain Ξ_o and the random number of grains overlapping a given point. Also properties of the random graph with nodes $\{x_n\}$ and edges connecting germs of overlapping grains and percolation are studied; see Sections 3.3.3 and 3.3.4.

6.5.5 Weighted grain distributions

The mark distribution M describes the shape and size of the typical grain of a germ–grain model. It is sometimes useful to weight the grain by a size parameter and to study the weighted

mark distribution of the grain. The *volume-weighted mark distribution* $M_{(v)}$ is an important special case. It is defined by

$$\int f(K)M_{(v)}(\mathrm{d}K) = \int f(K)v_d(K)M(\mathrm{d}K)\Big/\overline{V} \tag{6.118}$$

for nonnegative measurable functions $f(K)$ on $\mathbb{K}$, where $\overline{V}$ is the mean volume of the typical (unweighted) grain. A small number of large grains contribute to this distribution as much as a large number of small grains.

Such volume-weighted mark distributions can be of more interest than the unmodified or *number-weighted* mark distribution M. In the case of balls the term 'sieving distribution' is often used, since a series of sieving operations using sieves of different mesh sizes will produce an approximation to a volume-weighted distribution of balls.

Weighting can be carried out by using other functionals such as surface area rather than volume.

A series of moment formulae are implied by (6.118):

$$\int \big(v_d(K)\big)^n M_{(v)}(\mathrm{d}K) = \int \big(v_d(K)\big)^{n+1} M(\mathrm{d}K)\Big/\overline{V} \qquad \text{for } n \geq 1. \tag{6.119}$$

6.5.6 Intersection formulae

Many measurements tend to be of the form $h(\Xi \cap W)$ for a given test set or observation window W and suitable functionals $h(\cdot)$. Consequently formulae for the expectations of such quantities are important in statistical applications. Schneider and Weil (2008, Section 9.4) give formulae for such means in the case of stationary standard random sets (see p. 209), which can be decomposed into germ–grain models with convex grains (see p. 238).

There are two important special cases:

$$\mathbf{E}\big(v_d(\Xi \cap W)\big) = pv_d(W) \tag{6.120}$$

for the volume and

$$\mathbf{E}\big(S(\Xi \cap W)\big) = pS(W) + S_V^{(d)} v_d(W) \tag{6.121}$$

for the surface area. Formula (6.120) is clearly true for general stationary random closed sets under the sole assumption that $v_d(W)$ is finite. In Formula (6.121) S denotes the boundary length measure (surface area measure in the spatial case), while $S_V^{(d)}$ denotes the intensity of the fibre process (surface process) formed by the boundary (surface) $\partial\Xi$ of Ξ and is equal to the mean boundary length per unit area (mean surface area per unit volume in the spatial case). The first term on the right-hand side of Formula (6.121) results from the intersection of Ξ with the boundary of W.

If the standard random set Ξ is motion-invariant, and if W is convex and compact, then the following general formula holds for all intrinsic volumes of $\Xi \cap W$ (see e.g. Schneider

and Weil, 2008, p. 416):

$$\mathbf{E}\big(V_k(\Xi \cap W)\big) = \frac{1}{k!d!b_k b_d} \sum_{i=k}^{d} i!(d-i+k)!b_i b_{d-i+k}\, v_i\, V_{d-i+k}(W) \quad \text{for } k = 0, 1, \ldots, d, \tag{6.122}$$

where v_i is the specific i^{th} intrinsic volume (see p. 229). In stereological notation, as in Section 10.2,

$$\begin{aligned} &v_0 = N_A, \qquad v_1 = \frac{L_A}{2}, \qquad v_2 = A_A && \text{if } d = 2,\\ &v_0 = N_V, \qquad v_1 = \frac{M_V}{\pi}, \qquad v_2 = \frac{S_V}{2}, \qquad v_3 = V_V && \text{if } d = 3. \end{aligned}$$

Formula (6.122) follows from the Hadwiger characterisation theorem (1.44) since the functionals $h_k(\cdot) = \mathbf{E}\big(V_k(\Xi \cap \cdot)\big)$ are finite, monotone, C-additive, and motion-invariant.

In the planar case of $d = 2$ a particularly important version of (6.122) is that of $k = 0$. In that case

$$\begin{aligned} \mathbf{E}\big(\chi(\Xi \cap W)\big) &= \mathbf{E}\big(V_0(\Xi \cap W)\big)\\ &= \frac{2\pi v_0 V_2(W) + 4v_1 V_1(W) + 2\pi v_2 V_0(W)}{2\pi}\\ &= A_A + \frac{L_A L(W)}{2\pi} + N_A A(W), \end{aligned} \tag{6.123}$$

where $\chi(\cdot)$ denotes the connectivity number or Euler–Poincaré characteristic, $A_A = p$, and L_A, N_A and $A(W)$ are respectively the mean boundary length per unit area, the specific connectivity number and the area of W.

Proof of Formula (6.123). Consider the case of a germ–grain model with convex disjoint grains with rotation-invariant distribution. Since the grains are disjoint, the number of grains to hit W is given by $\chi(\Xi \cap W)$. Then the Campbell theorem (4.29) yields for the corresponding marked point process

$$\mathbf{E}\big(\chi(\Xi \cap W)\big) = \lambda \mathbf{E}\big(v_d(\check{\Xi}_0 \oplus W)\big), \tag{6.124}$$

where Ξ_0 denotes the typical grain and λ is the intensity of the germ process (so $\lambda = N_A$). Formula (6.124) is true because of

$$\begin{aligned} \mathbf{E}\big(\chi(\Xi \cap W)\big) &= \lambda \int_{C(\mathbb{K})} \int_{\mathbb{R}^d} \mathbf{1}_{H(W)}(x, K)\, \mathrm{d}x\, M(\mathrm{d}K)\\ &= \lambda \int_{C(\mathbb{K})} \int_{W \oplus \check{K}} \mathrm{d}x\, M(\mathrm{d}K)\\ &= \lambda \int_{C(\mathbb{K})} v_d(\check{K} \oplus W) M(\mathrm{d}K)\\ &= \lambda \mathbf{E}\big(v_d(\check{\Xi}_0 \oplus W)\big), \end{aligned}$$

where M is the distribution of Ξ_0, $H(W) = \{(x, K) \in \mathbb{R}^d \times C(\mathbb{K}) : (x + K) \cap W \neq \emptyset\}$ and K is a dummy variable of integration ranging over the system of convex bodies $C(\mathbb{K})$. □

The mean volume $\mathbf{E}\big(\nu_d(\check{\Xi}_0 \oplus W)\big)$ can be calculated by methods of integral geometry. If Ξ_0 is rotation-invariant then the generalised Steiner formula (6.29) can be used. In the case $d = 2$ Formula (6.30) yields the result.

6.5.7 Statistics for motion-invariant germ–grain models

Practical measurement procedures typically involve a sample of a germ–grain model Ξ via a convex compact sampling window W.

The fundamental statistical problems are estimation of the intensity λ of the germ process and some description of the grains. These problems are nontrivial because of edge-effects; some grains will only be partially observed as they do not lie completely in the window W. Measurements on these grains will be difficult or even impossible; the possibility of the presence of such grains introduces potential bias in counting procedures.

Determination of λ

(1) Counting rules

Baddeley and Jensen (2005, Section 3.3.5 and Chapter 10) describe various counting rules for the unbiased estimation of the germ density λ. The most natural procedure assigns to each grain a unique 'associated' point, such as the extremal point in a fixed direction or the centre of gravity. An unbiased estimator of λ is given by the number of these points in W divided by $\nu_d(W)$.

Another popular method uses the *Gundersen counting frame* or *Gundersen's tiling rule*, illustrated by Figure 6.10 for the planar case. Here all grains are counted which hit the rectangular window W but not the area on the left-hand side of the 'forbidden line' including the window's left vertical and lower horizontal sides; it must be possible to decide which grain fragments in W belong to the same grain and also to decide for each grain of interest whether or not it hits the 'forbidden line'. The number n_W of grains hitting W but not the 'forbidden lines' leads to the estimator

$$\hat{\lambda} = \frac{n_W}{A(W)}. \tag{6.125}$$

It is unbiased even if the germ–grain model is only stationary.

Proof of the unbiasedness of $\hat{\lambda}$. Consider

$$n_W = \sum_{[x_n;\Xi_n]\in\Psi} \mathbf{1}_{\mathcal{T}(\Xi_n)}(x_n),$$

where $\mathcal{T}(K) = \{x \in \mathbb{R}^2 : x + K \text{ is counted by the frame}\}$. Geometrical arguments show that for every K the set $\mathcal{T}(K)$ is a rectangle, which is congruent to W. Thus the Campbell theorem (4.29) for marked point processes gives

$$\mathbf{E}(n_W) = \lambda \int \int \mathbf{1}_{\mathcal{T}(K)}(x)\mathrm{d}x\, M(\mathrm{d}K) = \lambda A(W);$$

see Schwandtke *et al.* (1988). □

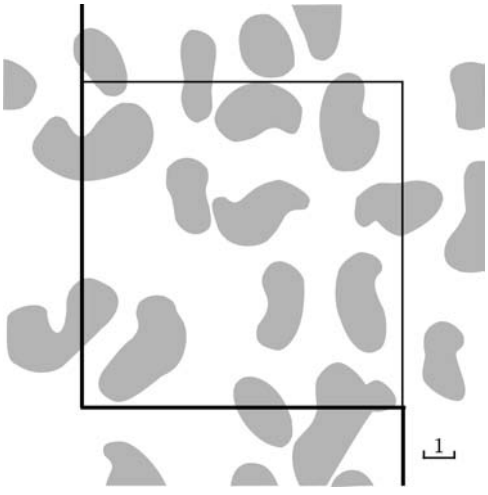

Figure 6.10 A sample of a germ–grain model in a window, to be considered together with Example 6.3 on p. 253, in which the length scale shown is used. The window W is the inner square; the additional space shown is needed for getting full information on the grains hitting the Gundersen counting frame, which is given for the inner square; the three bold lines are its 'forbidden lines'.

Note that the Gundersen frame uses more information than given in W: it is possible that grains intersect both W and the frame outside of W; see Figure 6.10.

In the three-dimensional case the Gundersen frame is constructed analogously; see Baddeley and Jensen (2005, Chapter 11).

(2) Disector

A simple three-dimensional method of measurement for the estimation of λ is the *disector*, which was invented by Sterio (1984); see also Baddeley and Jensen (2005, Section 3.3.5 and Chapter 10). It uses two parallel section planes of known distance t. The geometrical setup is shown in Figure 6.11. The lower plane is called the reference plane and the upper the look-up plane. The window of observation in the reference plane is W.

Let n_W be the number of grains which intersect the reference plane in W *but not* the look-up plane (which is deemed to be infinite in extent). Then λ is estimated by

$$\hat{\lambda} = \frac{n_W}{\nu_2(W)t}. \tag{6.126}$$

This is clearly an unbiased estimator of λ: assign to each particle (as associated point) its highest tangent point. These points form a stationary point process of intensity λ, and the disector finds the points which are between the two planes.

For purposes of estimation the phrase 'intersect the window' has to be made exact. An unbiased counting rule has to be used, such as described above; it can be implemented, for example, by the Gundersen frame.

Clearly, the distance t should be reasonably small, in order to minimise the possibility of there being grains which lie completely between the two planes without hitting either one. If

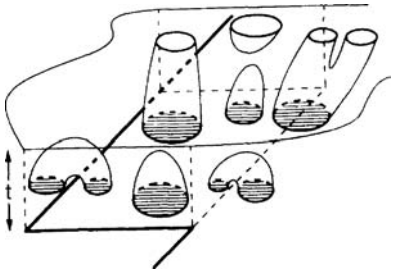

Figure 6.11 A schematic illustration of the disector. The rectangle below is the window in the reference plane, shown together with the Gundersen counting frame (the bold lines). The grains having contact with the window but not hitting the area on the left-hand side of the forbidden lines of the frame or the (upper) look-up plane are counted. In the illustration there are three such grains.

topologically complicated grains are considered, it is sometimes necessary to look below the reference plane in order to check connectivity properties of grain fragments.

Ohser and Mücklich (2000, Section 3.2.5) explained how the specific Euler–Poincaré characteristic N_V can be estimated by serial sections.

Simultaneous estimation of all intrinsic volume densities

In the planar case let $L(W)$ and $A(W)$ be the boundary length and area of W, and assume the grains are convex. The following quantities are measured:

$A(\Xi \cap W)$	the area of Ξ in W,
$L(\Xi \cap W)$	the boundary length of Ξ inside the interior of W plus the length of $\partial W \cap \Xi$,
$\chi(\Xi \cap W)$	the connectivity number of $\Xi \cap W$.

They satisfy the following system of equations:

$$\mathbf{E}\big(A(\Xi \cap W)\big) = A_A A(W), \tag{6.127}$$

$$\mathbf{E}\big(L(\Xi \cap W)\big) = A_A L(W) + L_A A(W), \tag{6.128}$$

$$\mathbf{E}\big(\chi(\Xi \cap W)\big) = A_A + \frac{L_A L(W)}{2\pi} + N_A A(W), \tag{6.129}$$

which is the particular case of (6.122) for $d = 2$ and $k = 0, 1, 2$. If the expectations on the left-hand side are replaced by the corresponding random quantities $A(\Xi \cap W)$, $L(\Xi \cap W)$ and $\chi(\Xi \cap W)$ then solving for A_A, L_A and N_A produces unbiased estimators for these fractions.

The same approach is possible in the spatial case.

However, the above presentation is somewhat naïve. The areas, lengths, and volumes do not appear from nowhere but must be somehow determined, a procedure which is not at all trivial if data are given as pixels. This book does not consider these problems; the methods needed in this case are described in Ohser and Schladitz (2009). The spatial case uses ideas of stereology, which are based on the Crofton formula.

A similar approach appears in Schmidt and Spodarev (2005), which is based on counting a topological index function of Ξ within the window W. Its algorithmic realisation is described in Klenk *et al.* (2006) and Guderlei *et al.* (2007). An alternative approach is presented in Mrkvička and Rataj (2008), where a local version of the Steiner formula is applied for various dilation radii r_i and linear regression then leads to estimates of the intrinsic volume densities.

Example 6.3. *Determination of λ, N_A, A_A and L_A for the pattern of Figure 6.10*
Figure 6.10 shows a sample of a planar motion-invariant germ–grain model Ξ observed through the window W, which is the *inner* square of side-length 10.5. The measurements made only through the window can be compared with others obtained by observing all of the grains that happen to intersect the window.

Image analyser measurements through the window give

$$A(\Xi \cap W) = 41.2,$$
$$L(\Xi \cap W) = 97.3,$$
$$\chi(\Xi \cap W) = 14,$$

using the unit of length of Figure 6.10. Thus the equation system (6.127) to (6.129) yields, assuming convexity (which is not given, but affects only N_A), the estimates

$$\hat{A}_A = 0.37,$$
$$\hat{L}_A = 0.74,$$
$$\hat{N}_A = 0.08.$$

All individual grains have connectivity number one. So the value $\hat{N}_A$ can be interpreted as estimating the mean number λ of grains per unit area. This number can also be estimated by counting associated points, for example the lower left boundary points of grains falling in W, which comes to 10, and so leads to an estimate of N_A as 0.09. The Gundersen frame method applied to the inner square W yields the estimate $\hat{N}_A = \hat{\lambda} = 9/A(W) = 0.08$. Note that the upper left particle must not be counted though it hits the window because it hits also the 'forbidden line'. However, both these measurement procedures utilise information exterior to the measurement window W.

The specific convexity number N_A^+ can be estimated as 0.11, by counting the lower tangent points with respect to the bottom line of Figure 6.10.

Schwandtke *et al.* (1987, 1988) study the estimation variances of these and other estimators of N_A and show that the estimator of N_A which results from the equation system above is more accurate than those arising from methods using associated points.

Tests of goodness-of-fit are carried out following the pattern of such tests in Sections 3.4.2 and 4.7.10, using summary characteristics and deviation tests.

Estimation of mean values for convex grains

Let $M(\cdot)$ be the distribution of the typical grain: so $M(\cdot)$ is a probability measure on the space $C(\mathbb{K})$ of convex bodies. Given a measurable nonnegative functional $f(K)$ the problem is to estimate the quantity

$$M_f = \int_{C(\mathbb{K})} f(K)M(\mathrm{d}K), \tag{6.130}$$

where as before K is a dummy variable of integration running through the space of convex bodies. Particular cases are

$$f(K) = \nu_d(K)$$

and

$$f(K) = \mathbf{1}(\mathrm{diam}(K) \leq r).$$

In the first case M_f is the mean grain volume and in the second for solid spherical grains the value of the distribution function of diameter at r.

There are two possible methods for the estimation of M_f.

(1) *Plus-sampling* (Miles, 1974b; Weil, 1982b). The values of $f(\Xi_i)$ are determined for all grains Ξ_i hitting the sampling window W. This may mean that information from outside of the window W must be gathered: hence the phrase 'plus-sampling'. An unbiased estimator for λM_f is $\hat{M}_f$:

$$\hat{M}_f = \sum_{[x_n;\Xi_n]\in\Psi} f(\Xi_n)\frac{\mathbf{1}_{W\oplus\check{\Xi}_n}(x_n)}{\nu_d(W\oplus\check{\Xi}_n)}. \tag{6.131}$$

The sum is taken only over those grains $[x_n; \Xi_n]$ that actually hit W as described above, since otherwise $\mathbf{1}_{W\oplus\check{\Xi}_n}(x_n) = 0$. The unbiased nature of M_f follows by an application of the Campbell theorem (4.29) for marked point processes to the germ–grain process $\Psi = \{[x_n; \Xi_n]\}$.

Formulae in integral geometry help simplify the evaluation of $\nu_d(W \oplus \check{\Xi}_n)$.

It is clear that in many cases plus-sampling will be unrealistic, since only the interior of the window W will be available for observation and so insufficient information for the determination of all $f(K)$-values is given.

(2) *Minus-sampling or Miles–Lantuéjoul sampling* (Miles, 1974b; Lantuéjoul, 1978a,b). Only the grains lying completely within W are considered. Analogous to $\hat{M}_f$ in (6.131), the quantity

$$\overline{M}_f = \sum_{[x_n;\Xi_n]\in\Psi} f(\Xi_n)\frac{\mathbf{1}_{W\ominus\check{\Xi}_n}(x_n)}{\nu_d(W\ominus\check{\Xi}_n)} \tag{6.132}$$

is an unbiased estimator for λM_f. Again the sum is restricted to particular grains, since $\mathbf{1}_{W\ominus\check{\Xi}_n}(x_n) = 0$ unless $x_n + \Xi_n \subset W$: only the grains fully contained in W are counted.

Matheron (1978) and Weil (1982b) discuss means of determination of $\nu_d(W \ominus \check{\Xi}_n)$.

Baddeley and Jensen (2005, p. 272) consider the case with associated points.

The simulation of germ–grain models follows the pattern of simulation of point processes and Boolean models as presented in Chapters 3, 4 and 5.

6.6 Other random closed set models

6.6.1 Gibbs discrete random sets

Usually in this book random sets are defined in the spirit of Euclidean geometry, as subsets of $\mathbb{R}^d$. However, random set data often appear in the form of discrete sets, as pixel structures. Therefore, it makes sense to build also models in this geometry. The following aims to give the reader some idea of such sets, following the paper Sivakumar and Goutsias (1997b). The exposition is restricted to the planar case, but generalisation to d dimensions is possible.

The space in which the sets are existing is the lattice W,

$$W = \{(m, n) : 1 \le m \le M, 1 \le n \le N\},$$

where M and N are natural numbers. The points $w = (m, n)$ are called *sites*. Subsets of W are denoted by X, $\mathcal{P}(W)$ is the power set of W, that is, the collection of all X, and $|X|$ is the cardinality of X, that is, number of sites of X. Assume that to each site $w \in W$ a corresponding random variable $x(w)$, called its *state*, is assigned, which takes the value 0 or 1. Then the set

$$\Xi = \{w \in W : x(w) = 1\}$$

is a discrete random set, whose distribution is given by the probabilities

$$\mathbf{P}(\Xi = X) \qquad \text{for } X \subset W,$$

saying that the random set Ξ is equal to the set X.

The particular case of discrete random sets considered in this section are *Gibbs discrete random sets*, the distribution of which is given by the elegant formula (6.133). These sets can be simulated in a well-established way and have found many successful applications. Goutsias and Sivakumar (1998) summarise advances of models based on Gibbs distributions. These are often natural choices, leading to a wide spectrum of distributions and making it possible to incorporate constraints and to model local interactions in a simple way.

A Gibbs distribution is given by

$$\mathbf{P}(\Xi = X) = \frac{1}{Z} \exp\bigl(-\beta U(X)\bigr) \qquad \text{for } X \subset W, \tag{6.133}$$

where Z, called *partition function*, is a normalising constant equal to

$$Z = \sum_{X \subset W} \exp\bigl(-\beta U(X)\bigr). \tag{6.134}$$

Furthermore, $U(X)$ is the *energy* of X and β a positive model parameter, called *inverse temperature*. Though it is notoriously difficult to calculate Z and numerical characteristics of the distribution such as the mean number $\mathbf{E}(|\Xi|)$ of sites in Ξ or the probability $\mathbf{P}(w \in \Xi)$ for a given site w, this model is very popular.

The inverse temperature β somehow controls the variability of a Gibbs discrete random set Ξ. If $\beta \to 0$ then Ξ becomes uniform, that is,

$$\lim_{\beta \to 0} \mathbf{P}(\Xi = X) = p \qquad \text{for } X \subset W, \tag{6.135}$$

where

$$p = 2^{-MN} \tag{6.136}$$

since 2^{MN} is the total number of all subsets X of W, that is, the number of elements of the power set $\mathcal{P}(W)$. If $\beta \to \infty$ then

$$\lim_{\beta \to \infty} \mathbf{P}(\Xi = X) = \begin{cases} q & \text{for } X \in \mathcal{U}, \\ 0 & \text{otherwise}, \end{cases} \tag{6.137}$$

with

$$q = |\mathcal{U}|^{-1},$$

in which $\mathcal{U}$ is the set of all $X \subset W$ with energy $U(X) = u$, where u is the global minimum of $U(X)$. The members in $\mathcal{U}$ are often called *ground states*.

Gibbs discrete random sets are usually simulated by the Markov chain Monte Carlo technique: A homogeneous ergodic Markov chain $\{X_n\}$ is constructed, the states of which are subsets of W, whose equilibrium distribution is just the Gibbs distribution (6.133). After sufficiently many jumps of the Markov chain any of its states can be approximately considered as a sample drawn from the Gibbs distribution.

Example 6.4. *The Ising model*
The energy is defined as

$$U(X) = \sum_{\substack{(v,w) \subset W \\ |v-w|=1}} \mathbf{1}\big(x(v) \neq x(w)\big), \tag{6.138}$$

where $|v - w| = |k - m| + |l - n|$ for $v = (k, l)$ and $w = (m, n)$. The energy $U(X)$ is high if X consists of many small components.

In the form given here the model is called the 'ferromagnetic' Ising model. Also the 'antiferromagnetic' case with $\beta < 0$ is of interest; see for example Georgii *et al.* (2001). Sivakumar and Goutsias (1997a,b, 1999) consider a more general energy function. Georgii (2000) and Georgii *et al.* (2001) show how to define Ising models on infinite lattices.

For the simulation of the Ising model here a quite simple form is described, the *Metropolis algorithm with single-site updating*. It works as follows.

Let X_n be the state of the Markov chain in the n^{th} iteration. The following state X_{n+1} is obtained in two steps:

(i) In W a site w is uniformly chosen. For X_{n+1} a proposal Y is made by changing the state of site w: either w is added to X_n (if not in X_n) or w is deleted from X_n (if in X_n); all other sites remain unchanged.

(ii) The proposal Y is accepted (i.e. $X_{n+1} = Y$) with probability

$$\min\{1, \exp(-\beta \Delta U)\},$$

where

$$\Delta U = U(Y) - U(X_n).$$

If Y is not accepted, then $X_{n+1} = X_n$.

It is clear that ΔU is completely given by the elements in $(B + w) \cap W$, where B is the *rhombus*

$$B = \{(0, -1), (0, 0), (0, 1), (-1, 0), (1, 0)\}.$$

Statistics for the Ising model is considered in Sherman (2011, Section 4.2), where also an example discussing cancer rates in the eastern USA is presented. In statistical applications, the Ising model often arises as a prior in Bayesian statistics.

Example 6.5. *Morphologically constrained discrete random sets*
These Gibbs discrete random sets, which were first used by Chen and Kelly (1992), have energies that lead to samples which tend to have prescribed morphological properties. A simple example is

$$U(X) = |X \setminus X \circ B| \qquad \text{for } X \subset W, \tag{6.139}$$

where $\circ$ denotes the opening operation on the lattice W and B is some structuring element. (Sivakumar and Goutsias, 1997c, present a theory of discretised morphological operators; see also Soille, 2003, Chapter 4.) The underlying idea is to have ground states that are B-open, in order to favour realisations X that are B-open: X and $X \circ B$ will differ only for a small number of sites, that is, X is 'smooth' in a sense determined by B. This class of Gibbs discrete random sets is thoroughly studied in a series of papers including Sivakumar and Goutsias (1999). Instead of defining the energy with opening, it can be defined also with respect to closing, as

$$U(X) = |X \bullet B \setminus X| \qquad \text{for } X \subset W, \tag{6.140}$$

or even

$$U(X) = |X \setminus X \circ B| + |X \bullet B \setminus X| \qquad \text{for } X \subset W. \tag{6.141}$$

The ground states are such sets that fulfill some morphological conditions. In the case of (6.139) this means that there are no components of a 'size' smaller than the 'size' of the structuring element B. Sivakumar and Goutsias (1999) present many interesting examples and extend the theory to the case of grey-tone-value fields. For simulation they use some multi-state updating Metropolis method. Finally, they show how to fit Gibbs discrete random sets to image data and use a maximum likelihood technique where the size density (6.143) plays an important rôle.

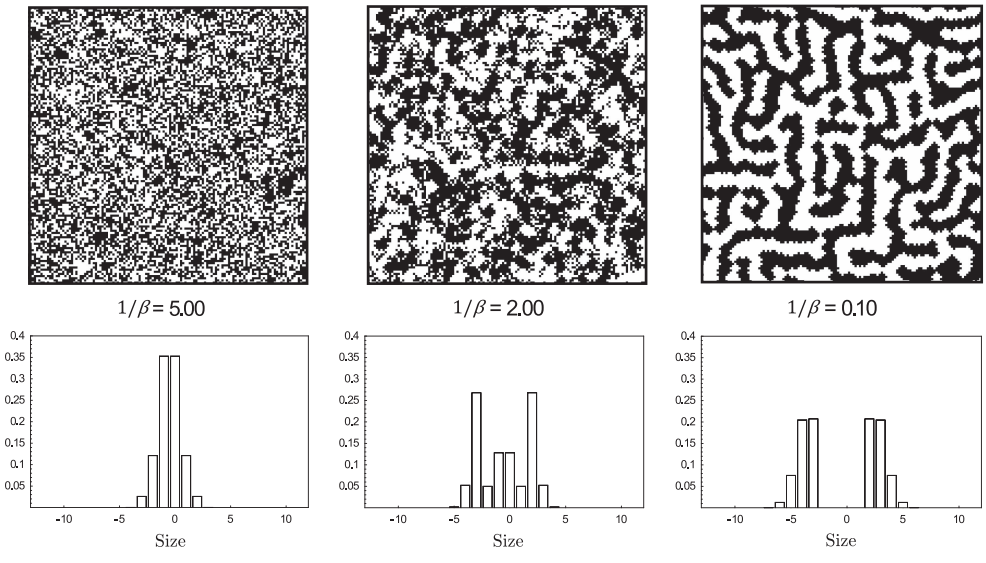

Figure 6.12 Realisations of the morphologically constrained Gibbs discrete random set as in Example 6.5 at three inverse temperatures β. The format of each figure is 128×128 pixels. The histograms show the corresponding size densities (6.143). Courtesy of K. Sivakumar.

Figure 6.12 shows three simulated morphologically constrained Gibbs discrete random sets as in Sivakumar and Goutsias (1999, Example 3.1). The energy function is

$$U(X) = \sum_{i=0}^{1} \left\| \gamma_i(X) \setminus \gamma_{i+1}(X) \right\|_W + \sum_{j=1}^{2} \left\| \phi_j(X) \setminus \phi_{j-1}(X) \right\|_W, \tag{6.142}$$

where

$$\gamma_k(X) = X \circ kB,$$

$$\phi_k(X) = X \bullet kB,$$

and

$$\|Y\|_W = \sum_{w \in W} Y(w)$$

for

$$Y(w) = \begin{cases} 0 & \text{if white,} \\ 1 & \text{if black,} \end{cases}$$

with B being the rhombus, so that $2B = B \oplus B$. The size density $s(k)$ of X is

$$s(k) = \begin{cases} \dfrac{1}{NM}\mathbf{E}\left(\left\|\gamma_k(X) - \gamma_{k+1}(X)\right\|_W\right) & \text{for } k = 0, 1, 2, \ldots, \\ \dfrac{1}{NM}\mathbf{E}\left(\left\|\phi_{|k|}(X) - \phi_{|k+1|}(X)\right\|_W\right) & \text{for } k = -1, -2, \ldots. \end{cases} \tag{6.143}$$

6.6.2 Dilated fibre and surface processes

Interesting random sets are obtained when the fibres (surfaces) of a fibre (surface) process are enlarged by set-theoretic dilation. An example is the *Boolean cylinder model*, which is obtained when the lines of a Poisson line process are dilated by the ball $B(o, r)$. Its basic characteristics are given in Ohser and Schladitz (2009, pp. 251–2) and Spiess and Spodarev (2011); see also Heinrich and Spiess (2009). A similar model is obtained by dilating the planes of a Poisson plane process. Redenbach (2011) studies the system of dilated Poisson-Voronoi tessellation faces.

6.6.3 Excursion sets

Random fields and u-level excursion sets

Excursion sets of random fields form another important class of random set models. The most well-studied case is that of excursion sets of stationary Gaussian and Gaussian-related random fields. A thorough mathematical treatment of the theory of random fields and excursion sets can be found in Adler (1981, 2000), Piterbarg (1996), Adler *et al.* (2010), Adler and Taylor (2007, 2011) and Vanmarcke (2010). This section presents a short introduction.

Excursion sets are a 'continuous alternative' to germ–grain models: the reader should compare Figures 3.2 and 6.13 to see the difference. The boundaries of excursion sets, typically, are 'smoother' than those of germ–grain models, but, by suitable choice of the covariance function of the underlying random field, can also be fractals; see the discussion of the smoothness parameter in Formulae (6.150) and (6.151) on p. 261. Random fractals will not be discussed here and the interested reader is referred to Stoyan and Stoyan (1994) and Mörters (2010).

A real-valued spatial process $\{Y(x) : x \in \mathbb{R}^d\}$, or $\{Y(x)\}$ for short, is called a *Gaussian (random) field* if the finite-dimensional distributions

$$\mathbf{P}(Y(x_1) \in B_1, \ldots, Y(x_n) \in B_n) \qquad \text{for Borel sets } B_1, \ldots, B_n \qquad \text{for } n \geq 1 \tag{6.144}$$

are multivariate normal. Hence a Gaussian field is completely characterised by its *mean function*

$$m(x) = \mathbf{E}\big(Y(x)\big) \qquad \text{for } x \in \mathbb{R}^d, \tag{6.145}$$

and *covariance function*

$$k(x_1, x_2) = \mathbf{E}\big((Y(x_1) - m(x_1))(Y(x_2) - m(x_2))\big) \qquad \text{for } x_1, x_2 \in \mathbb{R}^d. \tag{6.146}$$

A Gaussian field is stationary and isotropic, which is assumed throughout this section, if its $m(x)$ is a constant μ and $k(x_1, x_2)$ is a function only of the distance $r = \|x_1 - x_2\|$ of the

points x_1 and x_2. In this case, with some abuse of notation, write

$$k(x_1, x_2) = k(\|x_1 - x_2\|) = k(r), \qquad r \geq 0.$$

The value $\sigma^2 = k(0)$ is the *variance* of the random field $\{Y(x)\}$. Any Gaussian field can be normalised to have zero mean and unit variance. Hence, without loss of generality, hereinafter only normalised Gaussian fields, denoted by $\{Z(x)\}$, are considered.

If $k(r)$ is continuous, then the Gaussian field is *mean square continuous* in the sense that

$$\mathbf{E}\big(Z(x) - Z(x+\mathbf{r})\big)^2 = 2\big(k(0) - k(r)\big) \to 0 \qquad \text{for } r = \|\mathbf{r}\| \to 0, \tag{6.147}$$

but the realisations, known as *sample functions* or *sample paths*, are not necessarily continuous. A sufficient condition on $k(r)$ for almost surely continuous sample functions over $I \subset \mathbb{R}^d$ is that for some positive constants c and ε,

$$k(0) - k(\|x\|) \leq \frac{c}{|\log \|x\||^{1+\varepsilon}} \qquad \text{for all } x \in I \tag{6.148}$$

(Adler, 1981, p. 62).

Not any function can be used as a covariance function, because for any finite set of locations $\{x_1, \ldots, x_n\}$, the covariance matrix of the finite dimensional distribution (6.144) has to be nonnegative definite; functions that fulfil this condition are called *positive definite*; see Adler and Taylor (2007, Theorem 5.7.2) and Gneiting and Guttorp (2010, pp. 20–3) for necessary and sufficient conditions for positive definiteness.

Perhaps the most important class of covariance functions is the *Matérn* class (Matérn, 1986, p. 18), given by

$$k(r) = \frac{2^{1-\nu}}{\Gamma(\nu)} \left(\frac{r}{\theta}\right)^{\nu} K_\nu \left(\frac{r}{\theta}\right) \qquad \text{for } \nu, \theta > 0, \tag{6.149}$$

where $K_\nu(\cdot)$ is the modified Bessel function of the second kind, θ a scale parameter and ν a smoothness parameter such that the sample functions are m times differentiable if and only if $m < \nu$. Members of the *Matérn* class include

$$\nu = \tfrac{1}{2}, \quad k(r) = \exp\left(-\frac{r}{\theta}\right),$$

$$\nu = 1, \quad k(r) = \frac{r}{\theta} K_1 \left(\frac{r}{\theta}\right),$$

$$\nu = \tfrac{3}{2}, \quad k(r) = \left(1 + \left(\frac{r}{\theta}\right)\right) \exp\left(-\frac{r}{\theta}\right),$$

$$\nu = \tfrac{5}{2}, \quad k(r) = \left(1 + \frac{r}{\theta} + \frac{1}{3}\left(\frac{r}{\theta}\right)^2\right) \exp\left(-\frac{r}{\theta}\right).$$

Other important classes of covariance functions are the *powered exponential family*

$$k(r) = \exp\left(-\left(\frac{r}{\theta}\right)^{\alpha}\right) \qquad \text{for } 0 < \alpha \leq 2, \tag{6.150}$$

the *Cauchy family*

$$k(r) = \left(1 + \left(\frac{r}{\theta}\right)^{-\alpha}\right)^{-\beta/\alpha} \qquad \text{for } 0 < \alpha \leq 2 \text{ and } \beta > 0, \tag{6.151}$$

and the *spherical covariance function*

$$k(r) = \begin{cases} 1 + \dfrac{3}{2}\dfrac{r}{\theta} + \dfrac{1}{2}\left(\dfrac{r}{\theta}\right)^3 & \text{if } r \leq \theta, \\ 0 & \text{otherwise,} \end{cases} \tag{6.152}$$

where $\theta > 0$ is a scale parameter. The spherical covariance function is closely related to the set covariance of a three-dimensional ball with diameter θ. By the way, covariance functions related to balls of other dimensions are also used.

The long-memory parameter β in the Cauchy family (6.151) controls the decay rate of $k(r)$ such that the smaller the value of β, the stronger the long-range dependence.

Fractal structures are possible, and they could result from choosing small values for α in (6.150) and (6.151). The smoothness parameter α governs the behaviour of $k(r)$ at the origin, and the fractal dimension of the sample functions is equal to $d + 1 - \frac{\alpha}{2}$. Therefore, the larger the value of α, the smoother the sample functions. However, note that even the sample functions can be made smoother by increasing α, they are still not differentiable if $\alpha < 2$. Nevertheless, when $\alpha = 2$, the sample functions become infinitely differentiable.

Note that whilst the Matérn, the powered exponential and the Cauchy family are valid covariance functions for any $d \geq 1$, the spherical function is valid only for $d \leq 3$. For more possible forms; see Schlather (1999) and Gneiting and Guttorp (2010, pp. 24–6).

Gaussian fields may serve as building blocks for other random fields. An important example is the χ^2 *field with parameter* n:

$$\chi_n^2(x) = \sum_{i=1}^{n} Z_i(x)^2 \qquad \text{for } x \in \mathbb{R}^d, \tag{6.153}$$

where the $\{Z_i(x)\}$ are independent normalised Gaussian fields with the common covariance function $k(r)$. The mean and the covariance function of $\{\chi_n^2(x)\}$, denoted by $\mu^{*(n)}$ and $k^{*(n)}(r)$ respectively, are given by

$$\mu^{*(n)} = n, \tag{6.154}$$

$$k^{*(n)}(r) = 2nk(r)^2 \qquad \text{for } r \geq 0. \tag{6.155}$$

The *u-level excursion set* of a random field $\{Y(x)\}$, denoted by $\Xi_u(Y)$, results from truncating $\{Y(x)\}$ at level u, that is,

$$\Xi_u(Y) = \{x \in \mathbb{R}^d : Y(x) \geq u\}. \tag{6.156}$$

The closure of $\Xi_u(Y)$ is a random closed set, and if the sample functions are continuous, then $\Xi_u(Y)$ itself is a random closed set. Figure 6.13 on next page shows realisations of such random sets. These have boundaries 'smoother' than Boolean models, compare with Figure 3.2 on p. 66.

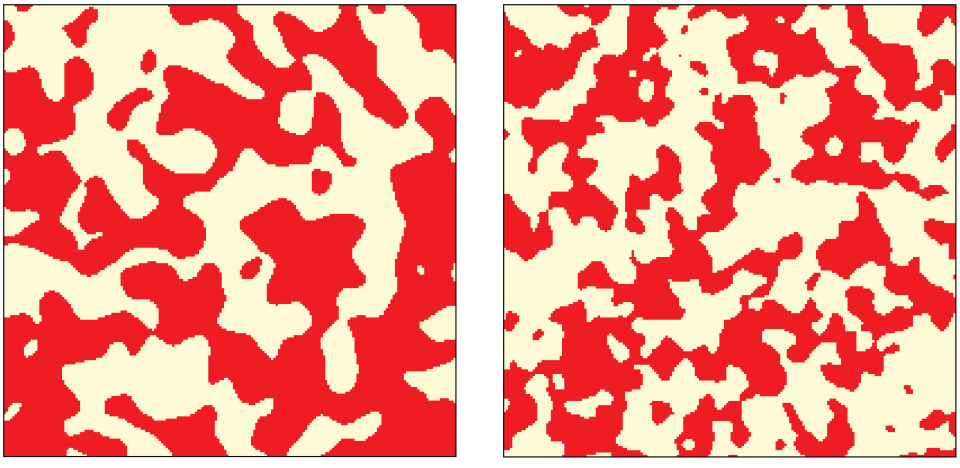

Figure 6.13 Simulated 0-level excursion sets in $[0, 20]^2$ of normalised Gaussian fields with covariance functions (a) $k(r) = \mathrm{e}^{-r^2}$ and (b) $k(r) = \left(1 + r^2\right)^{-2}$, $r \geq 0$. Note that for these models at the 0 level, because of symmetry, volume fraction is 0.5 and the number of holes and the number of connected components are, on average, the same and hence the specific connectivity number is zero. The structural difference results from different covariance functions: for case (a) the covariance function decreases more slowly for small r than for (b).

For a normalised Gaussian field $\{Z(x)\}$ the volume fraction p of $\Xi_u(Z)$ is clearly given by

$$p = \mathbf{P}\big(Z(0) \leq u\big) = 1 - \Phi(u), \tag{6.157}$$

where $\Phi(u)$ denotes the standard normal distribution function.

Also, for the planar case $d = 2$, the (noncentred) covariance $C_u(r)$ of $\Xi_u(Z)$ can be calculated for a normalised Gaussian field $\{Z(x)\}$ with covariance function $k(r)$:

$$C_u(r) = p^2 + \frac{1}{2\pi} \int_0^{k(r)} \frac{\mathrm{e}^{-\frac{u^2}{1+z}}}{\sqrt{1-z^2}}\, \mathrm{d}z \qquad \text{for } r \geq 0. \tag{6.158}$$

In particular, when $u = 0$,

$$C_0(r) = \frac{1}{4} + \frac{1}{2\pi} \sin^{-1} k(r) \qquad \text{for } r \geq 0. \tag{6.159}$$

For a χ^2 field, the planar u-level excursion set $\Xi_u(\chi_n^2)$ has the following covariance:

$$C_u^*(r) = p^2 + \frac{1}{\pi} \int_0^{|k(r)|} \frac{\mathrm{e}^{-\frac{u^2}{1+z}} - \mathrm{e}^{-\frac{u^2}{1-z}}}{\sqrt{1-z^2}}\, \mathrm{d}z \qquad \text{for } r \geq 0, \tag{6.160}$$

where $k(r)$ is the common covariance function of the underlying normalised Gaussian fields and p the volume fraction of $\Xi_u(\chi_n^2)$.

The linear contact distribution function $H_l(r)$ of $\Xi_u(Y)$ can sometimes be computed explicitly. It is related to the first passage time distribution of a certain associated process. For a normalised Gaussian field $\{Z(x)\}$ with twice differentiable covariance function $k(r)$, Nott and Wilson (1997) show that

$$H_l(r) = \mathbf{P}(T_u < r), \tag{6.161}$$

in which

$$T_u = \inf\{t > 0 : \xi_u(t) = u\} \tag{6.162}$$

is the first passage time of the process $\{\xi_u(t)\}$, defined as

$$\xi_u(t) = uk(t) - \eta\frac{k'(t)}{\lambda_2} + \zeta(t) \qquad \text{for } t > 0,$$

where λ_2 is the so-called *second spectral moment*, that is,

$$\lambda_2 = -k''(0), \tag{6.163}$$

which is assumed to be finite and positive throughout this section, η is a Rayleigh random variable with probability density function

$$f_\eta(t) = \lambda_2^{-1} t\mathrm{e}^{-t^2/(2\lambda_2)},$$

and $\{\zeta(t)\}$ is a zero mean nonstationary Gaussian process, independent of η, with covariance function

$$k_\zeta(s,t) = k(t-s) - k(t)k(s) - \frac{k'(t)k'(s)}{\lambda_2}.$$

There is no closed form expression for the distribution of T_u, and Lindgren and Rychlik (1991) suggest a regression approximation for this distribution.

For $S_V^{(d)}$, the specific surface area, Formula (6.48) gives

$$S_V^{(d)} = -\frac{db_d}{b_{d-1}}C_u'(0+). \tag{6.164}$$

Ballani *et al.* (2012) show that whenever $k(r)$ is twice differentiable, then

$$C_u'(0+) = -\frac{\sqrt{\lambda_2}}{2\pi}\mathrm{e}^{-u^2/2}, \tag{6.165}$$

where λ_2 is the second spectral moment defined in (6.163) above.

One-dimensional random sets are important when one considers linear sections, and such random sets are always unions of disjoint closed intervals. For a u-level excursion set in $\mathbb{R}$, the number of disjoint closed intervals will be the number of *upcrossings*, where an upcrossing happens whenever the sample function (which has been assumed to be continuous) crosses the level u from below.

Denote by N_u the number of upcrossings of the level u on $[0, 1]$ by a normalised one-dimensional Gaussian process with covariance function $k(r)$. Rice (1944, 1945) shows that

$$\mathbf{E}(N_u) = \frac{\sqrt{\lambda_2}}{2\pi} \mathrm{e}^{-u^2/2}, \tag{6.166}$$

which agrees with (6.164) and (6.165). Formula (6.166) immediately suggests unbiased estimators for λ_2, which is the only parameter for the limiting distribution of the maximum of $\{Z(x)\}$; see Adler (1981, pp. 68–9).

The number of upcrossings N_u in $[0, 1]$ is in fact the one-dimensional case of the specific connectivity number $v_0(u)$, which is also known as the *mean differential topology characteristic* per unit volume in the context of excursion sets. For a normalised Gaussian field $\{Z(x)\}$ under some smoothness and nondegeneracy regularity conditions,

$$v_0(u) = \frac{\mathrm{e}^{-u^2/2}\sqrt{\lambda_2^d}}{(2\pi)^{(d+1)/2}} \sum_{j=0}^{d-1} \frac{(d-1)!(-1)^j u^{d-2j-1}}{j!(d-2j-1)!2^j} \tag{6.167}$$

(Adler, 1981, Theorem 5.3.1, and Adler, 2000, Theorem 3.2.2). For $d = 1$, Formula (6.167) is the same as the Rice formula (6.166), whilst for the planar and spatial case, it leads to

$$N_A = \frac{u\mathrm{e}^{-u^2/2}\lambda_2}{(2\pi)^{3/2}}, \tag{6.168}$$

$$N_V = \frac{(u^2-1)\mathrm{e}^{-u^2/2}\sqrt{\lambda_2^3}}{(2\pi)^2}, \tag{6.169}$$

the specific connectivity number. Note that it is not the same as the mean Euler–Poincaré characteristic of the intersection of the excursion set and a unit cube, because of the complication at the intersection between the boundary and the excursion set. The interested reader is referred to Adler and Taylor (2007, pp. 140–1 and 289–98).

The chord lengths of sections of both Ξ_u and its complement are studied in Estrade *et al.* (2012). In general subsequent chords have dependent lengths, different to the case of a Boolean model. For the length distribution functions, bounds in terms of the random field characteristics can be given. The paper by Demichel *et al.* (2011) discusses the tails of chord length distributions and shows that the decay is always faster than for any negative power function.

Formula (6.169) shows that N_V as a function of the level u has zeros at $u = -1$ and $u = +1$. The presence of zeros can be explained intuitively by the relationship that the Euler–Poincaré characteristic in three dimensions is

$$\#\text{components} - \#\text{tunnels} + \#\text{holes};$$

see Section 1.8. Tunnels and holes, if any, are very rare for high u (positive N_V), tunnels dominate for u around 0 (negative N_V), and for deeply negative u there is one component and many holes (positive N_V). Thus there are zeros of N_V, and it is a matter of mathematical beauty that these are just at -1 and $+1$.

Worsley (1997) and Adler and Taylor (2011, Chapter 5) describe the applications of the Euler–Poincaré characteristic of the excursion set in astrophysics and medical imaging. Astrophysicists were able to construct a map of (standardised) galaxy density. At each level u, the empirical Euler–Poincaré characteristic of the u-level excursion set was plotted to obtain a function of u. Such a plot on one hand suggested a good agreement between the empirical Euler–Poincaré characteristics and the theoretical ones from the excursion sets of a Gaussian field, and on the other hand revealed the structure of the universe: at high levels of u, the topology of the universe is like a meatball, at medium levels a sponge and at low levels a bubble. Another example came from the cosmic microwave background radiation data across the full sky. These data are directional and hence can be modelled by a random field on the sphere. Again, the empirical Euler–Poincaré characteristics as a function of the level u were compared with the theoretical ones from the fitted Gaussian model. Some evidence of non-Gaussianity was found. This approach is quite common in comparing competing theories in cosmology.

For medical imaging, paired data on brain activities, taken by positron emission tomography or functional magnetic resonance imaging, were collected when the participants were performing a task and were at rest. Under the random noise hypothesis, the sample mean of the pointwise differences at each voxel inside the brain follows a normal distribution. Hence, these sample means, after normalisation, can be modelled by a Gaussian random field on a compact set, representing the brain, in $\mathbb{R}^3$. Consider its u-level excursion set. When u is sufficient high, only the global maximum will survive and the Euler–Poincaré characteristics is 1. Thus, for sufficient high levels, the mean Euler–Poincaré characteristics can approximate the tail distribution of supremum of the Gaussian field (Adler and Taylor, 2007, Formula (14.0.2)). Consequently a critical level u_0 can be obtained, exceeding which will lead to rejection of the random noise hypothesis; if the hypothesis is rejected then it is possible to identify the brain region associated with the task performed.

Arns *et al.* (2002) considered Mecke's morphological functions for excursion sets. Vogel (2002) discussed applications in soil research, in which excursion sets were used to model porous media. For three-dimensional reconstructions of porous networks using correlated Gaussian fields (and other characteristics of porous materials); see Schüth *et al.* (2002).

For a χ^2_n field in which the component normalised Gaussian fields satisfy some smoothness and nondegeneracy regularity conditions, the specific connectivity number for a general d is also explicitly known (Worsley, 1994). The formulae for the planar and spatial cases are

$$N_A = \frac{u^{(n-2)/2}\mathrm{e}^{-u/2}\lambda_2}{2^{n/2}\pi\Gamma(n/2)}\big(u-(n-1)\big), \tag{6.170}$$

$$N_V = \frac{u^{(n-3)/2}\mathrm{e}^{-u/2}\sqrt{\lambda_2^3}}{(2\pi)^{3/2}2^{(n-2)/2}\Gamma(n/2)}\big(u^2-(2n-1)u+(n-1)(n-2)\big). \tag{6.171}$$

Statistics

It is easy to see that in random-set statistics it suffices to use normalised Gaussian fields. If so, only the level parameter u and the covariance function $k(r)$ have to be estimated. The level u can be easily estimated from the relationship given in (6.157), where for p the observed area or volume fraction is plugged in. The covariance function can then be estimated nonparametrically, with the help of Formula (6.158), from an estimate of the random set covariance $C(r)$,

obtained from the binary image using the method described in Section 6.4.3. However, this way is difficult since inverting the integral in Formula (6.158) does not necessarily yield the positive definite function property required for a valid covariance function. Thus, again the two-step method is recommended, where in the first step a rough estimate of $k(r)$ is determined and in the second step parametric statistical methods are applied.

For the second step, parametric analysis, various approaches exist.

(1) *Method of moments*
If $k(r)$ contains one or two parameters, then plugging in the empirical specific surface area and specific connectivity number into Formulae (6.164), (6.165), and (6.168) or (6.169), gives estimates for the parameters.

(2) *Minimum contrast*
Another possibility is to minimise the distance between the theoretical form of some characteristic function and its empirical values. For example, the theoretical random set covariance $C_{\hat{u}}(r)$ of the excursion set at the estimated level $\hat{u}$ can be compared with the empirical covariance. However, there is a potential structural defect in this approach. Whilst $C_u(r)$ in Formula (6.158) is at least p^2, the empirical covariance can be smaller, due to for example holes around connected components.
A better candidate may be the linear contact distribution function $H_l(r)$, which can be easily estimated using the methods described in Section 6.4.5. Their theoretical counterparts given in Formulae (6.161) and (6.162) can be approximated efficiently (Rychlik and Lindgren, 1993). Thus, minimum contrast estimators for the parameters can be computed; see Nott and Wilson (1996).

(3) *Pairwise likelihood*
Denote by $\{z(x)\}$ a given binary image. Instead of full likelihood, Nott and Rydén (1999) considered pairwise likelihood

$$\prod_{i<j} p\big(\mathbf{1}(z(x_i) > u), \mathbf{1}(z(x_j) > u); \Theta\big)$$

where $p(\cdot, \cdot; \Theta)$ is the joint probability density function of the two binary random variables $\big(\mathbf{1}(Z(x_i) > u), \mathbf{1}(Z(x_j) > u)\big)$ and Θ the vector of parameters.

In practical implementation, the pairwise likelihood takes the product over distinct locations

$$L\big(\Theta; \Xi_u(z)\big) = \sum_{x \in \mathscr{L}} \prod_{x' \in \mathscr{L}'} p\big(\mathbf{1}(z(x) > u), \mathbf{1}(z(x + x') > u); \Theta\big), \qquad (6.172)$$

where $\mathscr{L}$ and $\mathscr{L}'$ are two finite sets of sites in the sampling window W such that $\mathscr{L} \subset \{x : x + \mathscr{L}' \in W\}$. The maximiser $\hat{\Theta}$ of $L\big(\Theta; \Xi_u(z)\big)$ is the maximum pairwise likelihood estimator for Θ. Nott and Rydén (1999) showed that $\hat{\Theta}$ is consistent and asymptotically follows the normal distribution.

Example 6.6. *Modelling heather pattern by excursion set*
Figure 6.14(a) shows a data set which has been already often analysed by random-set methods. The dark areas in the figure show areas covered by heather over a $10 \times 20\,\mathrm{m}^2$ rectangular

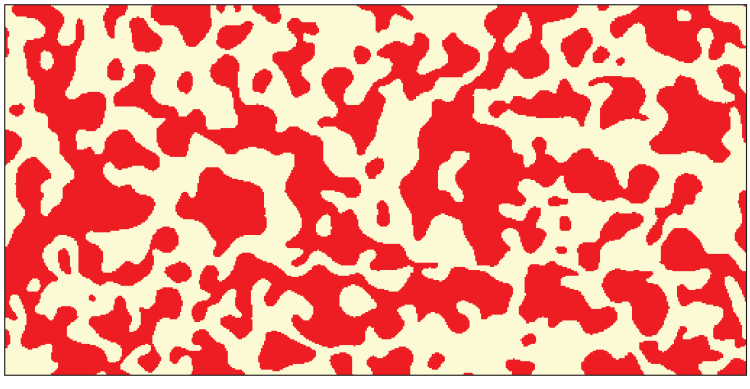

(a)

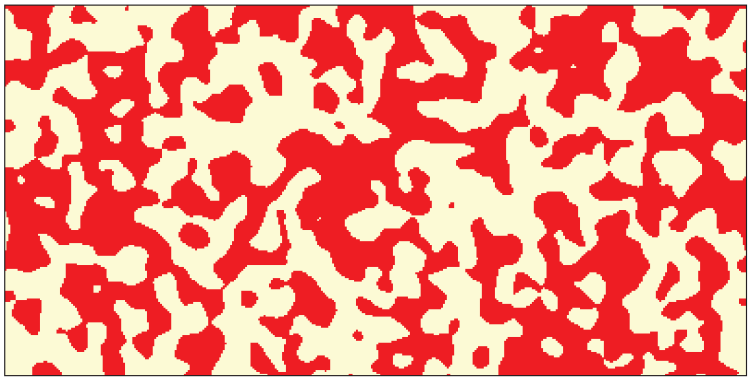

(b)

Figure 6.14 (a) The heather data in a $10 \times 20\,\mathrm{m}^2$ rectangle (available from the `spatstat` package in `R`); (b) a simulated realisation of a 0-level excursion set of a normalised Gaussian field in 10×20 rectangle, with covariance function $k(r) = \mathrm{e}^{-(r/0.4)^2}$.

window at Jädraås, Sweden. Since heather appears in bushes, it is natural to try a statistical fit with a germ–grain model, where the 'grains' are perhaps the heather bushes. In this spirit Diggle (1981) and Møller and Helisová (2010) try to fit a Boolean model with random discs or more general germ–grain models to the data. However, their results do not confirm the germ–grain model assumption. In contrast, visual inspection already raises doubt whether a model of this type is appropriate. Comparison between Figures 6.13 and 6.14(a) suggests that an excursion set, perhaps of a Gaussian field, may be a good model. The questions why the heather pattern sample looks like an excursion set and how the excursion set hypothesis can be tested against the germ–grain model hypothesis will not be discussed.

The estimates of the fundamental random-set characteristics are

$$\hat{A}_A = 0.50, \quad \hat{L}_A = 1.77\,\mathrm{m}^{-1} \quad \text{and} \quad \hat{N}_A = 0.185\,\mathrm{m}^{-2}.$$

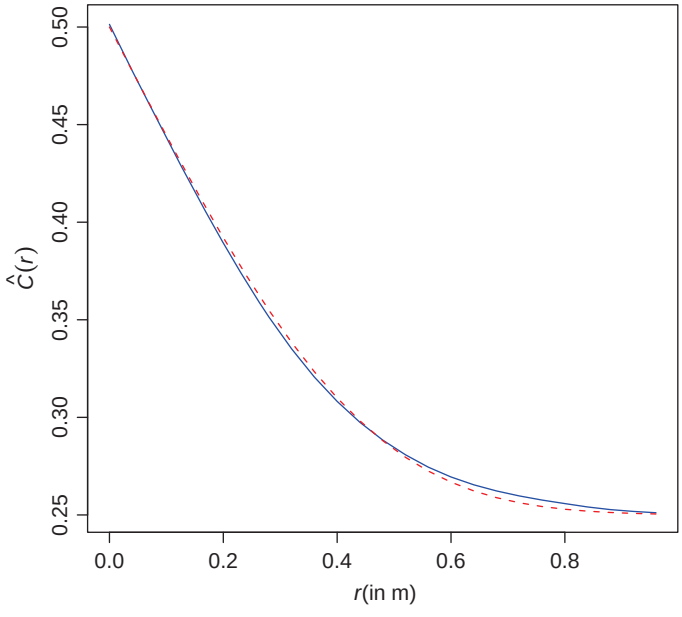

Figure 6.15 The empirical covariance (—) and the theoretical covariance (- - -) of the fitted excursion set model for the heather data. Courtesy of K. S. Helisová.

Figure 6.15 shows the empirical covariance $\hat{C}(r)$. (The authors thank K. S. Helisová for the numerical values of $\hat{A}_A$ and $\hat{L}_A$, estimated by the method of Mrkvička and Rataj, 2008, and for the values of $\hat{C}(r)$.)

These values can be used to estimate Boolean model parameters, by means of Formulae (3.50) to (3.52). Under the assumption that the grains are discs, for the mean radius the value 0.41 m is obtained and for the second moment of radius 0.162 m^2. This yields for the radius a negative variance, which seems to show that a Boolean model with discoidal grains is not suitable.

As an alternative, the u-level excursion set of a normalised Gaussian field is fitted to the heather data. For the covariance function $k(r)$ of the random field the simplest *ad hoc* choice,

$$k(r) = \exp\left(-\left(\frac{r}{\theta}\right)^2\right) \qquad \text{for } r \geq 0, \tag{6.173}$$

is made, in order to get smooth boundaries as observed.

Since (by good luck) $\hat{A}_A = 0.5$, u is estimated as $\hat{u} = 0$. Formulae (6.164) and (6.165) yield

$$L_A = -\pi C'(0+) = \frac{1}{\sqrt{2}\theta}.$$

This leads to the estimate

$$\hat{\theta} = 0.40\,\mathrm{m},$$

which is very close to the estimate 0.38 obtained by the pairwise likelihood approach (Nott and Rydén, 1999) and the estimate 0.39 obtained by minimising the L^2-norm of theoretical and empirical linear contact distribution of the right half of the data (Nott and Wilson, 1997).

Figure 6.15 shows, in addition to the empirical $\hat{C}(r)$, also the theoretical covariance of the excursion set model with covariance function given in (6.173) and $\theta = 0.4$, and a simulated realisation of the fitted model is given in Figure 6.14(b).

To check whether the model offers a good fit of the data, a parametric bootstrap test (see Sections 3.4.2 and 4.7.10) can be used. A summary characteristic such as the linear contact distribution function $H_l(r)$ or the covariance is chosen. Measured in, for example the L^2- or L^∞-norm, the deviations from the theoretical values of the empirical values in the given data and in 999 independent simulated realisations of the fitted models are then calculated. If the deviation calculated from the given data is not among the top 5% of these 1000 deviations, then the model is not rejected. Alternatively, simulated confidence envelopes can also be employed for visual inspection of the fit. Nott and Rydén (1999) has, using the covariance, adopted the latter approach, and found that such an excursion set model for the heather data was not rejected.

6.6.4 Birth-and-growth processes

Fundamentals

A birth-and-growth process $\{\Xi_t\}$ is a dynamic germ–grain model used for modelling situations in which germs (nuclei) are born at random instants at random spatial locations. Each germ x_i is the origin of a grain $\Xi_{t,i}$, which evolves in time according to a given growth law (Villa and Rios, 2010, and Aletti *et al.*, 2011). At time t the random closed set Ξ_t can be written as

$$\Xi_t = \bigcup_i (\Xi_{t,i} + x_i),$$

where the union is taken over all germs existing at time t. Symbolically, the evolution is written as

$$\Xi_t = \left(\Xi_0 \oplus \int_0^t G_\tau \mathrm{d}\tau\right) \cup \bigcup_{s\in[0,t]} \left(\mathrm{d}B_s \oplus \int_s^t G_\tau \mathrm{d}\tau\right), \tag{6.174}$$

where $\{G_\tau\}$ is an increasing compact convex set-valued process representing growth, and $\{B_s\}$ is an increasing closed set-valued process representing nucleation. The infinitesimal $\mathrm{d}B_s$ can be understood as $\lim_{\delta s\to 0}\left(B_{s+\delta s} - B_s^{\mathrm{int}}\right)$. Here growth is nonlocal since the same Minkowski-addend $G_t \mathrm{d}t$ is added to every $x \in \Xi_t$ to represent the growth between $(t, t + dt]$.

In some applications the growth depends on the 'ages' of the grains, so that at time t the model is given by

$$\Xi_t = \left(\Xi_0 \oplus \int_0^t G_\tau \mathrm{d}\tau\right) \cup \bigcup_{s\in[0,t]} \left(\mathrm{d}B_s \oplus \int_0^{t-s} G_\tau \mathrm{d}\tau\right). \tag{6.175}$$

An analogous model with discrete time is considered in Aletti *et al.* (2009), where also statistical problems are discussed.

This book considers only spatially stationary (or spatially statistically homogeneous) structures, where Ξ_t forms a stationary random closed set at each time t. Particular cases where the germs are located at single planes or lines (in $\mathbb{R}^3$) are considered in Cahn (1956) and Villa and Rios (2010). Bounded growing sets are considered in Cressie and Hulting (1992), Deijfen (2003) and Jónsdóttir *et al.* (2008); see also the references to random compact set models on p. 215.

The following construction is closely related to the Boolean model. The germ-birth rate is denoted by $\lambda(t)$. Births can happen anywhere in $\mathbb{R}^d$ and all germs born in the time interval $[0, t]$ form a homogeneous Poisson process in $\mathbb{R}^d$ of intensity λ_t,

$$\lambda_t = \int_0^t \lambda(u)\mathrm{d}u. \tag{6.176}$$

An important special case is

$$\lambda(t) = ct^{m-1} \qquad \text{for } t \geq 0, \tag{6.177}$$

where c and m are positive constants. (This intensity leads to the so-called Weibull theory; see below.) Important is also the so-called site-saturated case:

$$\lambda(t) = \lambda\delta(t) \qquad \text{for } t \geq 0, \tag{6.178}$$

in which $\delta(t)$ is the Dirac delta function and λ a positive constant, meaning that all germs, forming a homogeneous Poisson process of intensity λ, start to grow at time $t = 0$.

The grains grow according to some growth rate or velocity $v(t)$. If a grain with germ x grows spherically and born at time s, then the grain is at time t the ball $B(x, r_t)$ with radius

$$r_t = \int_s^t v(u)\mathrm{d}u. \tag{6.179}$$

In this case, if in addition $v(t)$ decays exponentially and $m = -d$ in (6.177), the resultant structure of such a birth-and-growth process is a fractal (Chiu, 1995c).

The definitions here have been given in terms of 'time t'. However, in some (mechanical) applications the rôle of time is played by some load σ. The germs then appear with increasing load and may lead to fractures.

In this book interactions of growing grains are excluded. In reality, for example, it may happen that a growing segment grain stops growing once it contacts another grain.

The main aim of this section is to calculate the volume fraction $V_V(t)$ of Ξ_t at time t. It is given by

$$V_V(t) = \mathbf{P}(o \in \Xi_t), \tag{6.180}$$

for which formulae will be given.

Birth-and-growth processes have found applications in the contexts of polymerisation (Capasso, 2003) and of nucleation of materials (Cahn, 1956).

Evolution processes for random closed sets are also modelled by stochastic differential equations; see Lorenz (2010, Section 3.7), Kloeden and Lorenz (2011) and Aletti *et al.* (2011). Lorenz and Kloeden speak about 'stochastic morphological evolution equations' and use ideas

from set-valued analysis as in Aubin (1999). By means of an extended form of differential equations beyond the body of vector spaces they could develop a general theory without the convexity assumption as, for example, in Malinowski and Michta (2010). It is to be expected that this approach will permit the pure geometrical modelling to be enriched with physical ideas.

The Weibull model

In this example, which follows Jeulin (1994), instead of time t some mechanical load σ is considered, which is increasing like time. According to a birth rate $\lambda(\sigma)$ germs are activated in the whole $\mathbb{R}^d$. The birth rate has the form

$$\lambda(\sigma) = c\sigma^{m-1} \qquad \text{for } \sigma \geq 0, \tag{6.181}$$

with $m \geq 1$; c is some positive constant. (The corresponding inhomogeneous Poisson process is sometimes called Weibull-Poisson process.)

A Borel set B of volume $v_d(B)$ is considered. It is said that B fails under load when the first germ is born in B. Let S be the random load under which B fails. Its distribution function $F(\sigma)$ is given by

$$F(\sigma) = \mathbf{P}\big(\Phi_B([0,t]) > 0\big),$$

where Φ_B is the one-dimensional point process of germ birth instants for B. This is a Poisson process of intensity $\lambda(\sigma)v_d(B)$. Consequently

$$\mathbf{P}\big(\Phi_B([0,t]) > 0\big) = 1 - \mathbf{P}\big(\Phi_B([0,t]) = 0\big) = 1 - \exp\left(-v_d(B)\int_0^t \lambda(u)\mathrm{d}u\right),$$

and for the birth rate given in (6.181),

$$F(\sigma) = 1 - \exp\left(-v_d(B)\,\frac{c\sigma^m}{m}\right),$$

or

$$F(\sigma) = 1 - \exp\left(-\Big(\frac{\sigma}{\sigma_0}\Big)^m\right) \qquad \text{for } \sigma \geq 0. \tag{6.182}$$

This is the well-known Weibull distribution. The parameter m is called *Weibull modulus*.

Length distribution of growing segments

In this example, t and 'time', instead of σ and 'load', are used, though the latter could also be applied. The planar case is considered. Each grain is a segment with one endpoint at its germ and the other endpoint moves with constant velocity v and without any interaction with other grains.

The birth rate is

$$\lambda(t) = ct^{m-1} \qquad \text{for } t \geq 0, \tag{6.183}$$

which is the same as (6.181) with $\sigma = t$.

The problem is the determination of the length probability density function $f(l)$ of the segments existing at time t_0. Only segments initiated before t_0 count and clearly older segments are longer than younger ones.

The probability density function $g(t)$ of the instants of initiation is

$$g(t) = \frac{\lambda(t)}{\int_0^{t_0} \lambda(u)\mathrm{d}u} \qquad \text{for } 0 \leq t \leq t_0.$$

The length of a segment initiated at time t is $l = v(t_0 - t)$ and thus the probability density function of segment length is

$$f(l) = \frac{g\left(t_0 - \frac{l}{v}\right)}{v}.$$

With (6.183) this yields

$$f(l) = \frac{m\left(t_0 - \frac{l}{v}\right)^{m-1}}{vt_0^m} \qquad \text{for } 0 \leq l \leq vt_0. \tag{6.184}$$

This gives $f(0) = m/(vt_0)$ and $f(vt_0) = 0$ and between 0 and vt_0 the length density $f(l)$ is decreasing.

Such a distribution is often observed in statistical analyses of the lengths of geological faults; see Stoyan and Gloaguen (2011). Figure 6.16 shows the empirical and the fitted density $f(l)$ of the fault lengths in Figure 8.1 on p. 298.

The causal cone

The causal cone $\mathcal{C}(t, x)$ helps calculate the volume fractions of birth-and-growth processes. It is the space–time region in which at least one birth event has to take place in order to cover the point x by the time t; see Villa and Rios (2010). In the case of spherical growth the causal cone is

$$\mathcal{C}(t, x) = \left\{(u, y) : 0 \leq u \leq t, y \in B\left(x, \int_u^t v(z)\mathrm{d}z\right)\right\} \qquad \text{for } t \geq 0 \text{ and } x \in \mathbb{R}^d. \tag{6.185}$$

If (spatially) stationary processes are studied (as here) it suffices to consider $x = o$, because of (6.180).

Let furthermore Φ_{st} (st = spatial–temporal) be the point process of germs in $\mathbb{R}^d \times \mathbb{R}_+$, where each germ is characterised by both location x and instant of initiation t. Under the

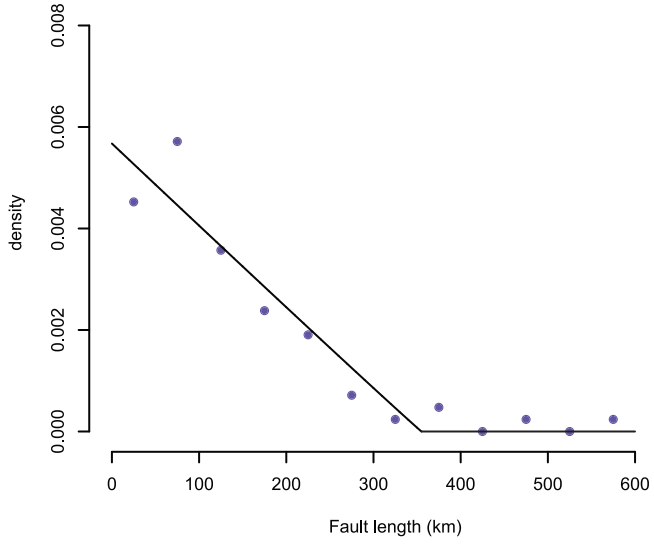

Figure 6.16 Empirical and fitted probability density function of the lengths of the geological faults of the NNE–SSW system in Figure 8.1. See Stoyan and Gloaguen (2011) for details and the estimation method. It is assumed that for very short faults there is some censoring.

assumptions above Φ_{st} is a Poisson process with intensity function $\lambda(t, x) = \lambda(t)$. The probability $\mathbf{P}(x \in \Xi_t)$ satisfies

$$\mathbf{P}(x \in \Xi_t) = \mathbf{P}\big(\Phi_{\mathrm{st}}(\mathcal{C}(t, x)) > 0\big),$$

and so putting $x = o$, one obtains

$$V_V(t) = 1 - \exp\left(-\int_0^t v_d\big(\mathcal{C}(t, o)\big)\lambda(u)\mathrm{d}u\right). \tag{6.186}$$

The KJMA theory

Kolmogorov (1937), Johnson and Mehl (1939) and Avrami (1939) developed a theory for the volume fractions $V_V(t)$ of birth-and growth processes as above, where the germs form a Poisson process in the whole $\mathbb{R}^d$. In the site-saturated case (6.178), Formula (3.45) for the volume fraction of a Boolean model can be used to obtain

$$V_V(t) = 1 - \exp\left(-b_d\lambda\left(\int_0^t v(u)\mathrm{d}u\right)^d\right) \qquad \text{for } t \geq 0, \tag{6.187}$$

since Ξ_t is a Boolean model with intensity λ and solid spherical grains of the same radius

$$r_t = \int_0^t v(u)\mathrm{d}u.$$

In the case of time-dependent $\lambda(t)$ again Ξ_t is a Boolean model, now with intensity $\lambda_t = \int_0^t \lambda(u)\mathrm{d}u$ and solid spherical grains with variable radii. Using the causal cone and (6.186)

yields

$$V_V(t) = 1 - \exp\left(-b_d \int_0^t \lambda(s) \left(\int_s^t v(u)\mathrm{d}u\right)^d \mathrm{d}s\right) \qquad \text{for } t \geq 0. \tag{6.188}$$

Balls on lines and planes

Cahn (1956) and Villa and Rios (2010) studied birth-and-growth processes where the germs are not scattered in the whole space but only on some planes or lines. In the spirit of these papers here two cases are discussed where the germs lie on the lines of a Poisson line process and on the planes of a Poisson plane process, both in $\mathbb{R}^3$. (These processes are explained in Section 8.2.2 and 8.2.3. Stationarity is always assumed.) For simplicity the case of constant growth velocity v and site-saturation (6.178) is considered.

The point process of all germs is the union of independent homogeneous one-dimensional (two-dimensional, respectively) Poisson processes of intensity ϱ on the lines (planes) of the line (plane) process. The result is a stationary Cox process in $\mathbb{R}^3$ of intensity ϱL_V (ϱS_V), where L_V (S_V) is the length (area) density of the line (plane) process.

According to the spirit of the causal cone, $V_V(t)$ is nothing else than the complement of the void-probability of the Cox process of germs:

$$V_V(t) = 1 - v_{B(o,vt)}, \tag{6.189}$$

as discussed in Section 5.2. Of course, the origin o is not covered by one of the balls $B(x, vt)$ centred at the germs if and only if the Cox process has no point within $B(o, vt)$.

The following gives the result for the line process, for the case known in the materials scientific context as 'grain edge nucleation', see Cahn (1956). The case of a plane process goes similarly.

The random number of lines of the line process hitting $B(o, vt)$ has a Poisson distribution of mean $\mu = \pi v^2 t^2 L_V$, which follows from (8.14). The lengths of the chords generated by intersection of lines with the ball $B(o, vt)$ are independent and have the probability density function

$$f(l) = \frac{l}{2(vt)^2} \qquad \text{for } 0 \leq l \leq 2vt;$$

see Formula (10.61). Since the germs on each line form a homogeneous Poisson process of intensity ϱ, the probability that on an intersecting line there is no point within $B(o, vt)$ is

$$p_0 = \int_0^{2vt} \exp(-\varrho\lambda) f(l)\mathrm{d}l = \frac{1 - (2vt\varrho + 1)\exp(-2vt\varrho)}{2(vt\varrho)^2}.$$

Then the void-probability is

$$v_{B(o,vt)} = \sum_{i=0}^{\infty} \frac{\mu^i}{i!} \mathrm{e}^{-\mu} p_0^i,$$

and

$$V_V(t) = 1 - \exp\bigl(-\mu(1 - p_0)\bigr). \tag{6.190}$$

For the plane process μ is $2rS_V$ and the radius distribution of the section discs of planes with the ball $B(o, vt)$ is the distribution given by Formula (10.42).

The case where the germs are scattered on the faces of tessellations is considered in Saxl *et al.* (2003).

Process duration

Suppose the birth-and-growth process takes place in a finite region, then the time until, if possible, the volume fraction becomes 1 (and hence the process stops) is of practical interest. Consider the model with birth rate given by (6.177) and spherical growth at a positive constant rate v, operating in a cube of side length L. The duration T_L of the process until the volume fraction in the cube reaches 1 can be approximated, when L is sufficiently large, by

$$T_L \simeq A_d^{-1} k c^{-1} b_d^{-1} v^{-d} \left(\frac{d+m}{m} \right)^{-1/(d+m)}, \tag{6.191}$$

where

$$A_d = \sum_{i=0}^{d} \binom{d}{i} \frac{(-1)^i}{i+m},$$

$$k = \log \left(\frac{1}{c b_d v^d} \left(\frac{c L^d}{m} \right)^{(d+m)/m} \right);$$

see Chiu (1995c), in which the limiting distributions of T_L for various forms of the birth rate are given.

Estimation of the birth rate and the growth speed

If the births of germs are observable only when they are born in places not occupied by any grains, then the actual birth rate $\lambda(t)$ will be different from the rate $\eta(t)$ of observable births.

At each time s, where $s \le t$, the process gives a (spatially) stationary Boolean model. Hence, for a model with spherical growth at a constant speed v, the two rates are related by

$$\eta(t) = \lambda(t) \exp \left(-b_d v^d \int_0^t (t-s)^d \lambda(s) \mathrm{d}s \right), \tag{6.192}$$

in which the term after $\lambda(t)$ on the right-hand side is the probability that a germ born is observable. Molchanov and Chiu (2000) suggest that by considering $\lambda(t)$ in (6.192) to be a constant λ_i in $[t_i, t_{i+1})$, where $t_i = i\delta$ for small $\delta > 0$, $\lambda(t)$ can be approximated by the solutions of

$$\lambda_i = \eta(t) \exp \left(\frac{b_d v^d \delta^{d+1}}{d+1} \sum_{k=0}^{i-1} \lambda_k \left((i-k)^{d+1} - (i-k-1)^{d+1} \right) \right) \qquad \text{for } i \ge 1, \tag{6.193}$$

with the initial value $\lambda_0 = \eta(\delta)$. A stepwise constant estimate of $\lambda(t)$ can then be obtained by replacing $\eta(t)$ in (6.193) by a kernel smoothed estimate of $\eta(t)$, based on the observed birth instants. If $\lambda(t)$ comes from some parametric family, minimising the distance between

the corresponding parametric form of $\eta(t)$ and a smoothed estimate of it yields the minimum contrast estimates of the parameters.

If v is unknown, the maximum likelihood approach suggested by Chiu *et al.* (2003) can be used. The likelihood $L(\lambda, v)$ of observing births at $\{(t_1, x_1), \ldots, (t_n, x_n) \in [0, \infty) \times \mathbb{R}^d\}$ is proportional to the product of the likelihood that there are births at t_i and the probability that, apart from those observed, there is no other birth in the causal cones $C(t_i, x_i)$, that is,

$$L(\lambda, v) \propto \left(\prod_{i=1}^{n} \lambda(t_i) \right) \exp\left(- \int_{\bigcup_{i=1}^{n} C(t_i, x_i)} \lambda(t) \mathrm{d}(t, x) \right). \tag{6.194}$$

Note that the larger the speed v, the bigger the causal cones. Thus, no matter what $\lambda(t)$ is, the likelihood in (6.194) increases with v and so the maximum likelihood estimator $\hat{v}$ of the speed v is the largest possible v such that none of the points (t_i, x_i) is contained in the interior of a causal cone.

When a parametric form of $\lambda(t)$ is given, maximising $L(\lambda, \hat{v})$ leads to the maximum likelihood estimators of the parameters of $\lambda(t)$.

Since the birth locations are stationary, even if only birth times but not birth locations can be observed, one still can express the likelihood in an integral form and consequently maximising it, often by numerical methods, to estimate the growth speed and the parameters of the birth rate; see Chiu *et al.* (2003).

6.7 Stochastic reconstruction of random sets

Often one is confronted with the problem of providing a quantitative description of the pore-space geometry and topology of a random-set-type structure. The starting point is data from a (small) sample, which may be only lower-dimensional, resulting from a planar (or even linear) section. The aim is to find a way to construct many samples of arbitrary size of the corresponding random set (typically one constituent of a random structure, e.g. the pore space of a porous medium) in full dimensionality. If a fully specified mathematical model is explicitly given, one can generate by simulation as many samples as one likes. Even if no model is specified, given such samples in a computer, as a pixel structure, one still can carry out calculations for the determination of characteristics of connectivity, flow and transport properties, etc. Of course, in the construction information from the original data is used and therefore one speaks about **re**construction.

The following sketches an approach for the case of a two- or three-dimensional stationary and isotropic random set Ξ, which is represented as a pixel structure, such that 0-pixels and 1-pixels, respectively, stand for pore and solid. The structure of Ξ is characterised by its volume fraction p and some summary characteristics $F_1(r), \ldots, F_m(r)$, for example $F_1(r) = C(r)$ (covariance) and $F_2(r) = L(r)$ (chord length distribution function). The aim is to obtain a pixel structure with periodic boundary conditions (to approximate stationarity) with summary characteristics $\hat{F}_1(r), \ldots, \hat{F}_m(r)$ which are as close as possible to the prescribed $F_1(r), \ldots, F_m(r)$. Thus in least-squares thinking the following minimisation problem has to be solved:

$$E = \alpha_1 \int \left(F_1(r) - \hat{F}_1(r)\right)^2 \mathrm{d}r + \ldots + \alpha_m \int \left(F_m(r) - \hat{F}_m(r)\right)^2 \mathrm{d}r \to \min! \tag{6.195}$$

The minimisation is by choosing an optimal pixel structure, where only such structures having a fraction p of 1-pixels are permitted. The coefficients α_i are weights, which should be chosen in such a way that the summands in (6.195) are of similar size order. Each integral is in practice often replaced by a summation over r going over suitable inter-pixel distances, which may by different for the different $F_i(r)$.

The term 'reconstruction' is appropriate, since the starting point is fragmentary information on Ξ and the above procedure is applied to build samples of Ξ that are in good agreement with these fragments. In the case of simulations from a parametric stochastic model one would not speak about reconstruction, even when the parameters come from a sample of Ξ.

The summary characteristics should be chosen in such a way that they describe possibly different aspects of the pixel distribution. If, for example, $F_1(r) = C(r)$ for the solid phase, then $F_2(r) = L(r) =$ chord length distribution function for the pore phase is a good choice, if $m = 2$ is wanted. In addition to the characteristics of 'one-dimensional nature' such as $C(r)$, $L(r)$ and $H_l(r)$, it may be valuable to use also 'higher-dimensional' ones, such as $H_d(r)$ and $H_s(r)$ or n-point probability functions, if available. However, it may happen that some of the summary characteristics prescribed are contradicting — there is perhaps no random set that possesses all of them as its summary characteristics.

The usual minimisation method is *simulated annealing* (Hazlett, 1997; Yeong and Torquato, 1998a,b; Hilfer, 2000; Torquato, 2002, 2010). This works as follows (Talukdar *et al.*, 2002,a,b): In the beginning the pixels are randomly marked as 0 (void) and 1 (solid), such that volume fraction is p. The start configuration then changes stepwise, at the k^{th} iteration step a void and a solid pixel are randomly chosen and their marks are interchanged. The change slightly modifies the functions $\hat{F}_i(r)$, which describe the actual pixel structure. Therefore, also the 'energy' E defined by (6.195) changes from E_k to E_{k+1}, while volume fraction p is preserved. A pixel change is accepted with probability p_k given by the Metropolis rule

$$p_k = \min\left\{1, \exp\left(-\frac{E_{k+1} - E_k}{T_k}\right)\right\}, \tag{6.196}$$

where T_k is a control parameter, called 'temperature'. It decreases as k increases with the goal that a global minimum is achieved as quickly as possible. Talukdar *et al.* (2002) sketches the choice of the temperature schedule. Experience shows that the simpler form

$$p_k = \begin{cases} 1 & \text{if } E_k > E_{k+1}, \\ 0 & \text{otherwise,} \end{cases} \tag{6.197}$$

meaning that one accepts 'improvements only', is also sufficient; see Tscheschel and Stoyan (2006).

For an efficient use of the reconstruction method it is important to calculate the functions $\hat{F}_i(r)$ in a way that uses the fact that the pixel interchanges are only local and thus one can reuse the functions $\hat{F}_i(r)$ measured in the k^{th} step, instead of recomputing them fully, at the $(k+1)^{\text{st}}$ step.

Examples for the application of the reconstruction method can be found in Manwart *et al.* (2000), Torquato (2002) and Talukdar *et al.* (2002,a,b), and in p. 418 in the context of stereology, when for a three-dimensional set only one- or two-dimensional information is given. For a realisation of Ξ observed in W, reconstruction of samples in $W \oplus B(o, r) \setminus W$ for

$r \geq 0$ enables one to apply the plus-sampling (Section 6.5.7) for the estimation of summary characteristics of Ξ. Tscheschel and Chiu (2008) apply such an approach, called *quasi-plus-sampling*, to point patterns and show empirically that it can yield more accurate estimates than many other edge-correction methods (see Section 4.7.2).

A reconstruction method in the spirit of germ–grain models is described in Singh *et al.* (2006). There the grains are empirically given, and the approach is to model the germs first and then place the grains.

As a by-product, the reconstruction method may also help characterise the information content of summary characteristics: those which enable a precise reconstruction can be considered as highly informative; see the discussion in Jiao *et al.* (2009).